Research Report
KTC-97-1

DYNAMIC SITE PERIODS FOR THE JACKSON PURCHASE REGION OF WESTERN KENTUCKY (KYSPR96-173)

by

Ron Street
Associate Professor, Department of Geological Sciences

Zhenming Wang and Edward Woolery
Research Assistants, Department of Geological Sciences

Issam E. Harik
Professor of Civil Engineering and Head, Structures Section,
Kentucky Transportation Center

David L. Allen
Transportation Engineer V, Kentucky Transportation Center

and

Kevin G. Sutterer
Assistant Professor, Department of Civil Engineering

Kentucky Transportation Center
College of Engineering, University of Kentucky
Lexington, Kentucky

in cooperation with

Kentucky Transportation Cabinet
Commonwealth of Kentucky

and

The Federal Highway Administration
U.S. Department of Transportation

February 1997

Commonwealth of Kentucky
Transportation Cabinet
Frankfort, Kentucky 40622

James C. Codell, III
Secretary of Transportation

T. Kevin Flanery
Deputy Secretary

Paul E. Patton
Governor

June 16, 1997

Mr. Dennis Luhrs
Acting Division Administrator
Federal Highway Administration
330 West Broadway
Frankfort, Kentucky 40602

Dear Mr. Luhrs:

RE: IMPLEMENTATION STATEMENT
KYSPR 96-173, "Evaluation and Analysis of Innovative Concepts for Bridge Seismic Retrofit"

The above referenced research study is divided into three major tasks:

TASK A: Dynamic Site Periods for the Jackson Purchase region of Western Kentucky

TASK B: Seismic Stability of Highway Bridge Approach Embankments and Retaining Structures

TASK C: Seismic Assessment of Selected Truss Bridges Crossing the Ohio River in Western Kentucky

TASK A has been completed, and the results of the work are presented in this report. The objectives of this task were defined as follows:

1. Determination of the depth to Paleozoic bedrock,

2. Determination of the shear-wave velocities of the overlying sediments, and

3. Determination of the predominant period at which seismically induced, vertically propagating, ground motions would be amplified in the Jackson Purchase region.

In order to assess these quantities, locations throughout the area were investigated using high-resolution P-wave and S-wave seismic techniques. This data was used to generate dynamic site periods for the counties in Western Kentucky which compose the Jackson Purchase region.

Using the information contained in this report, engineers may design structures in such a way as to withstand shaking from a moderate earthquake in the New Madrid or Wabash Valley Seismic Zones. If the structure is designed so that its natural period does not coincide with the dynamic site period, the chance of the structure surviving the seismic event and remaining "useful" will be greatly improved.

Sincerely,

J. M. Yowell, P.E.
State Highway Engineer

c: David Smith

Technical Report Documentation Page

1. Report No.	2. Government Accession No.	3. Recipient's Catalog No.
KTC-97-1		

4. Title and Subtitle	5. Report Date
DYNAMIC SITE PERIODS FOR THE JACKSON PURCHASE REGION OF WESTERN KENTUCKY	February 1997
	6. Performing Organization Code
7. Author(s) R. Street, Z. Wang, E. Woolery, I.E. Harik, D.L. Allen, and K.G. Sutterer	8. Performing Organization Report No. KTC-97-1
9. Performing Organization Name and Address Kentucky Transportation Center College of Engineering University of Kentucky Lexington, Kentucky 40506-0281	10. Work Unit No. (TRAIS) 11. Contract or Grant No. KYSPR-96-173
12. Sponsoring Agency Name and Address Kentucky Transportation Cabinet State Office Building Frankfort, Kentucky 40622	13. Type of Report and Period Covered Final 14. Sponsoring Agency Code

15. Supplementary Notes

Prepared in cooperation with the Kentucky Transportation Cabinet and the U.S. Department of Transportation, Federal Highway Administration

16. Abstract

Bridges, overpasses, and other engineered structures in the Jackson Purchase region of Western Kentucky are, of necessity, built on a thick column of loose to semi-consolidated sediments. Because these sediments tend to amplify seismically induced ground motions at preferred periods, structures with natural periods close to the preferred periods of amplification of the ground motions are particularly vulnerable to damages during an earthquake because of in-phase resonance.

For this report, conventional seismic refraction and reflection techniques were used to determine the shear-wave velocities of the more poorly consolidated, near-surface sediments for a matrix of sites in the region. Conventional seismic P-wave reflections along with existing drill hole and seismic reflection data in the region were then used to determine the depth to the top of the bedrock at the sites investigated. These data were used in SHAKE91 to calculate the fundamental period of the ground motion at the sites. This period, identified in the study as the dynamic site period, is the period at which ground motions in the sedimentary column are most apt to be amplified as a result of a seismic shear wave propagating from the top of the bedrock to the surface. Based on the results in this report, it is recommended that bridges, overpasses, and other engineered structures built in the region be designed so that their natural periods do not coincide with the fundamental period of the sedimentary column, thereby avoiding damage during an earthquake as a result of in-phase resonance.

17. Key Words	18. Distribution Statement
P-wave, shear-wave, seismicity, vibration, dynamic site period	Unlimited with approval of Kentucky Transportation Cabinet

19. Security Classif. (of this report)	20. Security Classif. (of this page)	21. No. of Pages	22. Price
Unclassified	Unclassified	123	

FormDOT 1700.7 (8-72) Reproduction of Completed Page Authorized

TABLE OF CONTENTS

LIST OF TABLES

LIST OF FIGURES

EXECUTIVE SUMMARY

Bridges, overpasses, and other structures built in the Jackson Purchase Region of Western Kentucky (i.e., Ballard, Calloway, Carlisle, Fulton, Graves, Hickman, McCracken, and Marshall Counties) will be subjected to severe motion in the event of a severe earthquake in the New Madrid or Wabash Valley Seismic Zones. The motion will be a consequence of the structure's proximity to the seismic zones and the thick layer of loose and poorly consolidated sediments upon which they are, of necessity, built. The modifying effects on earthquake waves propagating from bedrock to the surface through a thick layer of sediments are routinely modeled using one-dimensional nonlinear response analyses. To calculate the effects of the sediments on a propagating earthquake wave, the shear-wave velocities, damping ratios, and thicknesses of the sediments at a site need to be known.

High-resolution shear-wave data at sites throughout the Jackson Purchase Region were acquired to determine the depth to bedrock as well as shear-wave velocities and thicknesses of the sediments. These data have been incorporated into the computer program SHAKE91, and used to calculate the fundamental period at which the maximum amplification of earthquake waves occurs. The fundamental periods have then been mapped.

ACKNOWLEDGMENT

The financial support for this project was provided by the Kentucky Transportation Cabinet and the Federal Highway Administration. The authors would like to acknowledge the cooperation, suggestions, and advise of the members of the Study Advisory Committee: Donald Herd (Committee Chair), Glenn Givan, Ray Greer, David Moses, Ted Noe, N.B. Shah, and David Steele.

Thanks are also expressed to Jeff Griffin for his help in preparing this report.

1.0 INTRODUCTION

Transportation facilities in the Jackson Purchase Region of Western Kentucky (Fig. 1) are, of necessity, built on a thick layer of loose to semi-consolidated sediment that occurs throughout the Upper Mississippi Embayment. Recent earthquakes in North America and elsewhere have clearly demonstrated the correlation between damage and the depth of the soils at a specific site; this is particularly true for sites underlain by thick layers of Holocene soils. The shear-wave velocities and thicknesses of the soil layers at a site can dramatically alter earthquake-induced ground motions at that site through the mechanisms of amplification, deamplification, frequency modulation, and increased duration. Amplification is due to energy being conserved across impedance boundaries. Deamplification is primarily caused by damping. Frequency modulation is the result of selective filtering (including resonance). Finally, increased duration is caused by such mechanisms as resonance and basin-generated surface waves resulting from the conversion of S-waves to surface waves (Frankel, 1994; Street et al., 1995). Together, these mechanisms are referred to as site effects.

The objectives of this study were to determine: (1) the depth to the Paleozoic bedrock, (2) the shear-wave velocities of the overlying sediments, and (3) the predominant period at which seismically induced, vertically propagating, ground motions would be amplified in the Jackson Purchase Region. To determine these parameters, a matrix of sites throughout the area was investigated using high-resolution P- and S-wave seismic techniques.

2.0 BACKGROUND

As noted by Reiter (1990), site effects, under certain conditions, may have a more profound effect on the level of earthquake shaking than the magnitude of the earthquake itself. In the October 19, 1989, Loma Prieta, California, earthquake, approximately two-thirds of the $5.9 billion in property damage was caused by enhanced ground shaking resulting from site effects, while only 2 percent ($131 million) of the property losses were attributed to ground failure phenomena such as liquefaction, landslides, and tectonic ground failure (Holzer, 1994). Similar, although less quantitatively stated, observations have been made concerning the damages in Mexico City, Mexico; Northridge, California; and Kobe, Japan, as a result of the September 19, 1985, Michoacan; the January 17, 1994, California; and the January 17, 1995, Hyogo-ken Nambu, Japan, earthquakes, respectively.

The seismic risk in Western Kentucky is caused by its proximity to the New

Madrid and Wabash Valley Seismic Zones (Fig. 2). The most severe earthquakes experienced in Western Kentucky were the four great earthquakes that occurred during the winter of 1811-1812 (Nuttli, 1973; Street, 1982). In the winter of 1811-1812, Western Kentucky, a frontier area, was sparsely inhabited and had no infrastructure. If the 1811-1812 earthquakes were to repeat themselves today, Western Kentucky, as well as large parts of Indiana, Illinois, Missouri, Arkansas, and Tennessee, would suffer catastrophic levels of damages. Fortunately, most studies predict (e.g., Johnston and Nava, 1985) that the recurrence of a great earthquake in the New Madrid Seismic Zone is highly unlikely in the foreseeable future. Most seismologists believe that a far more likely scenario is the occurrence of a 6.0 to 6.5 magnitude event by the year 2035. A more complete discussion of the seismic risk to Western Kentucky by earthquakes in the New Madrid and Wabash Valley Seismic Zones is presented elsewhere (Street et al., 1996).

Ground motions from a magnitude 6.0 to 6.5 earthquake in the New Madrid Seismic Zone will be greatly enhanced at selected periods by the thick layer of soils in the Jackson Purchase Region of Western Kentucky. However, they will most likely be of insufficient amplitude to cause catastrophic ground failure, such as liquefaction, in the soils. If the natural period of an engineered structure, such as an overpass, unfortunately coincides with the natural period of the underlying sediments, the likelihood of damages to the structure increases dramatically, since natural periods of the incoming enhanced ground motions and structure are in-phase. In fact, the structure may well be damaged beyond repair even if it was designed to withstand a much larger magnitude earthquake.

A realistic goal in the design and construction of most structures in Western Kentucky is to build them in such a way as to withstand shaking from a moderate (6.0 to 6.5 magnitude) earthquake in the New Madrid or Wabash Valley Seismic Zones, without incurring any damage that would affect the usefulness of the structure. One way to achieve this goal in an economical manner is to determine the predominant periods of the enhanced ground shaking at sites throughout the Jackson Purchase Region, and then design structures so that their natural periods do not coincide with the predominant period at the site where the structures are to be built. If this process is done correctly, the chance of the structure surviving the seismic event would be greatly improved, regardless of the location or magnitude of the earthquake.

For the design of a structure situated on a thick soil column, the predominant period of greatest interest is the dynamic site period. As indicated in Section 1.0, vertically propagating seismic waves traversing from bedrock through a horizontally stratified soil column to the surface are affected by a number of mechanisms that can modify their amplitudes. One mechanism that can lead to both an increase in amplitude and duration of motion is resonance. In the simplest case, the maximum ground motion occurs for waves whose wavelengths are four times the thickness of the soil column layer in which the seismic waves are trapped. In other words, for shear waves the period that is amplified the most is equal to $4H/V_s$, where H is the thickness of the soil layer and V_s is its shear-wave velocity (Reiter, 1990). The period at which the fundamental mode of resonance occurs at a site is defined as the dynamic site period (DSP).

3.0 SITE INVESTIGATIONS

Figure 3 illustrates the geographic distribution of sites investigated in this study to determine dynamic site period (DSP). Table 1 gives the geographic coordinates and elevation (with respect to sea level) of the sites, as well as the type of data collected at the site. The numbering of the sites listed in Table 1 corresponds with those shown in Figure 3. All of the seismic data for the study were collected using an instantaneous floating-point engineering seismograph and were processed on a PC using the software package VISTA (Seismic Image Software Ltd., 1995). The shear-wave data were recorded using an in-line spread of 12 30-Hz horizontal geophones at spacings of 6.1-m (20-ft). The shear-wave energy source was a section of steel I-beam that was struck horizontally with a 4.5-kg (10-lb) sledgehammer in a direction perpendicular to the geophone spread, which generated horizontally polarized shear (SH) waves. The testing devices used to collect such data are pictured in Figure 4.

The hold-down weight of the I-beam was approximately 70 to 80-kg, and consisted of the weight of the person swinging the hammer and the steel I-beam section. The source (i.e., I-beam and hammer operator) was stepped out from the end of the geophone spread at offsets of 6.1-m (20-ft), 61-m (200-ft), 122-m (400-ft), 183-m (600-ft), and 244-m (800-ft). The individual offset panels were then combined to form shear-wave seismic sections that covered the entire range of source-receiver offsets. Because of the limited amount of shear-wave energy that could be generated using a seismic hammer, we were typically unable to obtain data for determining shear-wave velocities in the soil column for depths in excess of 100 to 150-m (328 to 492-ft).

In addition to the shear-wave investigations, seismic P-wave reflection data were also obtained at several sites to determine the depth to the Paleozoic bedrock. The P-wave data were gathered in much the same way that the SH-wave data were collected. That is, data were obtained from an in-line spread of 12 vertical geophones operating at 40-Hz. Records from 6.1-m (20-ft) intervals with stepouts of 6.1-m (20-ft), 61-m (200-ft), 122-m (400-ft), etc., were combined to form a single seismic section. The energy source used for the P-wave investigation was a trailer-mounted, vacuum-assisted weight drop that drives a 45-kg steel slug into an aluminum platen. The hold-down weight of the platen is imposed by jacking the trailer up so that most of the weight of the trailer is translated to the platen.

The composite SH- and P-wave seismic sections were interpreted using conventional techniques. Seismic velocities and depths to interfaces were interpreted from the refraction data by the intercept method. Stacking velocities and depths to interfaces were interpreted from the available reflection data by conventional X^2-T^2 analysis and computer displays by interactively fitting a hyperbolic curve to arrivals having moveouts that could be interpreted as reflected waves. Figure 5 illustrates the SH-wave composite section obtained at site K82 (Table 1), near Cayce, Ky. Superimposed on the figure are dashed lines indicating the choice of refractors and reflections in the section.

Appendix A illustrates the SH-wave seismic sections obtained and used in this study. Not shown in the appendix are the seismic sections not used in the study because of the poor quality of the data. In addition to making composites of the individual offset panels as described above, typical processing steps were filtered and an automatic gain control (AGC) was applied to the data. The AGC is a moving "window" designed to measure the average signal level over a short time interval; it is used to adjust the gain to keep the output more or less constant regardless of the input level (Telford et al., 1976).

Filtering was done in the frequency domain using the Ormsby filter module built into VISTA (Seismic Image Software Ltd., 1995). The amplitudes of the data are unaffected in the frequency band defined by the low-cut and high-cut frequencies (10 to 45 Hz), are linearly attenuated between the low-truncation and low-cut frequencies (5 to 10 Hz), and linearly attenuated between the high-cut and high-truncation frequencies (45 to 50 Hz). The AGC window used in processing the SH-wave sections was uniformly taken to be 300 ms in length.

Table 2 gives the shear-wave velocities and thicknesses of the velocity layers as interpreted from the walkaway SH-wave sections shown in Appendix A. Site numbers listed in Appendix A correspond to those shown in Figure 3 and listed in Table 1.

4.0 DYNAMIC SITE PERIODS

As indicated above, the DSP at a site for vertically propagating seismic waves in a soil layer are a function of the shear-wave velocities, damping, and thicknesses of the soil layers in the soil column that overlies the bedrock, as well as the depth to the top of the bedrock. Eighty-three sites were investigated in this study for either SH-wave or P-wave velocities, or both SH- and P-wave velocities. The SH-wave data were used to estimate the shear-wave velocities, thicknesses of the soil layers, and, where possible, the depth to bedrock. At sites where the depth to the bedrock was greater than several tens of meters, however, we were unable to generate sufficient shear-wave energy to determine the depth to bedrock. Near some of these sites, drill hole data were available and were used to estimate the depth to the top of the bedrock. At other sites, proprietary P-wave seismic reflection data were obtained and used to determine the depth to the top of the bedrock. If the shear-wave data were inadequate for estimating the depth to the top of the bedrock, and there were no existing drill hole or P-wave seismic reflection data, a P-wave walkaway investigation, as discussed above, was done to derive an estimate for the depth to the top of the bedrock. Bedrock in this study is defined as Paleozoic rock.

Table 3 gives the source and type of data used to estimate the depth to the top of the bedrock, as well as the location of the site investigated. Information from Table 3 was then used to derive the depth to the top of the bedrock in the Jackson Purchase Region as shown in Figure 6. The depths in the figure are given with respect to sea level; hence, a negative depth means that the top of the Paleozoic bedrock is below sea level at that location.

The shear-wave velocities, thicknesses of the soil layers, and depth to the top of the Paleozoic bedrock were used in the software program SHAKE91 (Idriss and Sun, 1992) to calculate the DSP at sites in the study area that were successfully investigated using SH-waves. Other information needed for input into SHAKE91 was the velocity of the Paleozoic bedrock and the damping ratio (D) for each soil layer.

Based on a limited number of observations, a shear-wave velocity of 1,158 m/s (3,800 ft/s) was used for the Paleozoic bedrock throughout the study area. This velocity is not well documented, but for the purposes of calculating the DSP, a more precise value is unimportant to the calculations.

Damping of the soil layers in the input models for SHAKE91 was estimated from the shear-wave velocities using the shear-wave quality factor (Q_s) and the relationship $D = (2\ Q_s)^{-1}$ which is frequently used for small strains (i.e., 10^{-5} percent) when the stress-strain behavior of the soil is approximately linear (Mok et al., 1988). Wang et al. (1994) found that for unconsolidated soils in the Mississippi embayment, Q_s could be related to the shear-wave velocity (V_s) of the soils by the relationship $Q_s = 0.08\ V_s + 6.99 \pm 12.10$.

Small strains were assumed in the analysis since, as indicated in Section 2.0, the most likely scenario for a damaging earthquake in the New Madrid Seismic Zone is a 6.0 to 6.5 magnitude event occurring within the foreseeable future. In the event of such an earthquake, it is highly unlikely that nonlinear conditions will occur anywhere in the soils of the Jackson Purchase Region, with the possible exception of areas in the floodplain of the Mississippi River (i.e., the western edge of Fulton, Hickman, and Carlisle Counties).

The dynamic site periods for the sites investigated in this study are listed in the right column of Table 2. The range of DSP values given per site in Table 2 (low, mean, and high) are meant to give the range of dynamic site periods at the location, assuming some error in the interpretation of the seismic data. The column of values under the headings "Low" and "High" were obtained by assuming a 10 percent error in the depth to bedrock and shear-wave velocities of the soils. For the DSP values in the column marked "Low," the depth to the top of the bedrock was assumed to be 10 percent greater than that estimated in this study, and the shear-wave velocities of the soils were assumed to be 10 percent less than those interpreted from the SH-wave data in this study. For the DSP values under the column marked "High," the shear-wave velocities were increased by 10 percent, and the depth to the top of the Paleozoic bedrock was decreased by 10 percent. These estimates are believed to represent a reasonable upper and lower estimate of DSP values at the sites investigated in this study.

Figure 7 illustrates the best (i.e., "mean") estimates of the DSP values at the sites investigated in this study. The DSP values have been contoured and, in general, increase from east to west and north to south; which more or less corresponds to the depth to the top of the bedrock shown in Figure 6.

5.0 RECOMMENDATIONS

The term "dynamic site period," as used in this study, represents the fundamental period at which the soils overlying bedrock in the Jackson Purchase Region will resonate in the event of a damaging earthquake in the New Madrid or Wabash Valley Seismic Zones. To significantly lessen the likelihood of damage to engineered structures in the area, such as bridges, overpasses, schools, hospitals, etc., such structures need to be deigned so that their natural periods do not coincide with the DSP values shown in Figure 7. Furthermore, since the depth to bedrock and shear-wave velocities of the sediments can and sometimes do vary appreciably even over short distances, we recommend that site-specific studies be undertaken to verify or modify the suggested DSP values shown in Figure 7 for particularly sensitive structures, such as major bridges over the Ohio or Mississippi Rivers.

REFERENCES CITED

1. Ali-Yazdi, A.A. (1994). *Paleozoic Bedrock Depth Investigation in the Jackson Purchase Region of Western Kentucky Using P-Wave Seismic Reflection Technique for the Purpose of Regional 1-D Site Effects Estimation*, M.S. thesis, University of Kentucky, Lexington, 109 pp.

2. Dart, R.L. (1992). Catalog of the Pre-Cretaceous geologic drill-hole data from the Upper Mississippi Embayment: A revision and update of Open-File Report 90-260, *U.S. Geological Survey Open-File Report 92-685*, 253 pp.

3. Frankel, A. (1994). Dense array recordings in the San Bernardino Valley of Landers-Big Bear aftershocks; basin surface waves, moho reflections, and three-dimensional simulations, *Bulletin of the Seismological Society of America*, **84**, 613-624.

4. Holzer, T.L. (1994). Loma Prieta damage largely attributed to enhanced ground shaking, *EOS, Transactions of the American Geophysical Union*, **75**, 299-301.

5. Idriss, I.M., and Sun, J.I. (1992). *User's Manual for SHAKE91, A Computer Program for Conducting Equivalent Linear Seismic Response Analyses of Horizontally Layered Soil Deposits*, Center for Geotechnical Modeling, Department of Civil and Environmental Engineering, University of California, Davis, Calif., 13 pp., and 2 Appendices.

6. Johnston, A.C., and Nava, S.J. (1985). Recurrence rates and probability estimates for the New Madrid Seismic Zone, *Journal of Geophysical Research*, **90**, 6737-6753.

7. Mok, Y.J., I. Sanchez-Salinero, K.H. Stoke, and J.M. Rosset (1988). In situ damping measurements by crosshole seismic methods, *Earthquake Engineering and Soil Dynamics II-Recent Advances in Ground-Motion Evaluation, Proc. of the ASCE Specialty Conference*, June 27-30, Park City, Utah, 103-155.

8. Nuttli, O.W. (1973). The Mississippi Valley earthquakes of 1811-1812: Intensities, ground motion, and magnitudes, *Bulletin of the Seismological Society of America*, **63**, 227-248.

9. Reiter, L. (1990). *Earthquake Hazard Analysis: Issues and Insights*, Columbia University Press, New York, 254 pp.

10. Seismic Image Software Ltd., 1995, VISTA 6.61 Notes, 477 pp.

11. Street, R. (1982). A contribution to the documentation of the 1811-1812 Mississippi Valley earthquake sequence, *Earthquake Notes*, **53**, 39-52.

12. Street, R., Wang, Z., Harik, I. and Allen, D. (1996). Source zones, recurrence rates, and time histories, for earthquakes affecting Kentucky, *Kentucky Transportation Center Report KTC-96-4*, 187 pp.

13. Street, R., Woolery, E., Wang, Z., and Harris, J. (1995). A short note on shear-wave velocities and other site conditions at selected strong-motion stations in the New Madrid Seismic Zone, *Seismological Research Letters*, **66(1)**, 56-63.

14. Telford, W.M., Geldart, L.P., Sheriff, R.E., and Keys, D.A. (1976). *Applied Geophysics*, Cambridge University Press, New York, 860 pp.

15. Wang, Z., Street, R., Harris, J., and Woolery, E. (1994). Q_s estimation for unconsolidated sediments using first-arrival SH-refractions, *Journal of Geophysical Research*, **99 B**4, 13,543-13551.

TABLE 1

GEOGRAPHIC LOCATIONS OF SITES INVESTIGATED IN THE JACKSON PURCHASE REGION

Site No.	Quadrangle	Elevation (m)	Location		Wave	
			°N	°W	SH-	P-
K01	Joppa	107	37.164	88.852	Y	Y
K02	Bandana	113	37.146	88.901	Y	Y
K03	Bandana	116	37.139	88.977	Y	
K04	Bandana	99	37.200	88.988		Y
K05	Olmsted	101	37.164	89.027	Y	
K06	Calvert City	105	37.019	88.317	Y	
K07	Calvert City	122	37.004	88.297	Y	
K08	Paducah West	117	37.024	88.703	Y	
K09	Heath	149	37.005	88.853	Y	
K10	LaCenter	113	37.068	88.925	Y	Y
K11	LaCenter	125	37.014	88.972	Y	
K12	Barlow	140	37.042	89.000	Y	
K13	Barlow	101	37.111	89.022	Y	Y
K14	Barlow	104	37.093	89.069	Y	Y
K15	Birmingham Point	116	36.984	88.225	Y	Y
K16	Briensburg	146	36.891	88.315	Y	Y
K17	Briensburg	105	36.965	88.316	Y	Y
K18	Briensburg	143	36.956	88.365	Y	Y
K19	Elva	137	36.967	88.419	Y	Y

TABLE 1 (CONTINUED)

GEOGRAPHIC LOCATIONS OF SITES INVESTIGATED IN THE JACKSON PURCHASE REGION

Site No.	Quadrangle	Elevation (m)	Location		Wave	
			°N	°W	SH-	P-
K20	Elva	119	36.907	88.448	Y	Y
K21	Symsonia	104	36.899	88.538	Y	
K22	Symsonia	105	36.953	88.552	Y	
K23	Symsonia	110	36.941	88.606	Y	
K24	Melber	116	36.971	88.644	Y	
K25	Melber	137	36.893	88.733	Y	
K26	Lovelaceville	110	36.950	88.758	Y	
K27	Lovelaceville	116	36.919	88.794		Y
K28	Lovelaceville	107	36.961	88.849	Y	Y
K29	Blandville	102	36.930	88.906		Y
K30	Blandville	116	36.970	88.926	Y	
K31	Blandville	143	36.993	88.943		Y
K32	Wickliffe	107	36.906	89.005	Y	
K33	Wickliffe	93	36.998	89.114	Y	Y
K34	Hardin	117	36.810	88.284	Y	
K35	Hardin	162	36.784	88.351	Y	
K36	Oak Level	149	36.805	88.413	Y	
K37	Oak Level	140	36.840	88.453	Y	
K38	Oak Level	117	36.796	88.458	Y	

TABLE 1 (CONTINUED)

GEOGRAPHIC LOCATIONS OF SITES INVESTIGATED IN THE JACKSON PURCHASE REGION

Site No.	Quadrangle	Elevation (m)	Location		Wave	
			°N	°W	SH-	P-
K39	West Plains	108	36.841	88.525	Y	
K40	West Plains	131	36.823	88.621	Y	
K41	Hickory	133	36.779	88.730	Y	
K42	Hickory	131	36.841	88.797	Y	
K43	Fancy Farm	131	36.767	88.764	Y	
K44	Milburn	110	36.842	88.897	Y	
K45	Milburn	130	36.868	88.898	Y	
K46	Milburn	107	36.858	88.927		Y
K47	Milburn	122	36.821	88.982	Y	
K48	Arlington	107	36.867	89.023	Y	
K49	Arlington	111	36.804	89.023	Y	
K50	Hico	162	36.684	88.178	Y	
K51	Hico	165	36.628	88.226	Y	Y
K52	Hico	165	36.656	88.237	Y	
K53	Dexter	131	36.690	88.271	Y	
K54	Dexter	162	36.708	88.338	Y	
K55	Kirksey	165	36.713	88.375	Y	
K56	Kirksey	134	36.693	88.469	Y	
K57	Farmington	168	36.684	88.538	Y	

TABLE 1 (CONTINUED)

GEOGRAPHIC LOCATIONS OF SITES INVESTIGATED IN THE JACKSON PURCHASE REGION

Site No.	Quadrangle	Elevation (m)	Location		Wave	
			°N	°W	SH-	P-
K58	Farmington	142	36.681	88.597	Y	
K59	Mayfield	128	36.662	88.695	Y	
K60	Dublin	117	36.690	88.789	Y	
K61	Dublin	116	36.674	88.838	Y	
K62	Clinton	113	36.726	88.900	Y	
K63	Clinton	120	36.654	88.941	Y	
K64	Oakton	101	36.740	89.045	Y	Y
K65	Oakton	93	36.650	89.104	Y	Y
K66	New Concord	162	36.570	89.136		Y
K67	New Concord	123	36.533	88.183	Y	Y
K68	New Concord	165	36.556	88.231	Y	
K69	Murray	165	36.615	88.255	Y	
K70	Murray	166	36.559	88.285	Y	Y
K71	Murray	155	36.556	88.356	Y	
K72	Lynn Grove	165	36.573	88.406	Y	
K73	Lynnville	174	36.604	88.502	Y	
K74	Lynnville	168	36.564	88.607	Y	
K75	Cuba	142	36.604	88.672		Y
K76	Cuba	155	36.556	88.706	Y	

TABLE 1 (CONTINUED)

GEOGRAPHIC LOCATIONS OF SITES INVESTIGATED IN THE JACKSON PURCHASE REGION

Site No.	Quadrangle	Elevation (m)	Location		Wave	
			°N	°W	SH-	P-
K77	Water Valley	119	36.567	88.800	Y	
K78	Water Valley	140	36.520	88.835	Y	
K79	Crutchfield	125	36.520	88.901	Y	
K80	Crutchfield	105	36.597	88.909	Y	
K81	Crutchfield	101	36.536	88.962	Y	
K82	Cayce	94	36.574	89.017	Y	Y
K83	Cayce	107	36.524	89.073	Y	

TABLE 2

SOIL COLUMN THICKNESSES, SHEAR-WAVE VELOCITIES, AND DYNAMIC SITE PERIODS FOR SITES INVESTIGATED

Site	Layer Thickness (m)	Velocity (m/s)	Density (gm/m^3)	Damping Ratio	Period (sec)		
					Low	Mean	High
K01	12.8	196.3	1.95	0.022	0.73	0.89	1.00
	23.2	500.3	2.00	0.011			
	113.4	697.3	2.20	0.008			
		1158.5	2.50	0.005			
K02	3.7	204.9	1.95	0.021	0.23	0.28	0.33
	14.3	409.5	2.00	0.013			
	13.7	595.1	2.10	0.009			
	10.4	740.5	2.20	0.008			
		1158.5	2.50	0.005			
K03	5.2	168.0	1.90	0.024	0.73	0.89	1.14
	43.3	338.4	2.00	0.015			
	38.4	399.4	2.10	0.013			
		1158.5	2.50	0.005			
K05	2.7	177.1	1.90	0.024	0.40	0.50	0.62
	37.8	531.7	2.10	0.010			
	34.5	630.5	2.20	0.009			
		1158.5	2.50	0.005			
K06	5.5	249.1	1.95	0.019	0.62	0.73	0.89
	23.5	393.9	2.00	0.013			
	82.0	580.2	2.20	0.009			
		1158.5	2.50	0.005			

TABLE 2 (CONTINUED)

SOIL COLUMN THICKNESSES, SHEAR-WAVE VELOCITIES, AND DYNAMIC SITE PERIODS FOR SITES INVESTIGATED

Site	Layer Thickness (m)	Velocity (m/s)	Density (gm/m^3)	Damping Ratio	Period (sec)		
					Low	Mean	High
K07	1.2	98.5	1.85	0.034	0.57	0.67	0.89
	2.7	305.8	2.00	0.016			
	89.9	542.7	2.10	0.010			
		1158.5	2.50	0.005			
K08	2.1	156.1	1.90	0.026	0.73	0.89	1.00
	14.3	272.9	2.00	0.017			
	61.6	531.4	2.10	0.010			
	57.0	672.0	2.20	0.008			
		1158.5	2.50	0.005			
K09	1.8	98.2	1.90	0.034	1.33	1.60	2.00
	8.8	220.1	1.95	0.020			
	27.7	369.8	2.00	0.014			
	57.6	617.4	2.10	0.009			
	222.6	731.7	2.20	0.008			
		1158.5	2.50	0.005			
K10	12.8	175.6	1.90	0.024	0.89	1.14	1.33
	34.5	254.0	2.00	0.018			
	30.2	425.6	2.10	0.012			
	67.7	609.8	2.20	0.009			
		1158.5	2.50	0.005			

TABLE 2 (CONTINUED)

SOIL COLUMN THICKNESSES, SHEAR-WAVE VELOCITIES, AND DYNAMIC SITE PERIODS FOR SITES INVESTIGATED

Site	Layer Thickness (m)	Velocity (m/s)	Density (gm/m^3)	Damping Ratio	Period (sec)		
					Low	Mean	High
K12	8.5	193.6	1.95	0.022	0.67	0.80	1.00
	55.5	417.1	2.00	0.012			
	49.1	638.4	2.20	0.009			
		1158.5	2.50	0.005			
K14	7.3	132.9	1.90	0.028	0.50	0.62	0.80
	40.2	579.6	2.00	0.009			
	62.5	708.8	2.20	0.008			
		1158.5	2.50	0.005			
K15	10.1	158.8	1.90	0.025	2.00	2.67	4.00
	39.0	328.7	2.00	0.015			
	41.2	487.5	2.10	0.011			
	406.7	731.7	2.20	0.008			
		1158.5	2.50	0.005			
K16	10.1	141.8	1.90	0.027	2.00	2.67	4.00
	13.7	250.0	2.00	0.019			
	33.8	451.5	2.10	0.012			
	437.8	731.7	2.20	0.008			
		1158.5	2.50	0.005			

TABLE 2 (CONTINUED)

SOIL COLUMN THICKNESSES, SHEAR-WAVE VELOCITIES, AND DYNAMIC SITE PERIODS FOR SITES INVESTIGATED

Site	Layer Thickness (m)	Velocity (m/s)	Density (gm/m^3)	Damping Ratio	Period (sec)		
					Low	Mean	High
K17	3.0	132.9	1.90	0.028	2.00	2.67	4.00
	6.1	250.3	1.95	0.019			
	47.3	433.8	2.00	0.012			
	449.7	731.7	2.20	0.008			
		1158.5	2.50	0.005			
K18	1.8	96.6	1.85	0.034	2.00	2.67	2.67
	11.0	350.0	2.00	0.014			
	32.9	472.6	2.10	0.011			
	399.4	731.7	2.20	0.008			
		1158.5	2.50	0.005			
K19	1.2	152.1	1.90	0.026	1.60	2.00	2.67
	7.9	341.5	1.95	0.015			
	27.7	379.9	2.00	0.013			
	51.2	554.3	2.10	0.010			
	256.4	731.7	2.20	0.008			
		1158.5	2.50	0.005			
K20	0.9	212.5	1.95	0.021	1.33	1.60	2.00
	11.0	327.1	2.00	0.015			
	47.6	435.7	2.10	0.012			
	251.5	751.2	2.20	0.007			
		1158.5	2.50	0.005			

TABLE 2 (CONTINUED)

SOIL COLUMN THICKNESSES, SHEAR-WAVE VELOCITIES, AND DYNAMIC SITE PERIODS FOR SITES INVESTIGATED

Site	Layer Thickness (m)	Velocity (m/s)	Density (gm/m^3)	Damping Ratio	Period (sec)		
					Low	Mean	High
K21	1.8	132.9	1.90	0.028	1.14	1.33	1.60
	29.3	447.9	2.00	0.012			
	42.1	559.5	2.10	0.010			
	195.1	774.4	2.20	0.007			
		1158.5	2.50	0.005			
K22	2.4	236.3	1.95	0.019	0.73	0.89	1.14
	22.3	548.2	2.10	0.010			
	155.2	784.5	2.20	0.007			
		1158.5	2.50	0.005			
K24	7.6	145.1	1.90	0.027	0.73	0.89	1.14
	40.9	344.5	2.00	0.014			
	94.5	650.9	2.20	0.008			
		1158.5	2.50	0.005			
K28	6.1	182.3	1.95	0.023	0.67	0.89	1.00
	58.2	487.8	2.00	0.011			
	60.4	618.9	2.10	0.009			
		1158.5	2.50	0.005			

TABLE 2 (CONTINUED)

SOIL COLUMN THICKNESSES, SHEAR-WAVE VELOCITIES, AND DYNAMIC SITE PERIODS FOR SITES INVESTIGATED

Site	Layer Thickness (m)	Velocity (m/s)	Density (gm/m^3)	Damping Ratio	Period (sec)		
					Low	Mean	High
K31	1.5	163.7	1.90	0.025	2.00	2.67	2.67
	11.0	183.2	1.95	0.23			
	16.2	289.0	2.00	0.017			
	43.9	326.8	2.10	0.015			
	375.6	736.6	2.20	0.008			
		1158.5	2.50	0.005			
K32	2.7	88.7	1.80	0.035	2.00	2.67	2.67
	12.5	165.9	1.90	0.025			
	42.4	336.3	2.00	0.015			
	18.6	571.6	2.10	0.009			
	378.0	731.7	2.20	0.008			
		1158.5	2.50	0.005			
K34	7.0	151.8	1.90	0.026	0.44	0.53	0.67
	12.8	455.2	2.10	0.012			
	57.3	580.5	2.20	0.009			
		1158.5	2.50	0.005			
K35	2.4	250.3	1.95	0.019	0.53	0.67	0.80
	9.8	376.5	2.00	0.013			
	64.9	555.5	2.10	0.010			
	24.1	759.8	2.20	0.007			
		1158.5	2.50	0.005			

TABLE 2 (CONTINUED)

SOIL COLUMN THICKNESSES, SHEAR-WAVE VELOCITIES, AND DYNAMIC SITE PERIODS FOR SITES INVESTIGATED

Site	Layer Thickness (m)	Velocity (m/s)	Density (gm/m^3)	Damping Ratio	Period (sec)		
					Low	Mean	High
K36	3.0	118.3	1.90	0.030	0.73	0.89	1.14
	95.1	523.5	2.10	0.010			
	46.0	744.8	2.20	0.008			
		1158.5	2.50	0.005			
K37	1.5	131.1	1.90	0.029	0.62	0.73	0.89
	30.2	429.3	2.10	0.012			
	105.2	731.4	2.20	0.008			
		1158.5	2.50	0.005			
K38	8.5	106.4	1.90	0.032	0.57	0.73	0.89
	8.2	531.4	2.10	0.010			
	101.2	660.1	2.20	0.008			
		1158.5	2.50	0.005			
K40	2.7	163.7	1.90	0.025	0.80	1.00	1.14
	21.0	285.4	2.00	0.017			
	28.0	481.7	2.10	0.011			
	87.2	593.3	2.20	0.009			
		1158.5	2.50	0.005			
K41	3.4	136.9	1.90	0.028	0.67	0.80	1.00
	27.4	304.0	1.95	0.016			
	36.0	339.9	2.00	0.015			
		1158.5	2.50	0.005			

TABLE 2 (CONTINUED)

SOIL COLUMN THICKNESSES, SHEAR-WAVE VELOCITIES, AND DYNAMIC SITE PERIODS FOR SITES INVESTIGATED

Site	Layer Thickness (m)	Velocity (m/s)	Density (gm/m³)	Damping Ratio	Period (sec)		
					Low	Mean	High
K42	2.4	152.4	1.90	0.026	0.33	0.40	0.50
	32.3	531.7	2.10	0.010			
	36.9	744.8	2.20	0.008			
		1158.5	2.50	0.005			
K43	2.1	152.4	1.90	0.026	0.57	0.73	0.89
	13.4	359.1	2.00	0.010			
	115.2	731.7	2.20	0.008			
		1158.5	2.50	0.005			
K44	9.5	214.0	1.95	0.021	0.80	1.00	1.14
	11.3	322.6	2.00	0.015			
	68.0	441.2	2.10	0.012			
	33.2	620.4	2.20	0.009			
		1158.5	2.50	0.005			
K46	5.5	164.6	1.90	0.025	0.89	1.00	1.33
	9.1	376.5	2.00	0.013			
	76.8	426.8	2.10	0.012			
	65.9	732.3	2.20	0.008			
		1158.5	2.50	0.005			

TABLE 2 (CONTINUED)

SOIL COLUMN THICKNESSES, SHEAR-WAVE VELOCITIES, AND DYNAMIC SITE PERIODS FOR SITES INVESTIGATED

Site	Layer Thickness (m)	Velocity (m/s)	Density (gm/m^3)	Damping Ratio	Period (sec)		
					Low	Mean	High
K47	2.4	131.1	1.90	0.029	1.00	1.33	1.60
	26.2	505.5	2.10	0.011			
	176.5	657.3	2.20	0.008			
		1158.5	2.50	0.005			
K48	1.8	177.1	1.90	0.024	1.33	1.60	2.00
	10.1	336.3	2.00	0.015			
	52.1	434.5	2.05	0.012			
	70.4	683.5	2.10	0.008			
	143.0	731.7	2.20	0.008			
		1158.5	2.50	0.005			
K49	2.7	163.4	1.90	0.025	1.14	1.60	2.00
	71.6	425.6	2.00	0.012			
	70.7	683.5	2.10	0.008			
	117.1	731.7	2.20	0.008			
		1158.5	2.50	0.005			
K50	3.0	224.7	1.95	0.020	1.33	1.60	2.00
	31.1	371.3	2.00	0.014			
	39.0	514.9	2.10	0.010			
	79.3	670.7	2.15	0.008			
	135.7	731.7	2.20	0.008			
		1158.5	2.50	0.005			

TABLE 2 (CONTINUED)

SOIL COLUMN THICKNESSES, SHEAR-WAVE VELOCITIES, AND DYNAMIC SITE PERIODS FOR SITES INVESTIGATED

Site	Layer Thickness (m)	Velocity (m/s)	Density (gm/m^3)	Damping Ratio	Period (sec)		
					Low	Mean	High
K51	2.1	125.3	1.90	0.029	1.60	2.00	2.67
	43.6	480.2	2.00	0.011			
	61.0	688.7	2.10	0.008			
	274.4	731.7	2.20	0.008			
		1158.5	2.50	0.005			
K52	5.5	120.4	1.90	0.030	1.33	1.60	2.00
	12.8	236.9	1.95	0.019			
	18.3	335.4	2.00	0.015			
	36.6	554.3	2.10	0.010			
	98.2	612.2	2.15	0.009			
		731.7	2.20	0.008			
K53	6.1	168.0	1.95	0.024	1.60	2.00	2.00
	35.7	368.9	2.00	0.014			
	77.4	637.5	2.10	0.009			
	211.9	731.7	2.20	0.008			
		1158.5	2.50	0.005			

TABLE 2 (CONTINUED)

SOIL COLUMN THICKNESSES, SHEAR-WAVE VELOCITIES, AND DYNAMIC SITE PERIODS FOR SITES INVESTIGATED

Site	Layer Thickness (m)	Velocity (m/s)	Density (gm/m^3)	Damping Ratio	Period (sec)		
					Low	Mean	High
K54	3.4	193.3	1.90	0.022	0.89	1.14	1.33
	19.5	398.8	2.00	0.013			
	97.0	519.8	2.10	0.010			
	32.6	590.9	2.20	0.009			
		1158.5	2.50	0.005			
K55	7.3	274.4	2.00	0.017	0.80	1.00	1.33
	69.8	791.2	2.10	0.011			
	75.0	625.6	2.20	0.009			
		1158.5	2.50	0.005			
K57	4.0	141.8	1.90	0.027	1.33	1.60	2.00
	10.7	277.1	2.00	0.017			
	31.1	415.9	2.10	0.012			
	25.9	668.6	2.15	0.008			
	242.4	731.7	2.20	0.008			
		1158.5	2.50	0.005			
K58	7.3	146.3	1.90	0.027	0.80	1.00	1.14
	41.5	625.0	2.10	0.009			
	127.7	733.8	2.20	0.008			
		1158.5	2.50	0.005			

TABLE 2 (CONTINUED)

SOIL COLUMN THICKNESSES, SHEAR-WAVE VELOCITIES, AND DYNAMIC SITE PERIODS FOR SITES INVESTIGATED

Site	Layer Thickness (m)	Velocity (m/s)	Density (gm/m^3)	Damping Ratio	Period (sec)		
					Low	Mean	High
K59	1.8	255.8	1.95	0.018	0.62	0.73	0.89
	5.2	384.5	2.00	0.013			
	77.1	858.4	2.10	0.009			
	44.8	759.8	2.20	0.007			
		1158.5	2.50	0.005			
K60	10.7	129.0	1.90	0.029	1.60	2.00	2.00
	25.3	551.2	2.10	0.010			
	306.1	762.2	2.20	0.007			
		1158.5	2.50	0.005			
K61	6.7	187.5	1.95	0.023	1.60	2.00	2.00
	36.9	414.6	2.00	0.012			
	30.5	632.3	2.10	0.009			
	267.4	751.2	2.20	0.007			
		1158.5	2.50	0.005			
K62	7.3	120.4	1.90	0.030	1.33	1.60	2.00
	27.4	475.6	2.00	0.011			
	36.9	532.0	2.10	0.010			
	300.3	866.2	2.20	0.007			
		1158.5	2.50	0.005			

TABLE 2 (CONTINUED)

SOIL COLUMN THICKNESSES, SHEAR-WAVE VELOCITIES, AND DYNAMIC SITE PERIODS FOR SITES INVESTIGATED

Site	Layer Thickness (m)	Velocity (m/s)	Density (gm/m^3)	Damping Ratio	Period (sec)		
					Low	Mean	High
K64	0.9	212.5	1.95	0.021	2.00	2.00	2.67
	14.3	255.2	2.00	0.018			
	27.7	491.2	2.10	0.011			
	45.1	591.2	2.15	0.009			
	320.4	731.7	2.20	0.008			
		1158.5	2.50	0.005			
K65	3.7	118.3	1.85	0.030	1.60	2.00	2.67
	15.9	172.3	1.95	0.024			
	4.0	455.8	2.05	0.012			
	49.1	532.0	2.10	0.010			
	282.6	731.7	2.20	0.008			
		1158.5	2.50	0.005			
K66	5.2	182.3	1.95	0.023	1.33	1.60	2.00
	32.0	317.1	2.00	0.015			
	29.6	579.9	2.10	0.009			
	254.6	731.7	2.20	0.008			
		1158.5	2.50	0.005			

TABLE 2 (CONTINUED)

SOIL COLUMN THICKNESSES, SHEAR-WAVE VELOCITIES, AND DYNAMIC SITE PERIODS FOR SITES INVESTIGATED

Site	Layer Thickness (m)	Velocity (m/s)	Density (gm/m^3)	Damping Ratio	Period (sec)		
					Low	Mean	High
K67	6.1	118.3	1.85	0.030	2.00	2.67	2.67
	25.3	268.3	1.95	0.018			
	36.6	439.3	2.00	0.012			
	32.9	533.5	2.05	0.010			
	168.6	632.3	2.10	0.009			
	189.3	731.7	2.20	0.008			
		1158.5	2.50	0.005			
K68	5.8	182.9	1.90	0.023	1.60	2.00	2.67
	58.8	341.5	2.00	0.015			
	97.6	531.4	2.10	0.010			
	218.9	731.7	2.20	0.008			
		1158.5	2.50	0.005			
K69	4.3	202.4	1.90	0.022	1.14	1.33	1.60
	38.4	384.1	2.00	0.013			
	55.8	531.7	2.10	0.010			
	154.6	731.7	2.20	0.008			
		1158.5	2.50	0.005			

TABLE 2 (CONTINUED)

SOIL COLUMN THICKNESSES, SHEAR-WAVE VELOCITIES, AND DYNAMIC SITE PERIODS FOR SITES INVESTIGATED

Site	Layer Thickness (m)	Velocity (m/s)	Density (gm/m^3)	Damping Ratio	Period (sec)		
					Low	Mean	High
K70	3.0	193.6	1.95	0.022	0.73	0.89	1.14
	85.7	486.3	2.10	0.011			
	60.7	773.2	2.20	0.007			
		1158.5	2.50	0.005			
K71	2.7	192.7	1.95	0.022	0.89	1.14	1.33
	29.0	300.3	2.00	0.016			
	73.2	439.9	2.10	0.012			
	51.5	709.1	2.20	0.008			
		1158.5	2.50	0.005			
K72	6.7	176.8	1.90	0.024	0.53	0.67	0.80
	104.3	827.1	2.20	0.007			
	32.3	884.1	2.30	0.006			
		1158.5	2.50	0.005			
K73	4.0	235.4	1.95	0.019	0.62	0.80	1.00
	20.7	432.9	2.10	0.012			
	104.9	665.2	2.20	0.008			
		1158.5	2.50	0.005			

TABLE 2 (CONTINUED)

SOIL COLUMN THICKNESSES, SHEAR-WAVE VELOCITIES, AND DYNAMIC SITE PERIODS FOR SITES INVESTIGATED

Site	Layer Thickness (m)	Velocity (m/s)	Density (gm/m³)	Damping Ratio	Period (sec)		
					Low	Mean	High
K74	2.1	121.6	1.90	0.030	0.50	0.62	0.73
	10.1	414.9	2.10	0.012			
	109.8	786.3	2.20	0.007			
		1158.5	2.50	0.005			
K78	4.9	216.2	1.95	0.021	0.67	0.80	1.00
	150.6	759.8	2.20	0.007			
		1158.5	2.50	0.005			
K79	10.7	158.5	1.90	0.025	2.00	2.67	2.67
	9.1	293.3	1.95	0.016			
	20.1	360.4	2.00	0.014			
	91.5	497.6	2.10	0.011			
	339.6	731.7	2.20	0.008			
		1158.5	2.50	0.005			
K80	4.3	122.0	1.85	0.030	1.33	1.60	2.00
	28.4	316.8	1.95	0.015			
	85.4	354.6	2.00	0.014			
	55.8	476.2	2.10	0.011			
		1158.5	2.50	0.005			

TABLE 2 (CONTINUED)

SOIL COLUMN THICKNESSES, SHEAR-WAVE VELOCITIES, AND DYNAMIC SITE PERIODS FOR SITES INVESTIGATED

Site	Layer Thickness (m)	Velocity (m/s)	Density (gm/m^3)	Damping Ratio	Period (sec)		
					Low	Mean	High
K81	12.5	170.7	1.90	0.024	0.62	0.80	1.00
	37.8	451.2	2.00	0.012			
	58.5	580.2	2.20	0.009			
		1158.5	2.50	0.005			
K82	4.3	92.4	1.85	0.035	0.67	0.80	1.00
	36.9	360.1	2.00	0.014			
	75.0	609.8	2.20	0.009			
		1158.5	2.50	0.005			
K83	7.0	121.6	1.85	0.030	0.73	0.89	1.14
	7.9	278.0	1.95	0.017			
	62.5	377.4	2.00	0.013			
	31.4	719.2	2.20	0.008			
		1158.5	2.50	0.005			
K84	8.8	182.6	1.90	0.023	1.00	1.14	1.60
	30.2	330.2	2.00	0.015			
	36.3	356.7	2.10	0.014			
	42.4	404.6	2.20	0.013			
		1158.5	2.50	0.005			

TABLE 3

TYPE AND SOURCE OF DATA USED TO ESTIMATE THE DEPTH TO BEDROCK IN THE STUDY AREA

1. Depths to bedrock based on drill hole logs in the Jackson Purchase Region, as summarized in Dart (1992):

County	Latitude (°N)	Longitude (°W)	Elevation With Respect to Sea Level (m)
Fulton	36.5208	89.3238	-518
Fulton	36.5316	89.3374	-508
Fulton	36.5478	89.2818	-491
Fulton	36.5455	88.8886	-381
Ballard	37.0704	88.9747	-2
Ballard	37.0844	89.1160	-7
Calloway	36.5737	88.2155	41
Calloway	36.6490	88.3729	-36
Calloway	36.5646	88.1632	61
Calloway	36.5616	88.1680	4
Carlisle	36.8250	89.0916	-253
Carlisle	36.9052	88.8843	-124
Graves	36.6866	88.5007	-127
Graves	36.7826	88.8072	-251
Graves	36.9174	88.6815	-73
McCracken	36.9800	88.5000	2
McCracken	37.0338	88.6270	-15
McCracken	37.0219	88.5587	-6

TABLE 3 (CONTINUED)

TYPE AND SOURCE OF DATA USED TO ESTIMATE THE DEPTH TO BEDROCK IN THE STUDY AREA

1. Depths to bedrock based on drill hole logs in the Jackson Purchase Region, as summarized in Dart (1992) (continued):

County	Latitude (°N)	Longitude (°W)	Elevation With Respect to Sea Level (m)
McCracken	37.0062	88.5315	-28
McCracken	37.0768	88.5985	2
Marshall	36.7598	88.4151	-36
Marshall	36.9503	88.3846	34

2. Depths to bedrock based on P-wave soundings in the Jackson Purchase Region.

Site Designation*	Latitude (°N)	Longitude (°W)	Elevation (m)
B	36.775	89.067	-344
C	36.783	89.021	-366
E	36.803	88.954	-260
H	36.793	88.814	-230
K	36.739	88.515	-263
N	36.799	88.739	-212
P	36.811	88.567	-124
V	36.733	88.406	-60
W	36.743	88.369	-15
X	36.772	88.339	10

* From Al-Yazdi (1994).

TABLE 3 (CONTINUED)

TYPE AND SOURCE OF DATA USED TO ESTIMATE THE DEPTH TO BEDROCK IN THE STUDY AREA

3. Depths to bedrock based on proprietary P-wave seismic reflection profiles in the Jackson Purchase Region (data being used with permission):

Site Designation*	Latitude (°N)	Longitude (°W)	Elevation (m)
1	36.840	88.863	-198
2	36.763	88.870	-202
3	36.692	88.870	-201
4	36.607	88.872	-245
5	36.567	89.154	-411
6	36.558	89.038	-369
7	36.550	88.975	-395
8	36.547	88.800	-289
9	36.547	88.727	-189
10	36.562	88.597	-143
11	36.570	88.430	-18

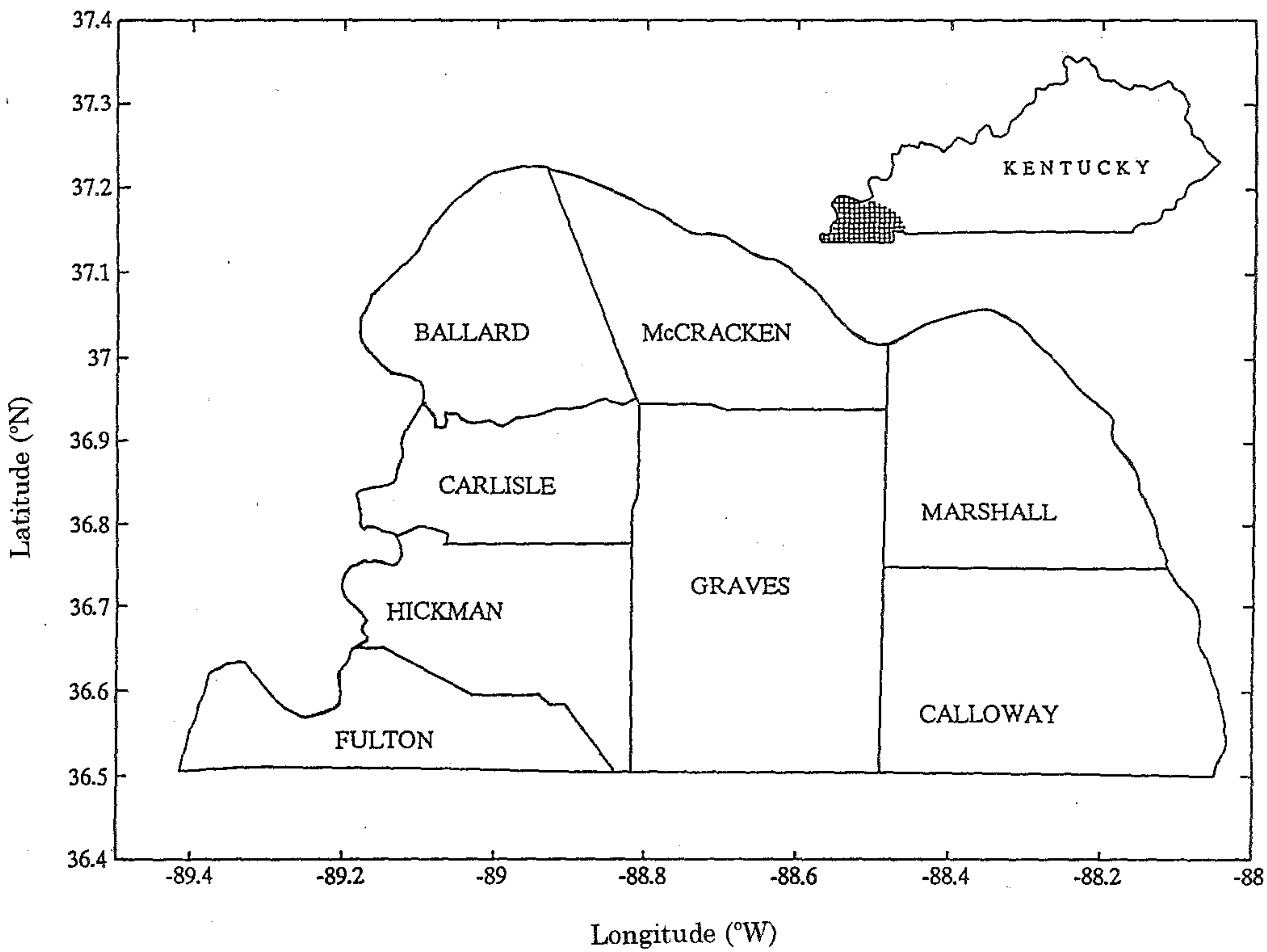

Figure 1. Map of the Jackson Purchase Region Showing County Lines.

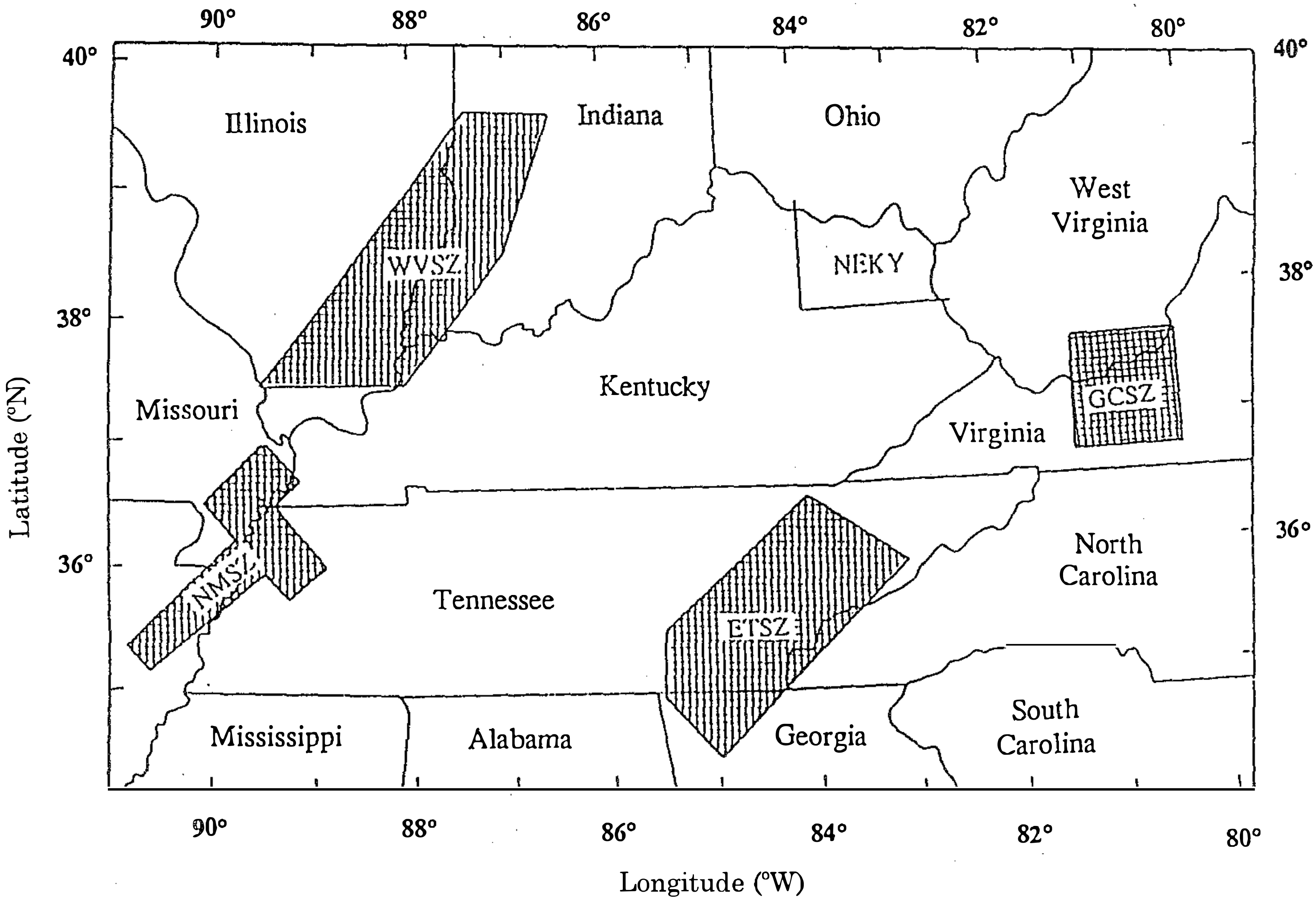

Figure 2. Map Showing the Geographic Locations of the New Madrid and Wabash Valley Seismic Zones.

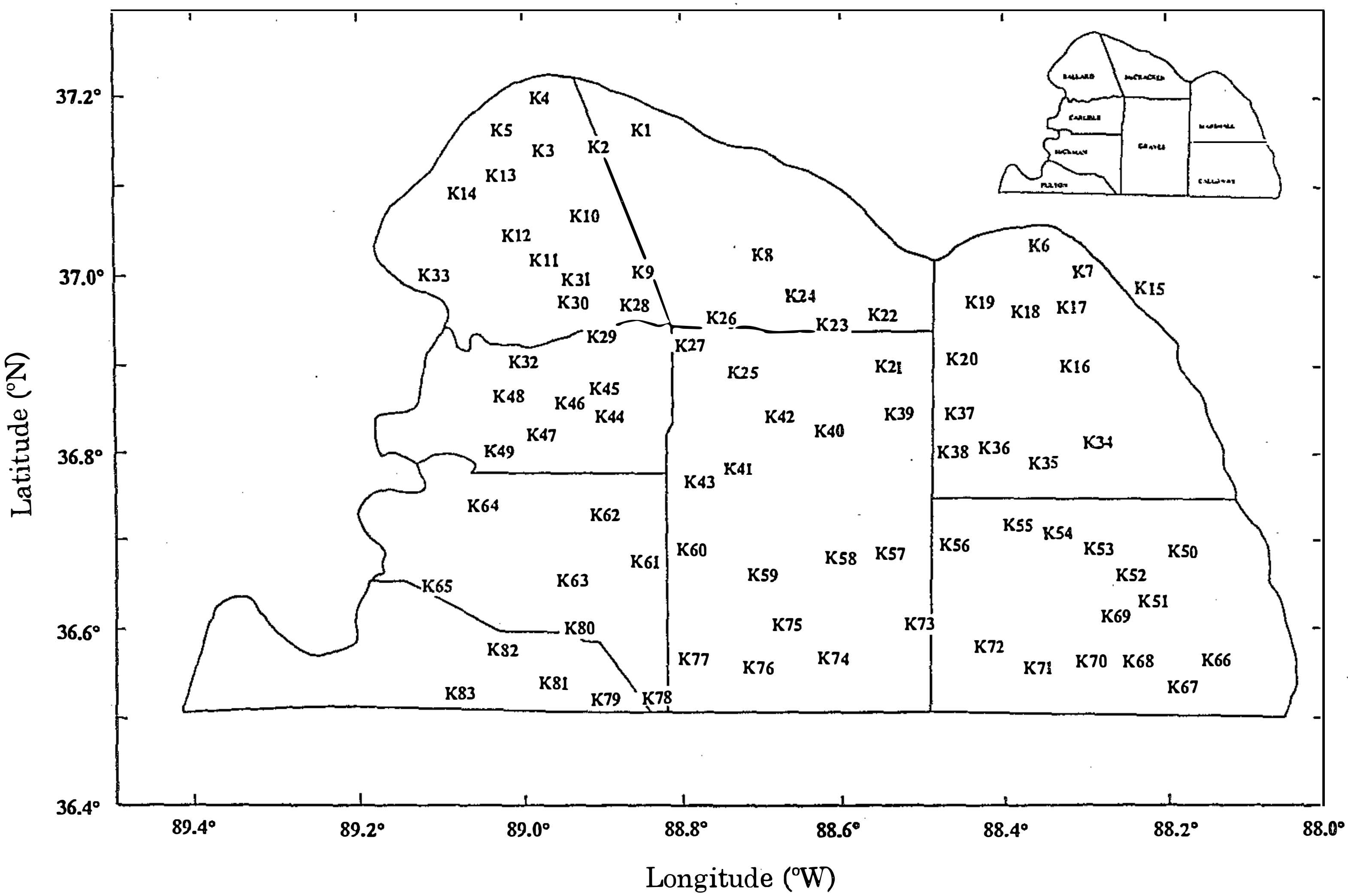

Figure 3. Map Showing Locations of Sites Investigated for the Study.

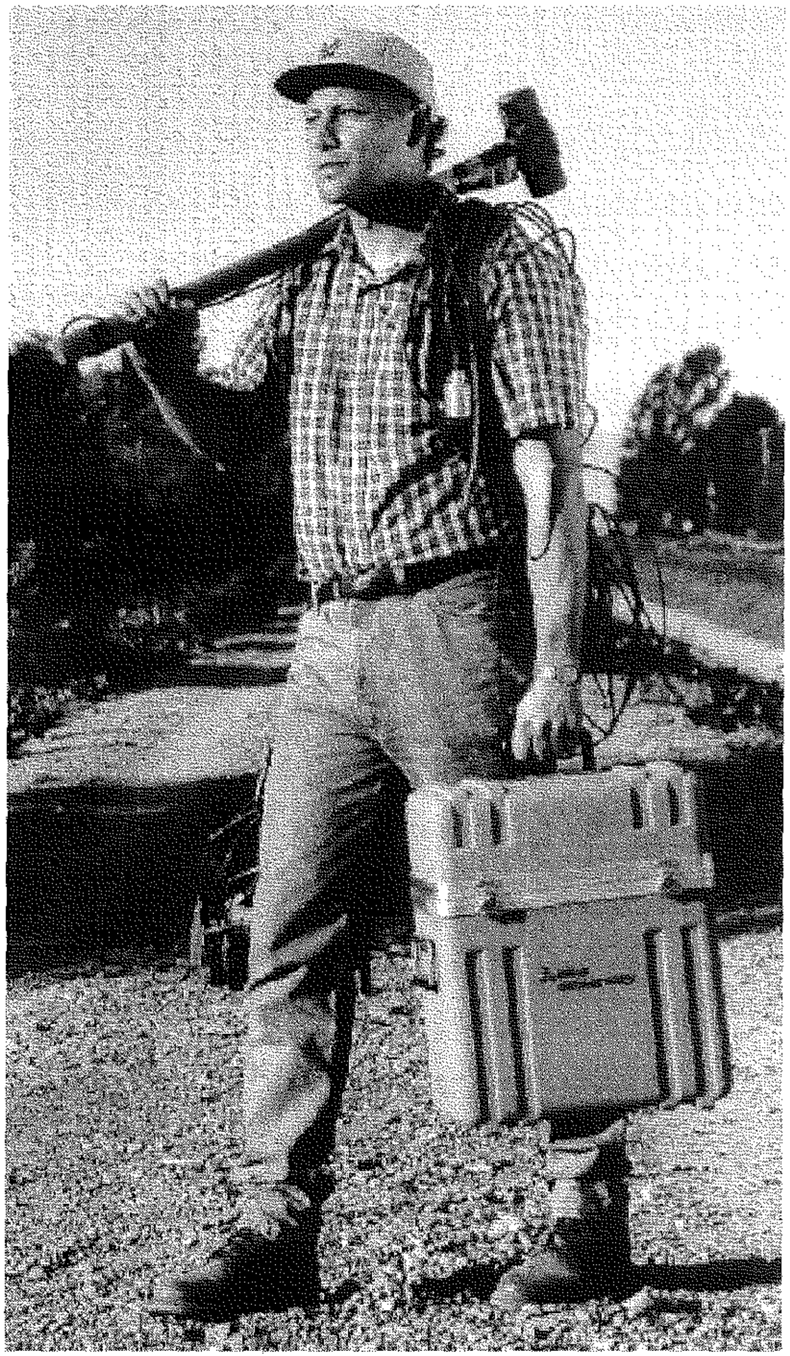

Figure 4. Typical Equipment Used on Site Investigations: Seismograph, Geophones, and Sledgehammer.

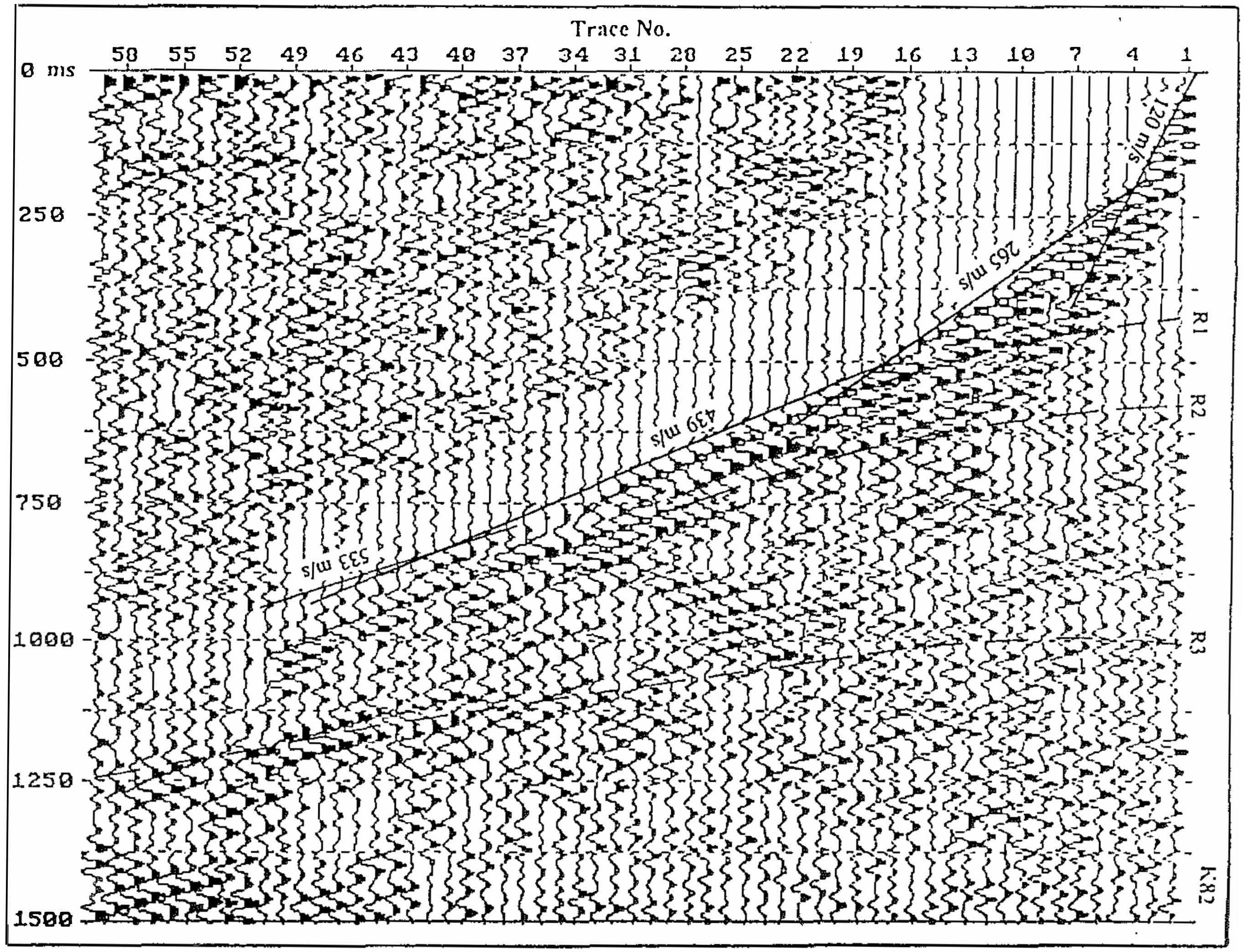

Figure 5. SH-wave Walkaway Seismic Section Obtained at Site K82.

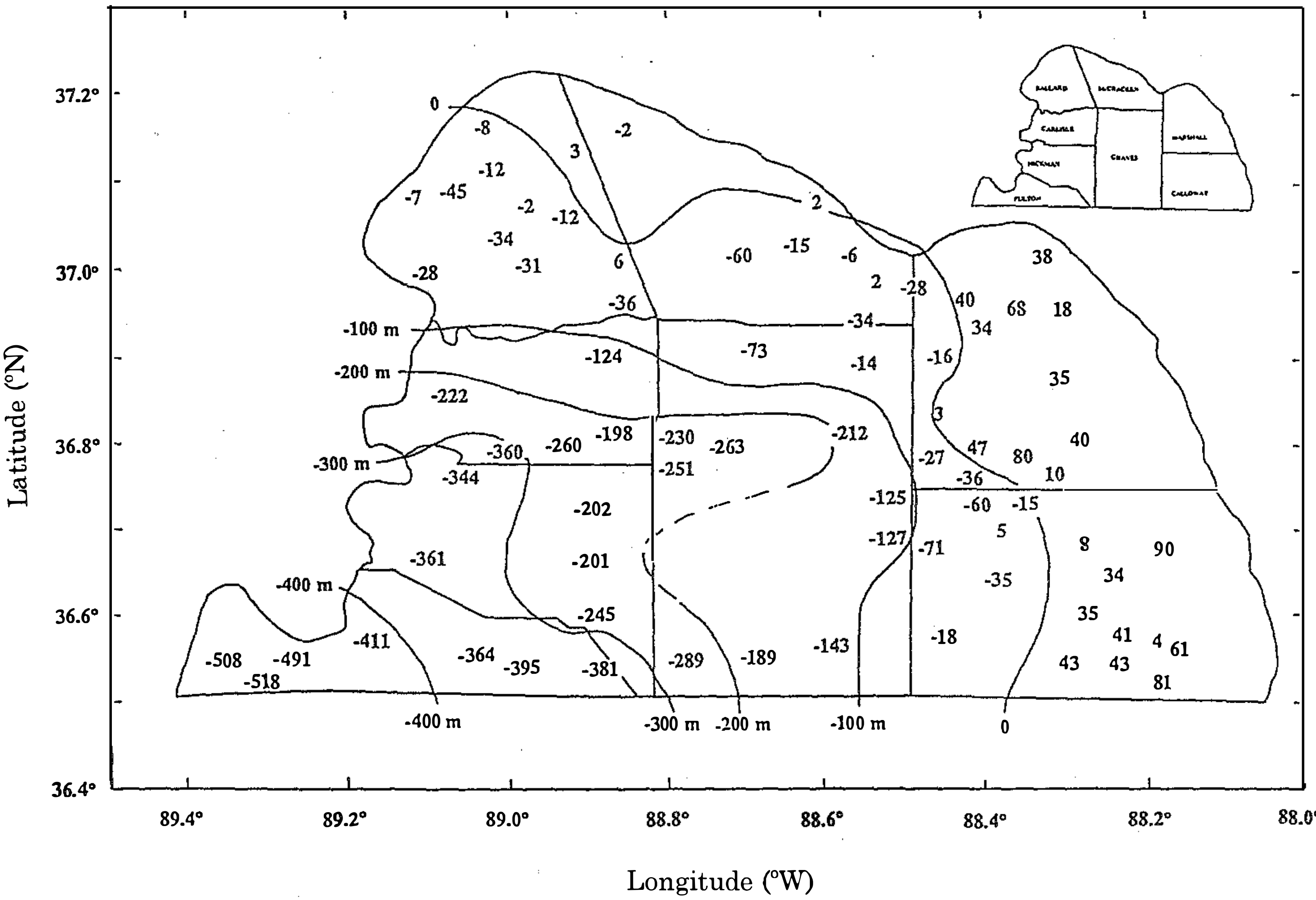

Figure 6. Contour Map of the Depths (m) to Bedrock in the Jackson Purchase Region.

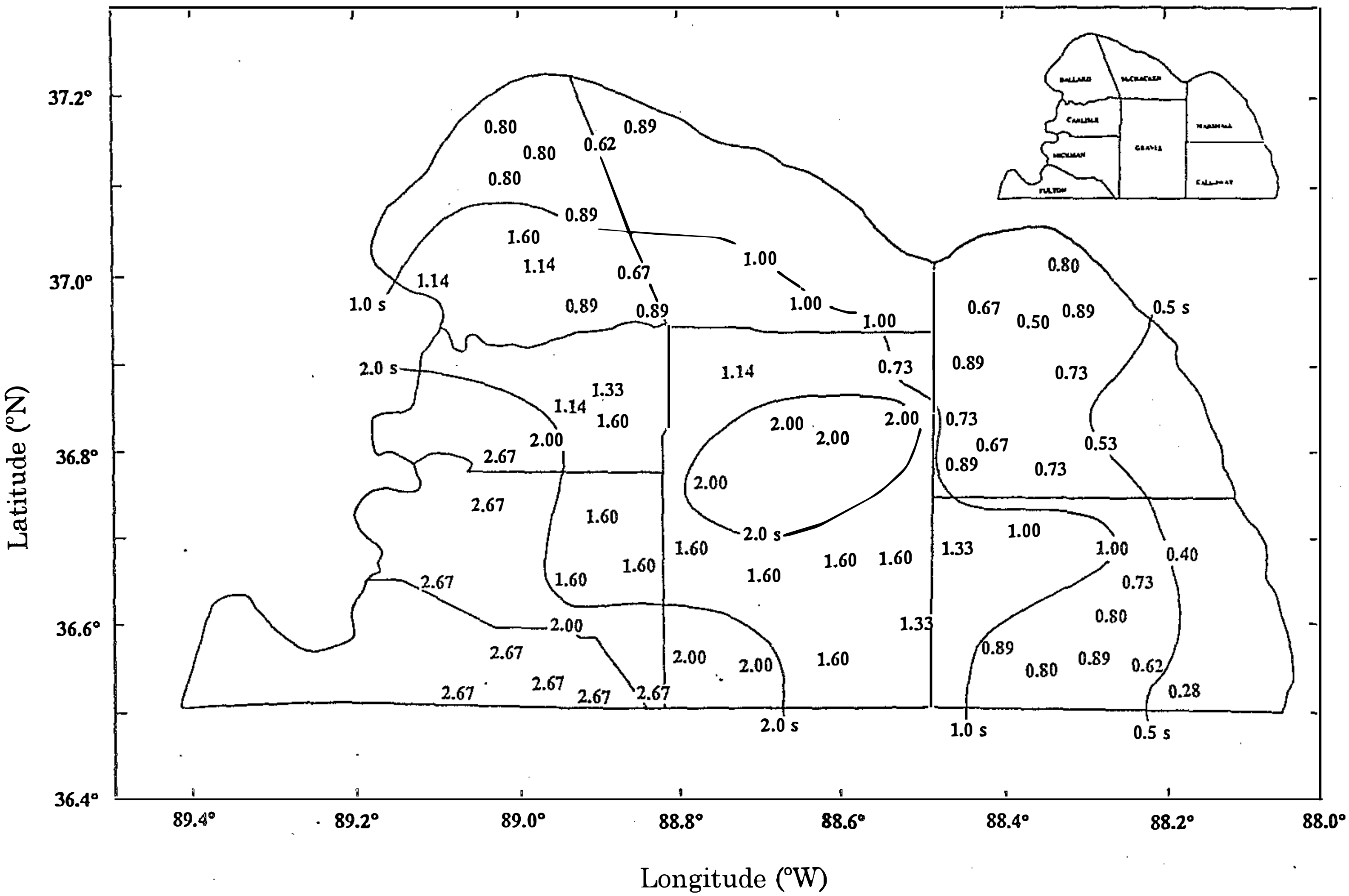

Figure 7. Contour Map of the Dynamic Site Periods for the Jackson Purchase Region.

APPENDIX A

SEISMIC SECTIONS USED FOR CALCULATING VELOCITIES

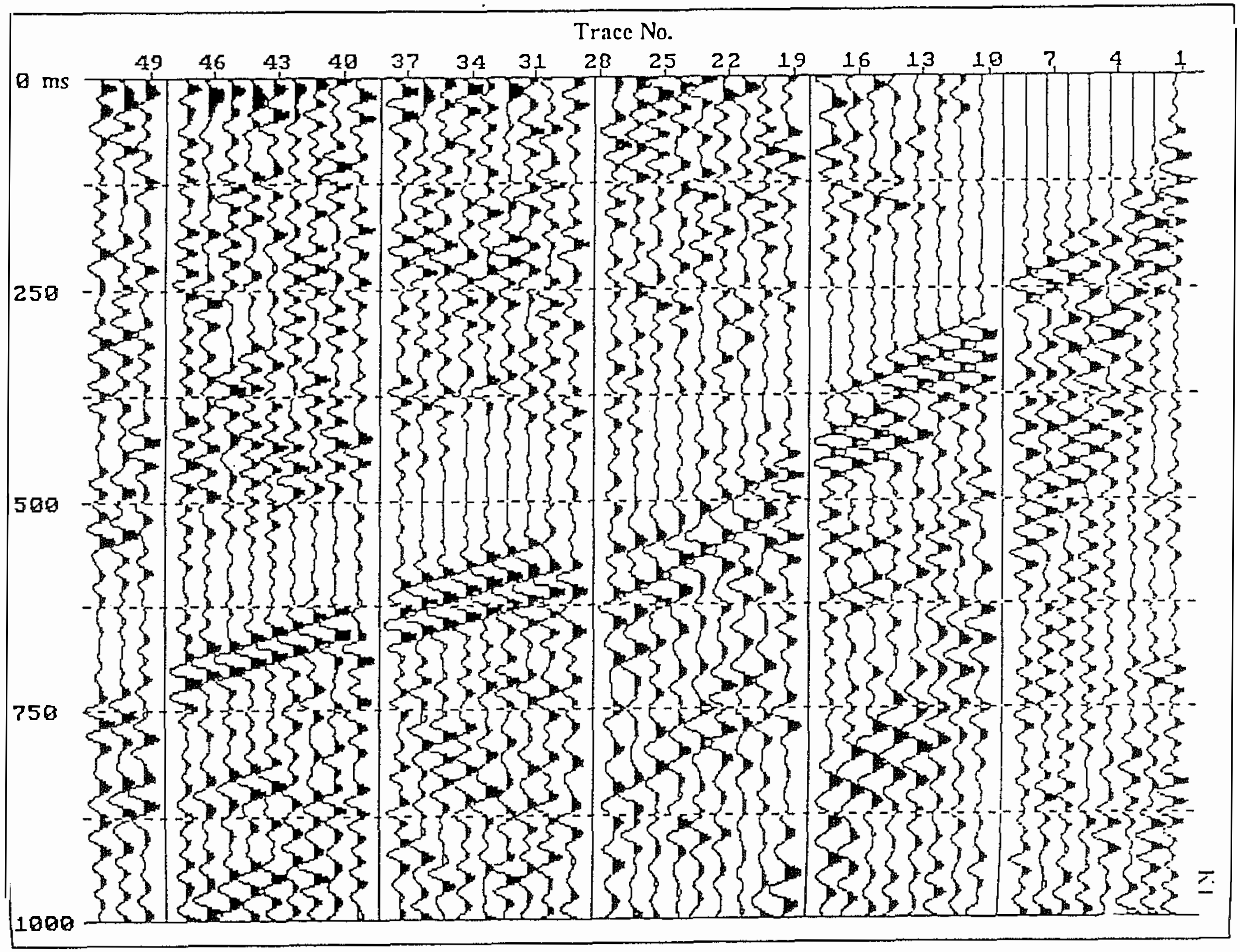

Figure A.1. Site K1 in McCracken County (Joppa Quadrangle).

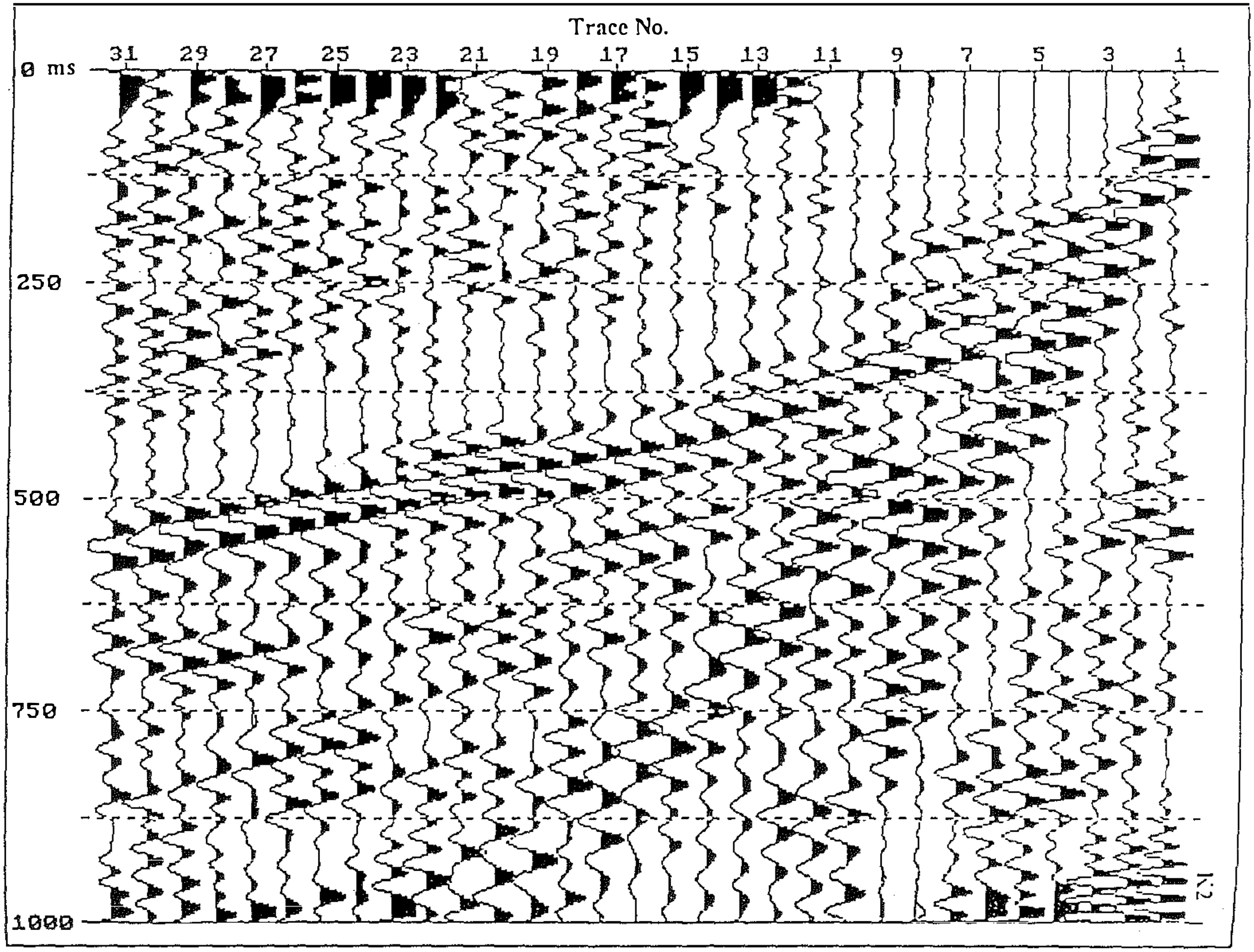

Figure A.2. Site K2 in Ballard County (Bandana Quadrangle).

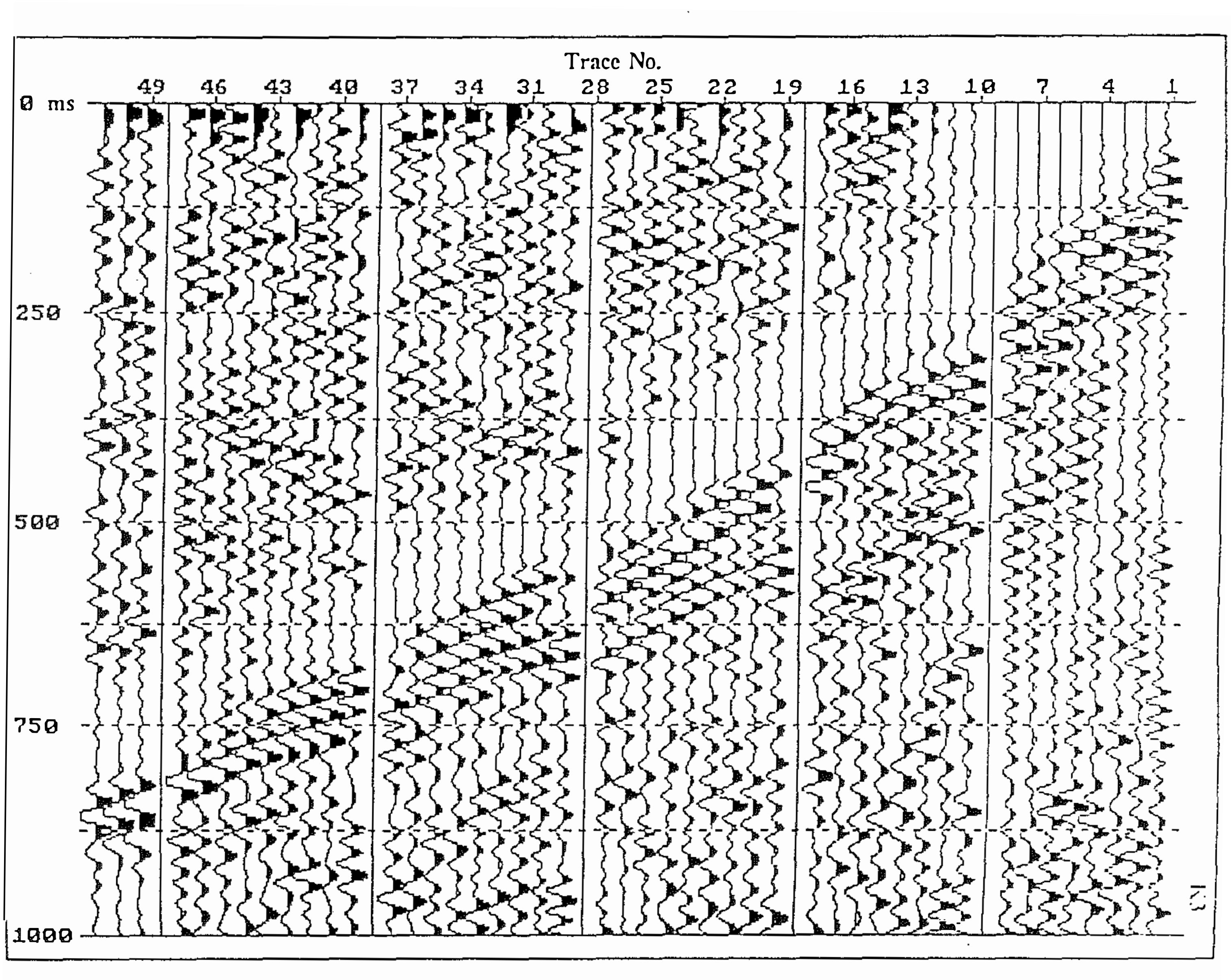

Figure A.3. Site K3 in Ballard County (Bandana Quadrangle).

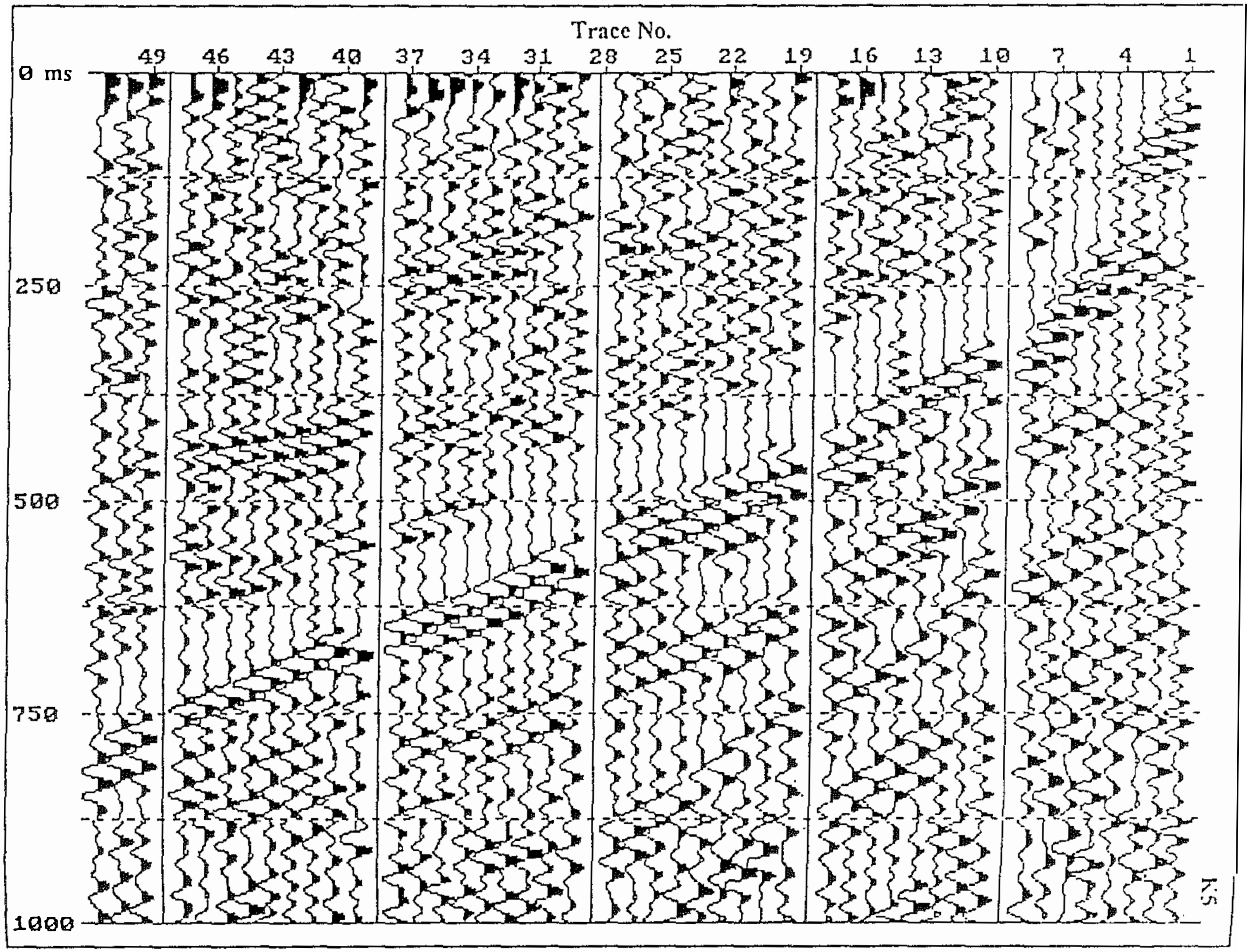

Figure A.4. Site K5 in Ballard County (Olmsted Quadrangle).

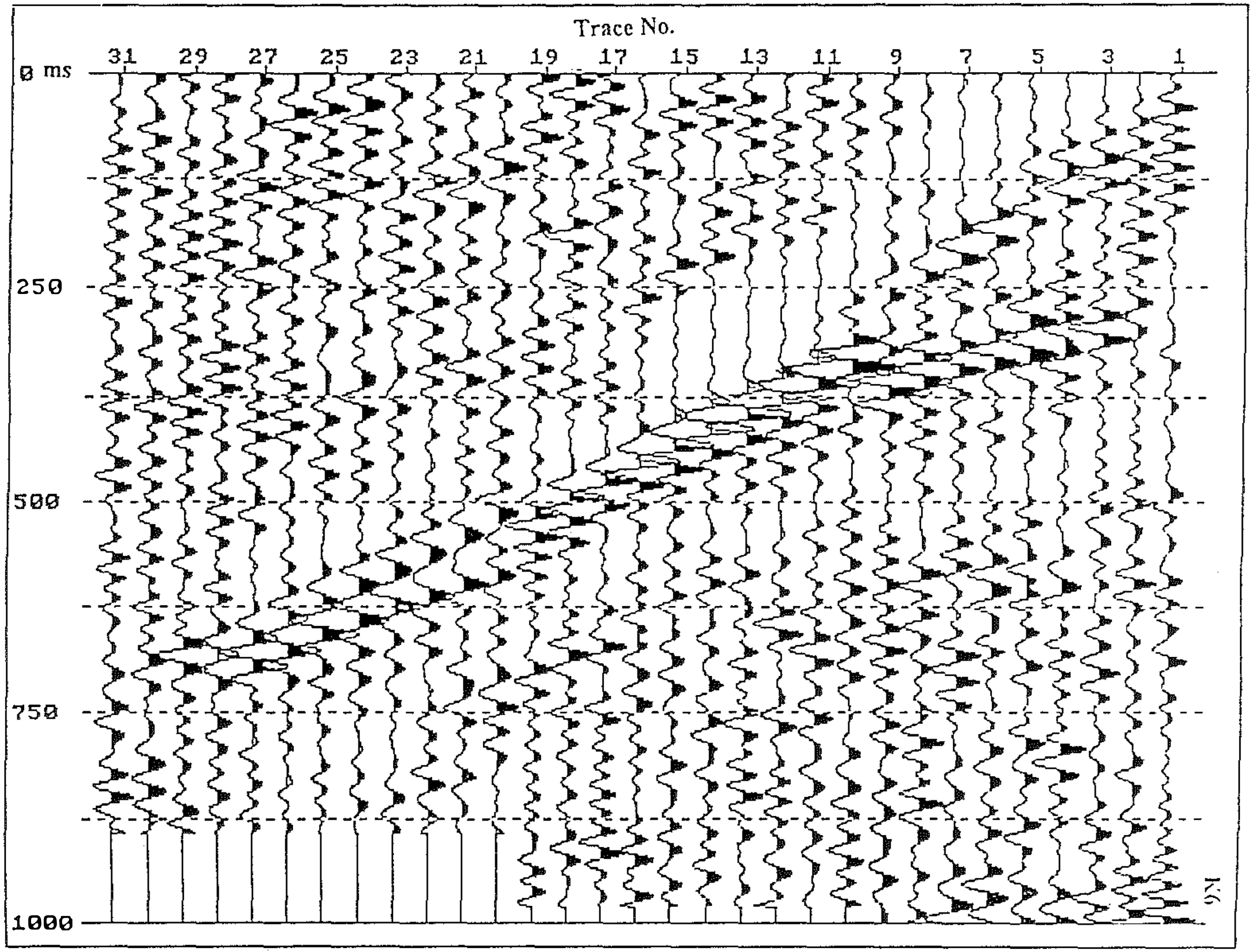

Figure A.5. Site K6 in Marshall County (Calvert City Quadrangle).

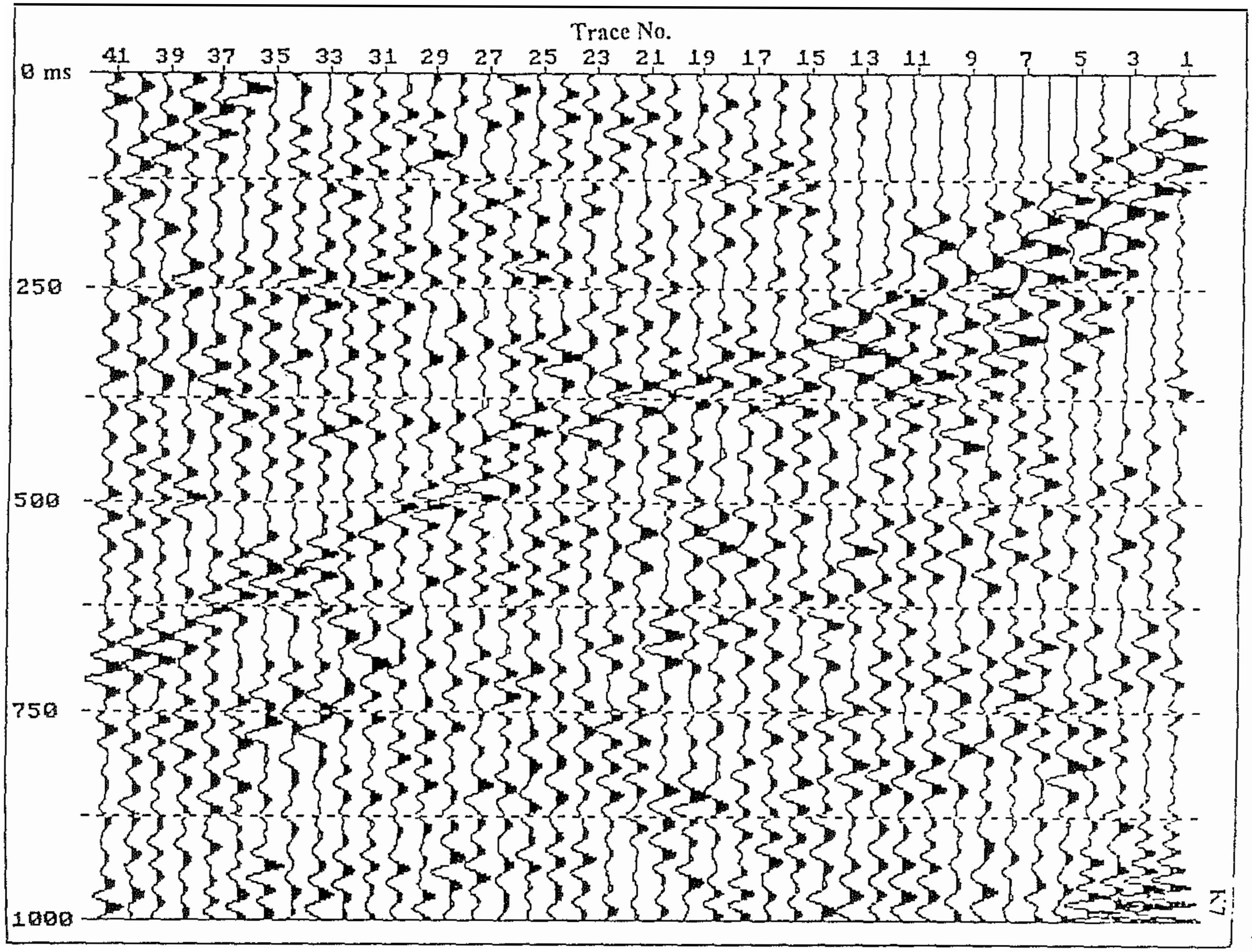

Figure A.6. Site K7 in Marshall County (Calvert City Quadrangle).

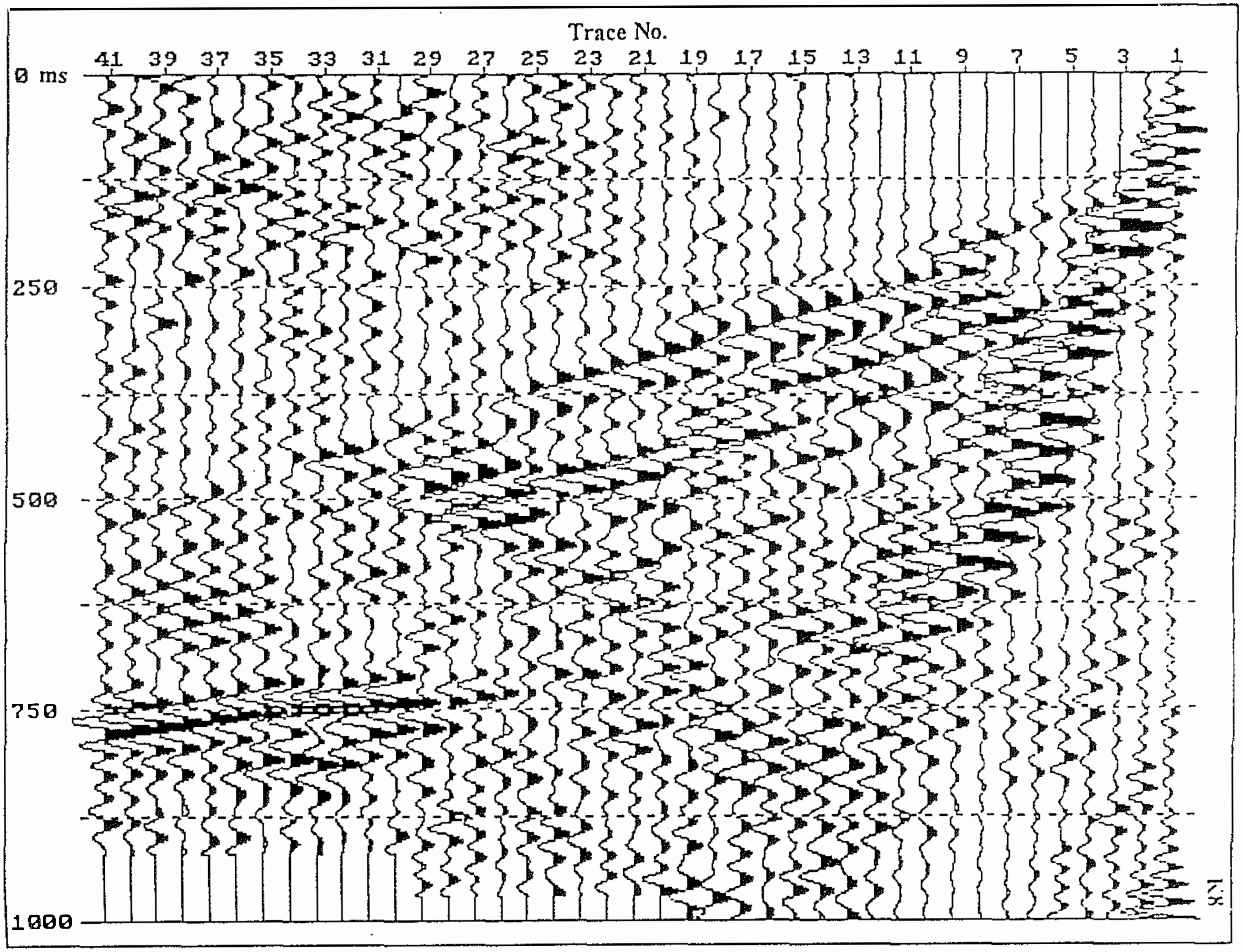

Figure A.7. Site K8 in McCracken County (Paducah West Quadrangle).

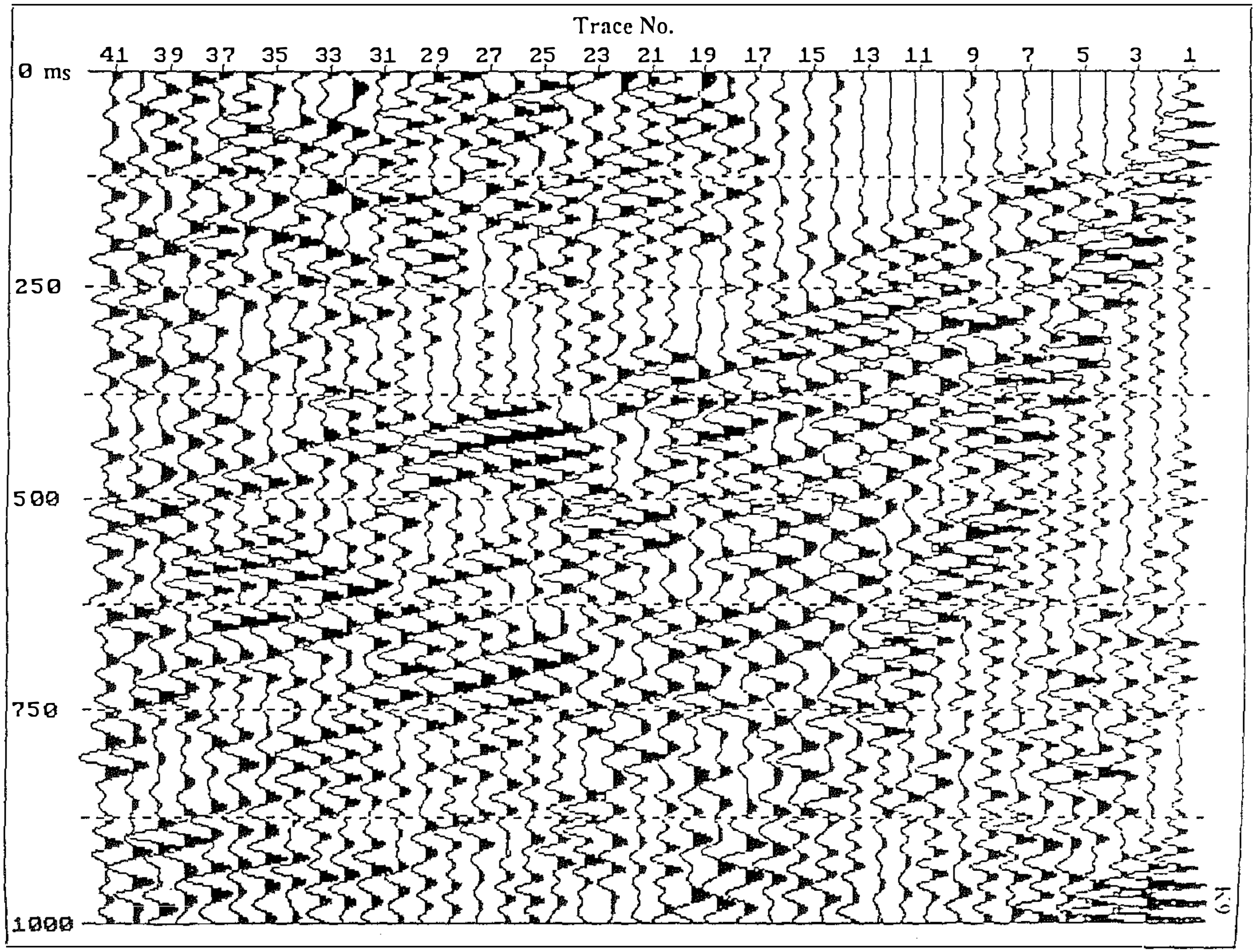

Figure A.8. Site K9 in Ballard County (Heath Quadrangle).

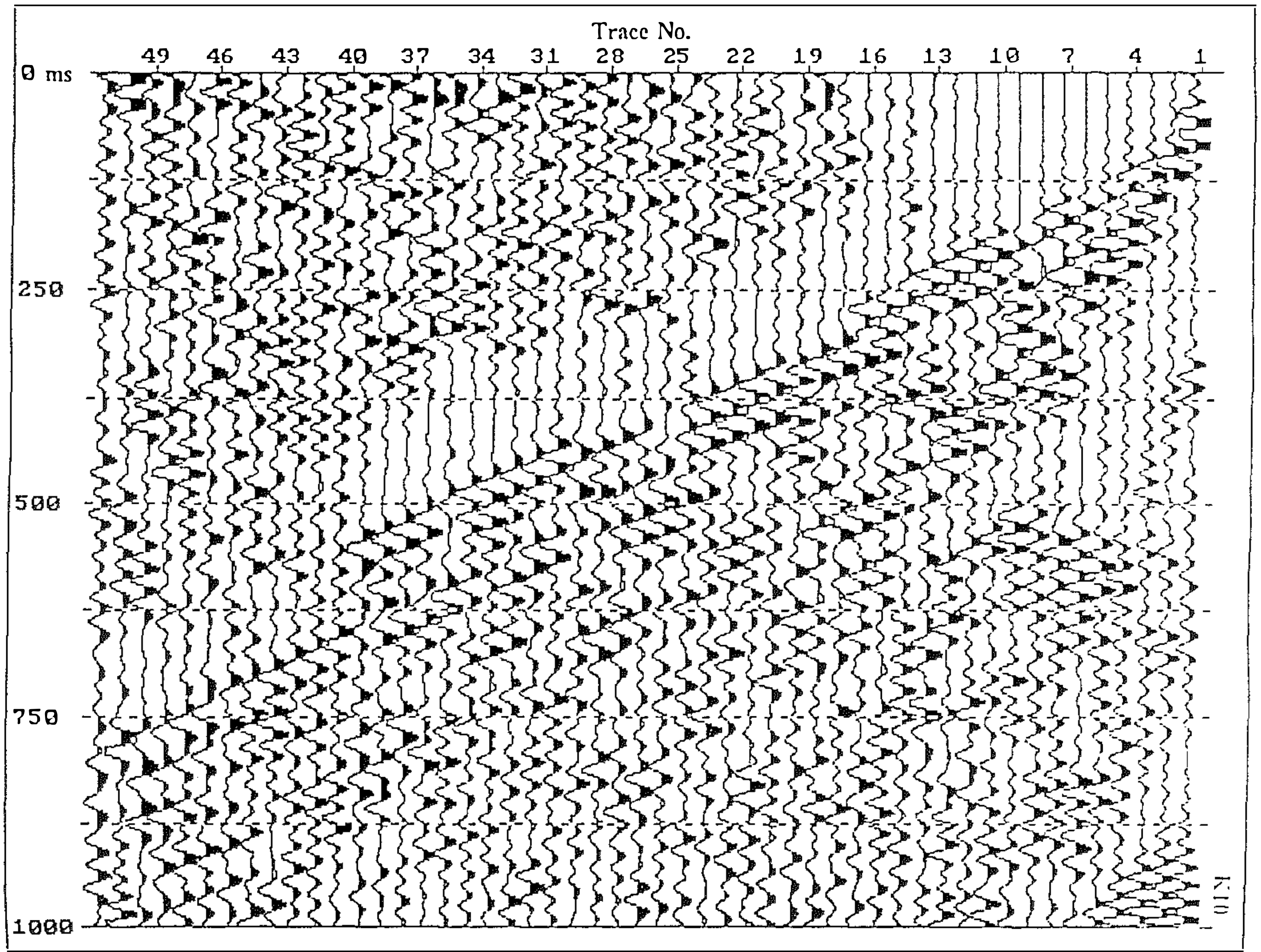

Figure A.9. Site K10 in Ballard County (LaCenter Quadrangle).

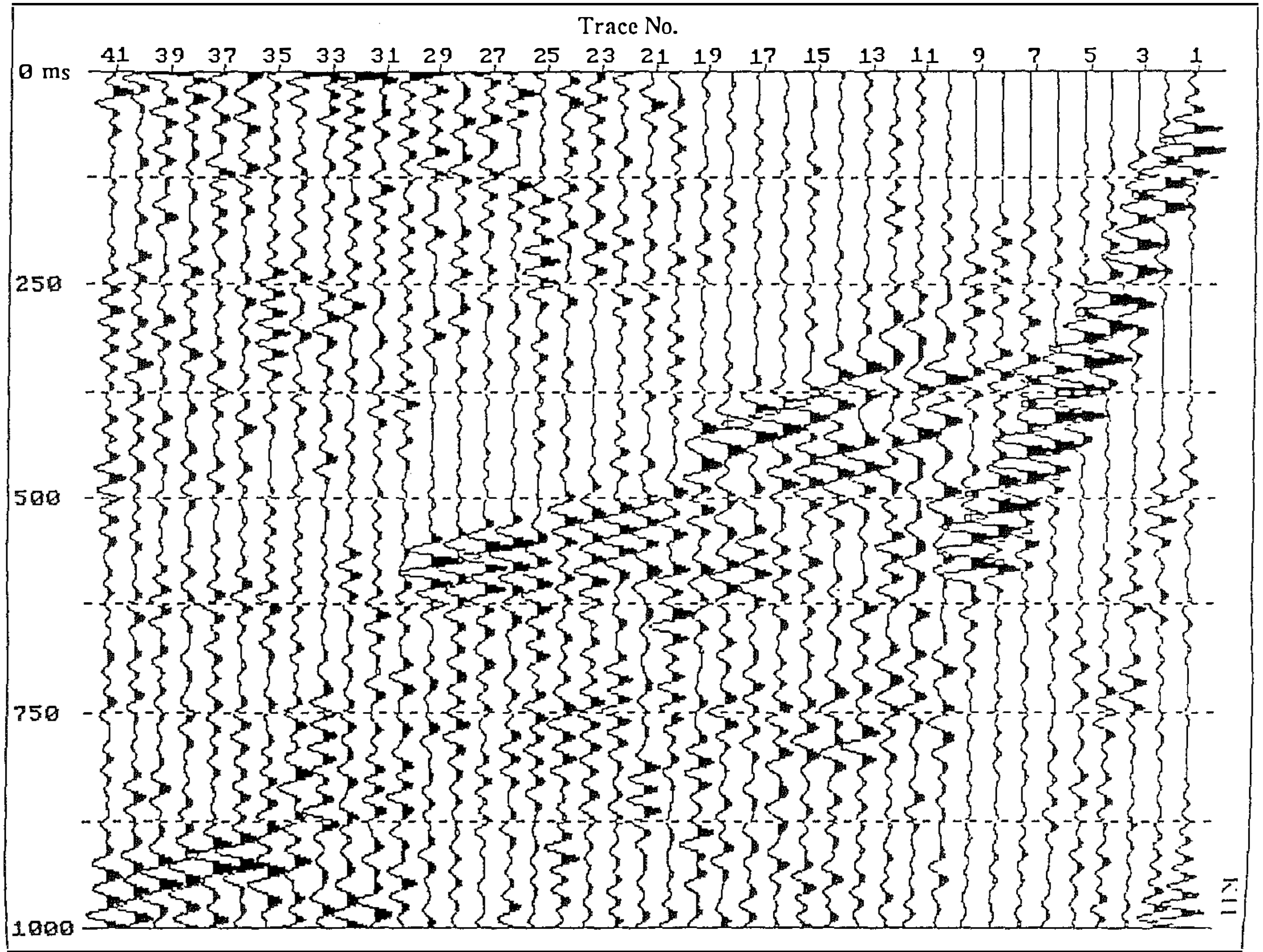

Figure A.10. Site K11 in Ballard County (LaCenter Quadrangle).

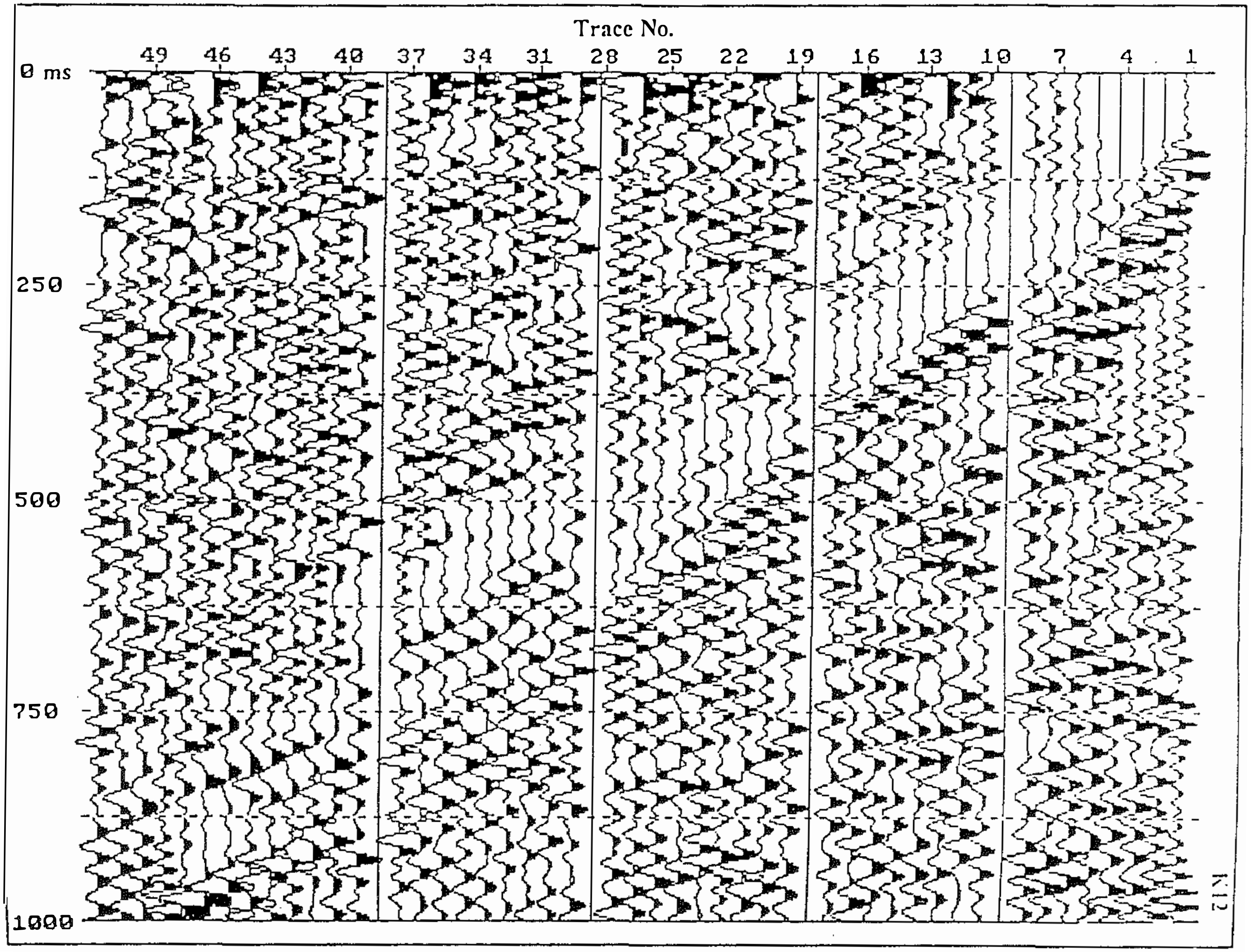

Figure A.11. Site K12 in Ballard County (Barlow Quadrangle).

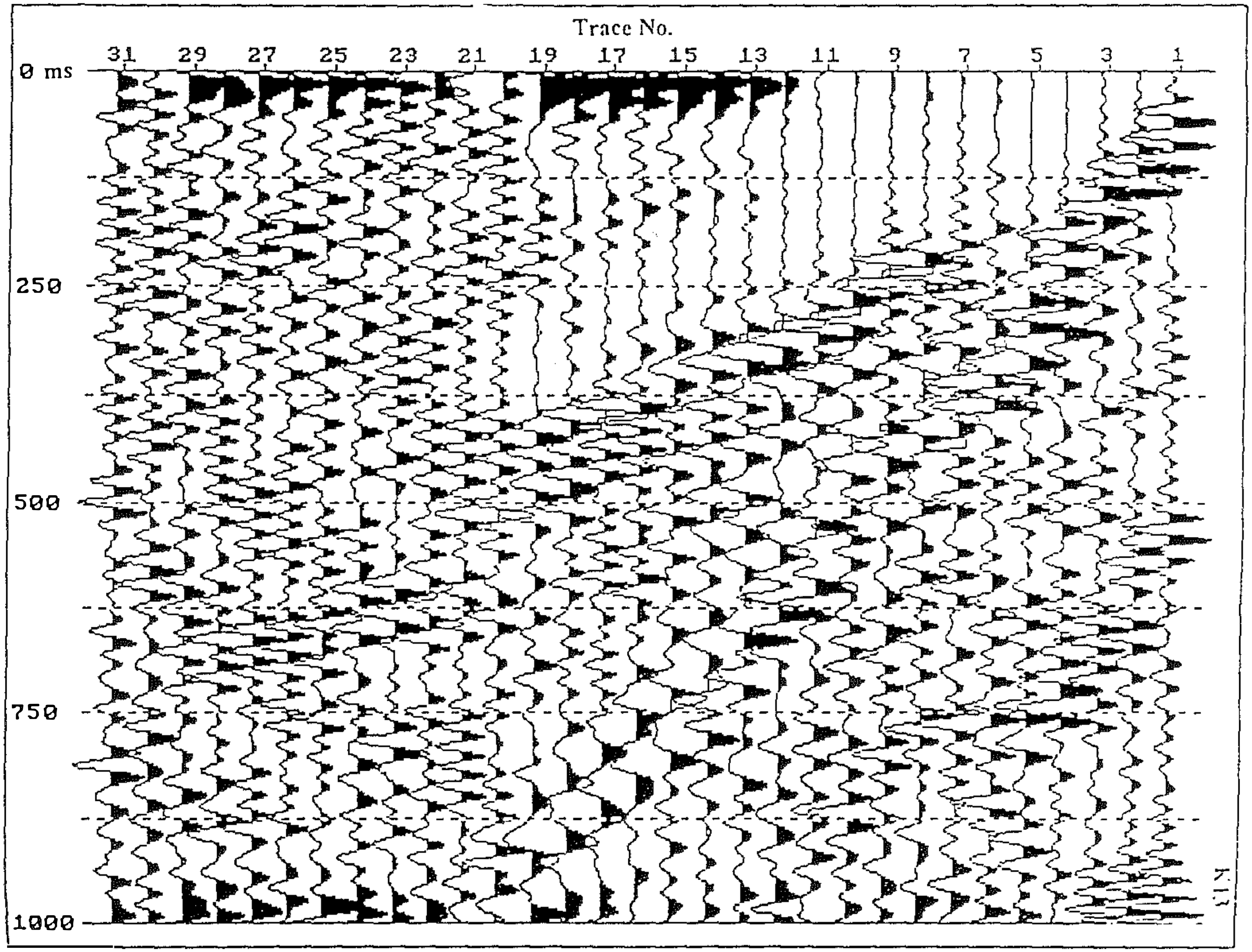

Figure A.12. Site K13 in Ballard County (Barlow Quadrangle).

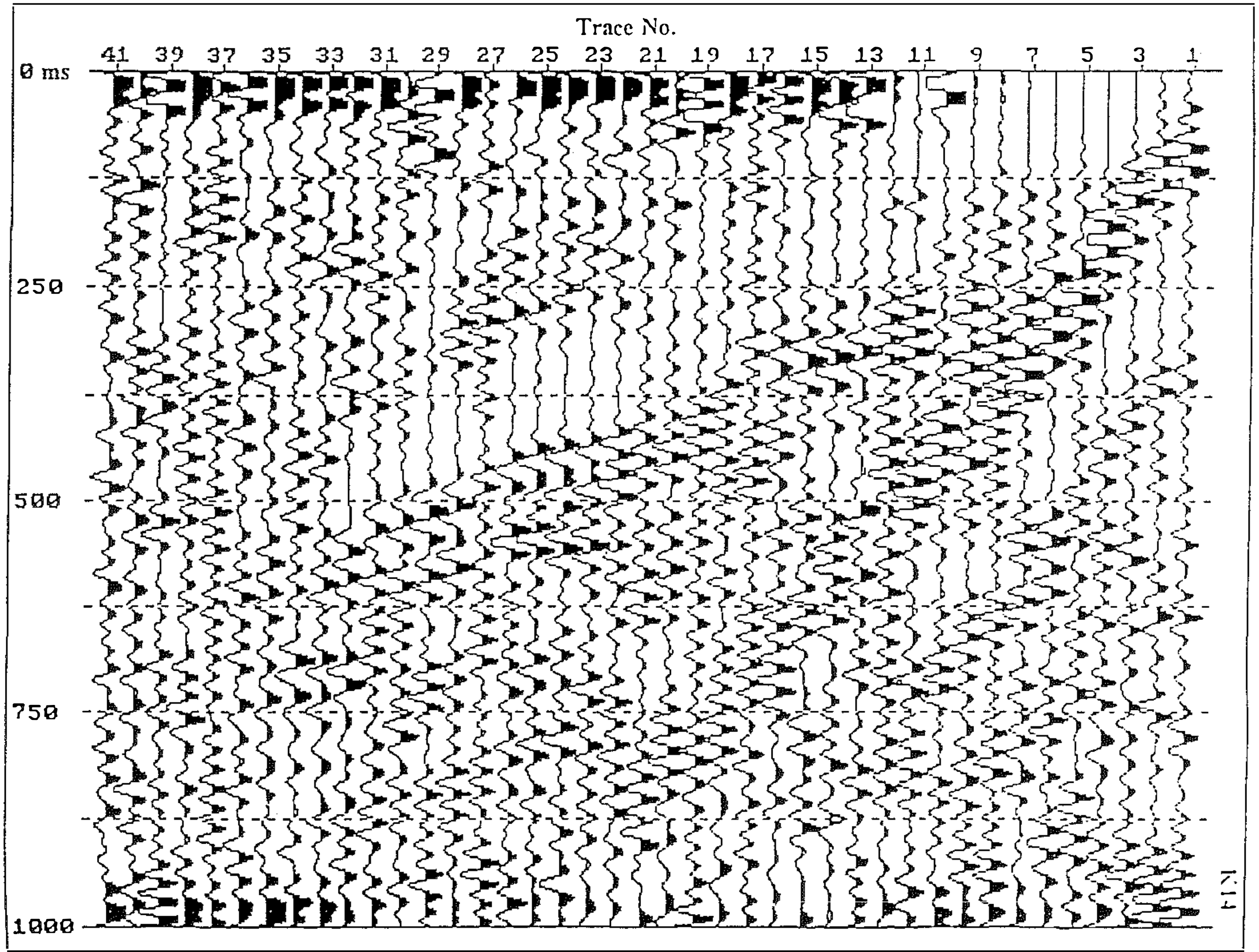

Figure A.13. Site K14 in Ballard County (Barlow Quadrangle).

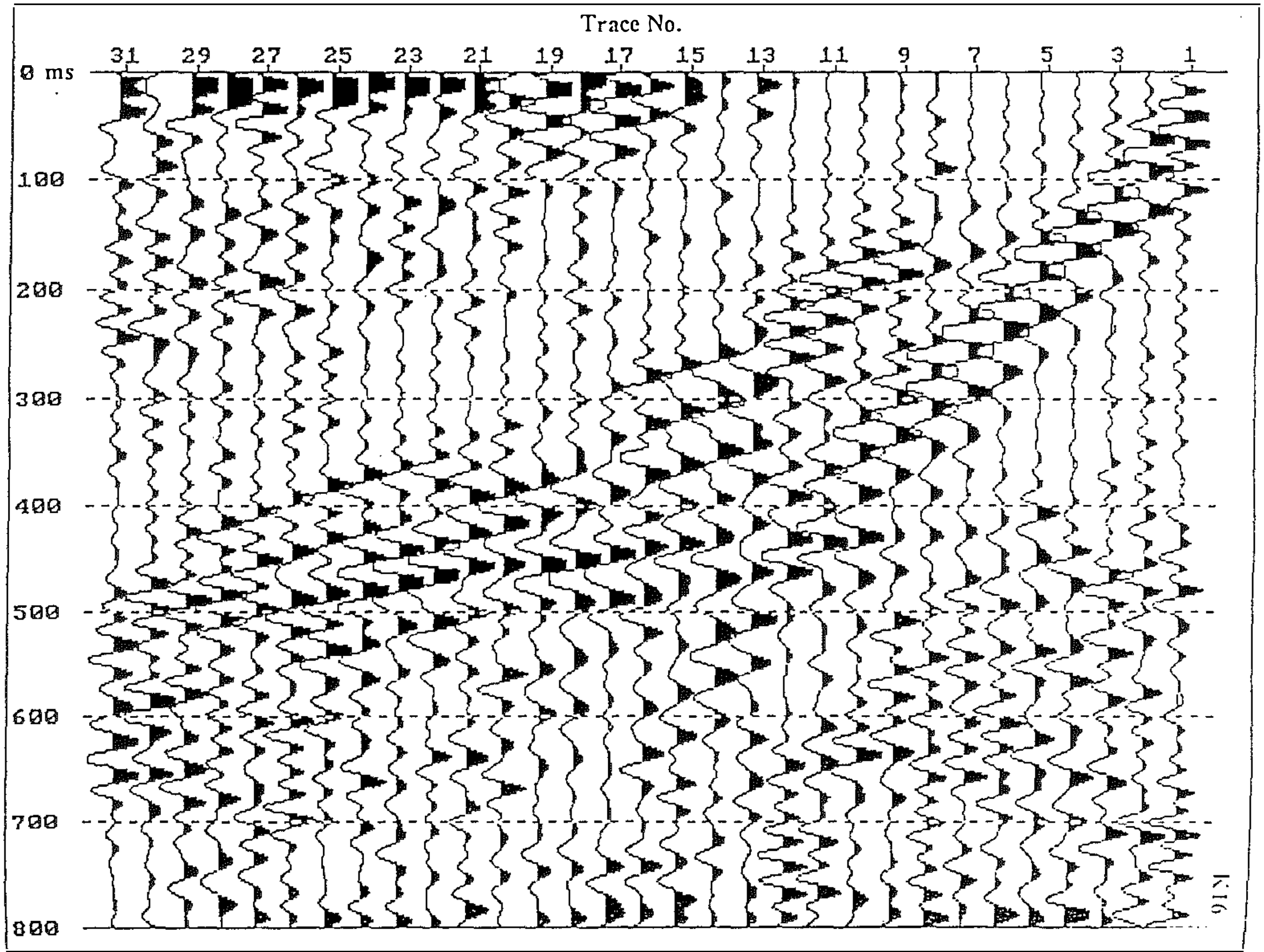

Figure A.14. Site K16 in Marshall County (Briensburg Quadrangle).

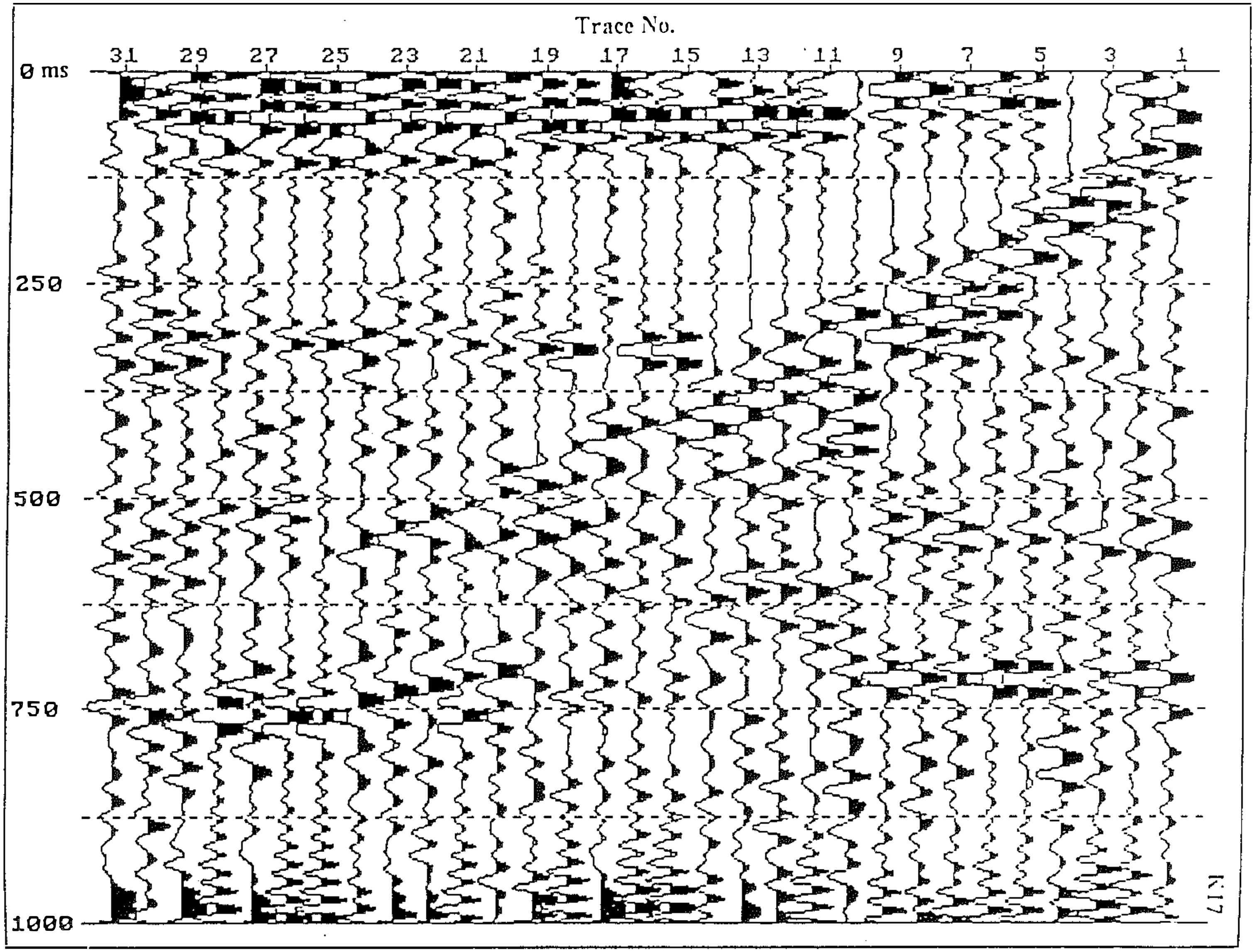

Figure A.15. Site K17 in Marshall County (Briensburg Quadrangle).

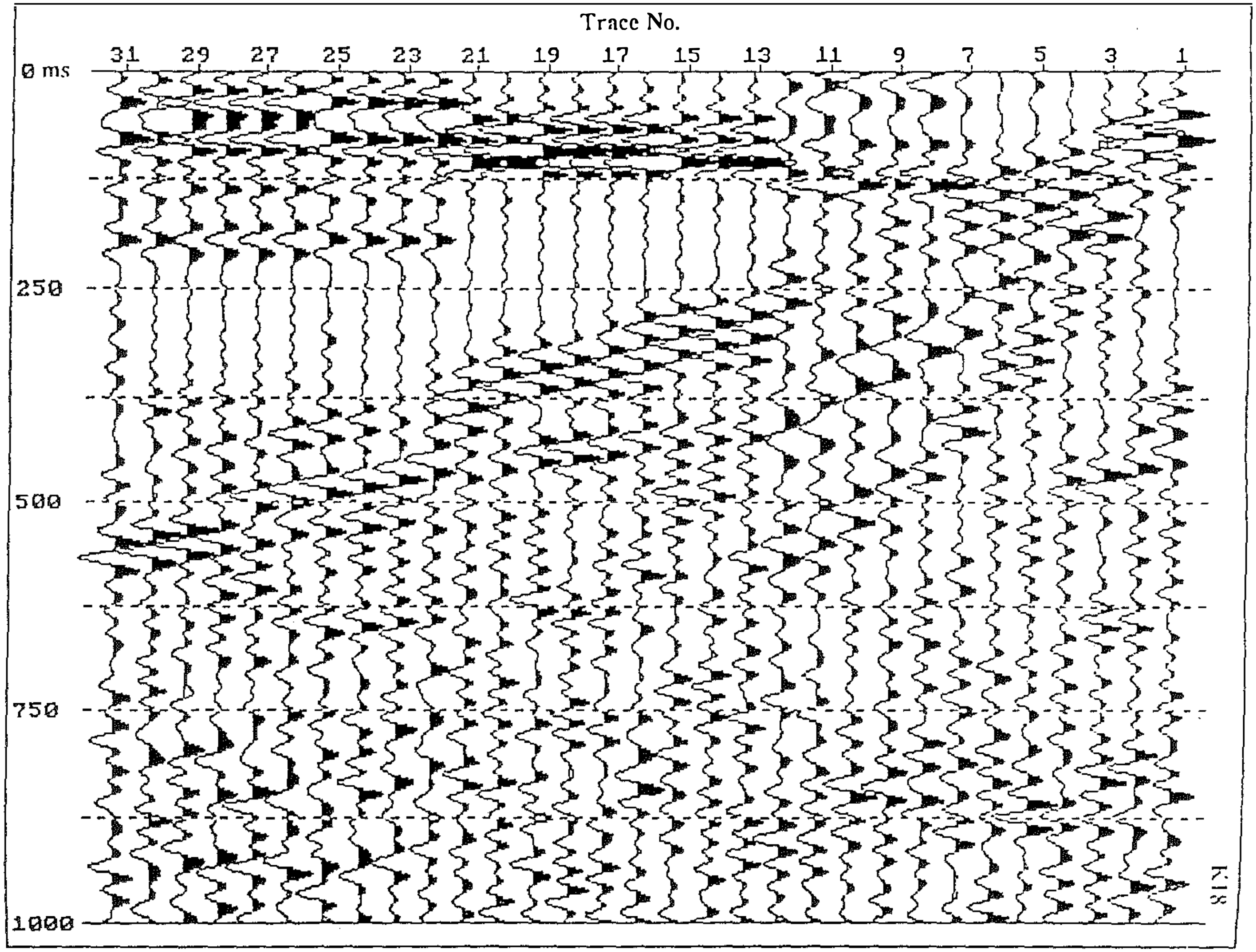

Figure A.16. Site K18 in Marshall County (Briensburg Quadrangle).

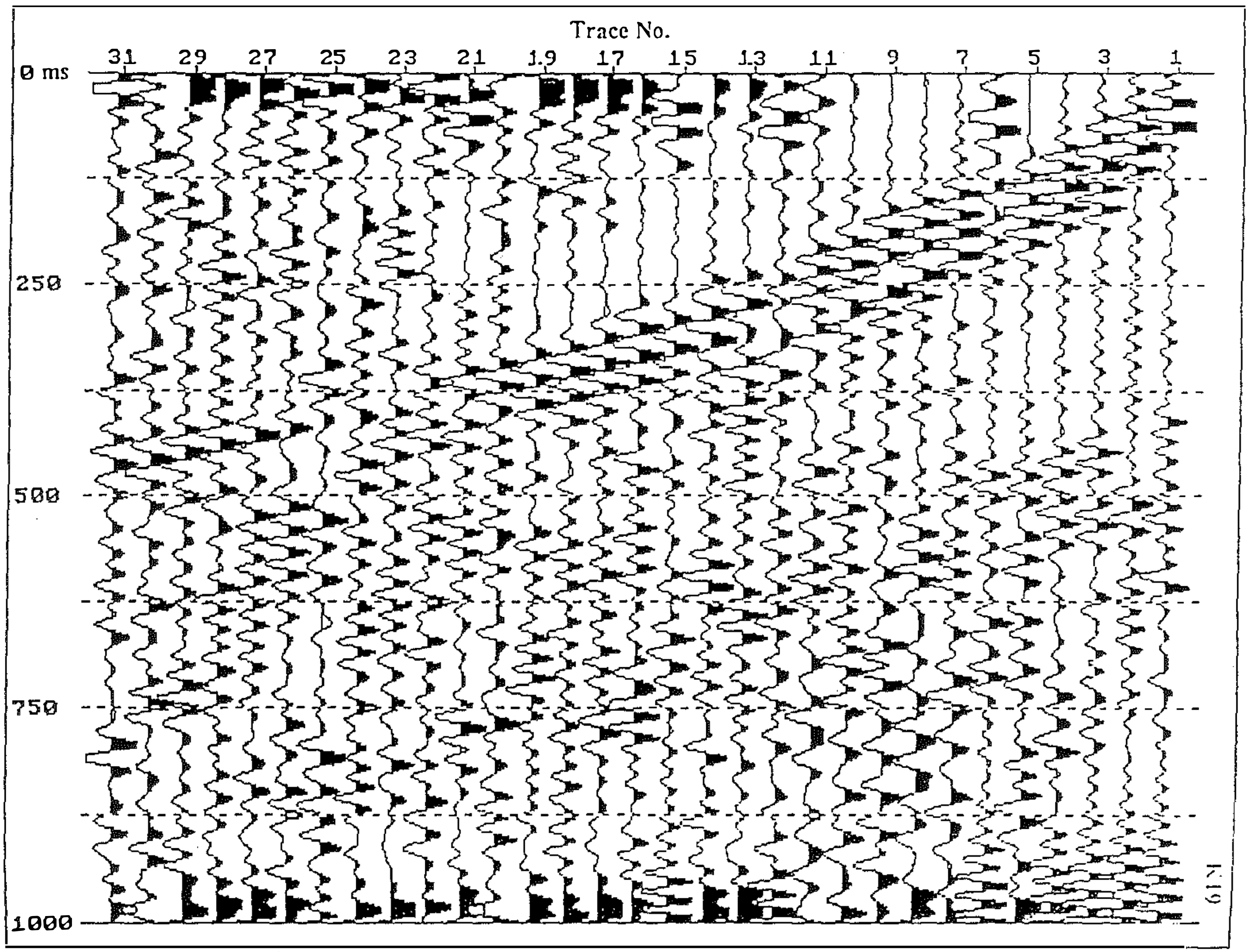

Figure A.17. Site K19 in Marshall County (Elva Quadrangle).

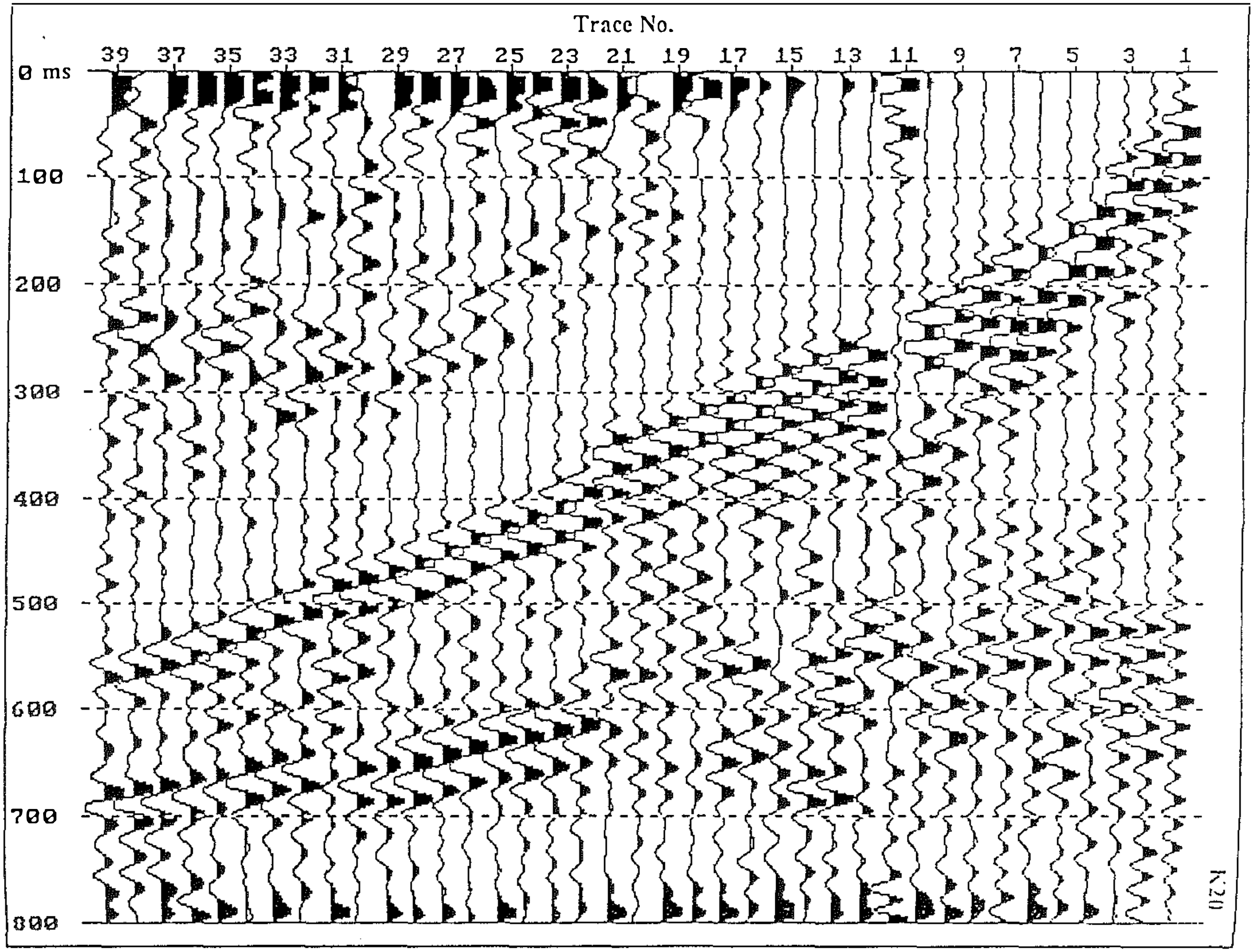

Figure A.18. Site K20 in Marshall County (Elva Quadrangle).

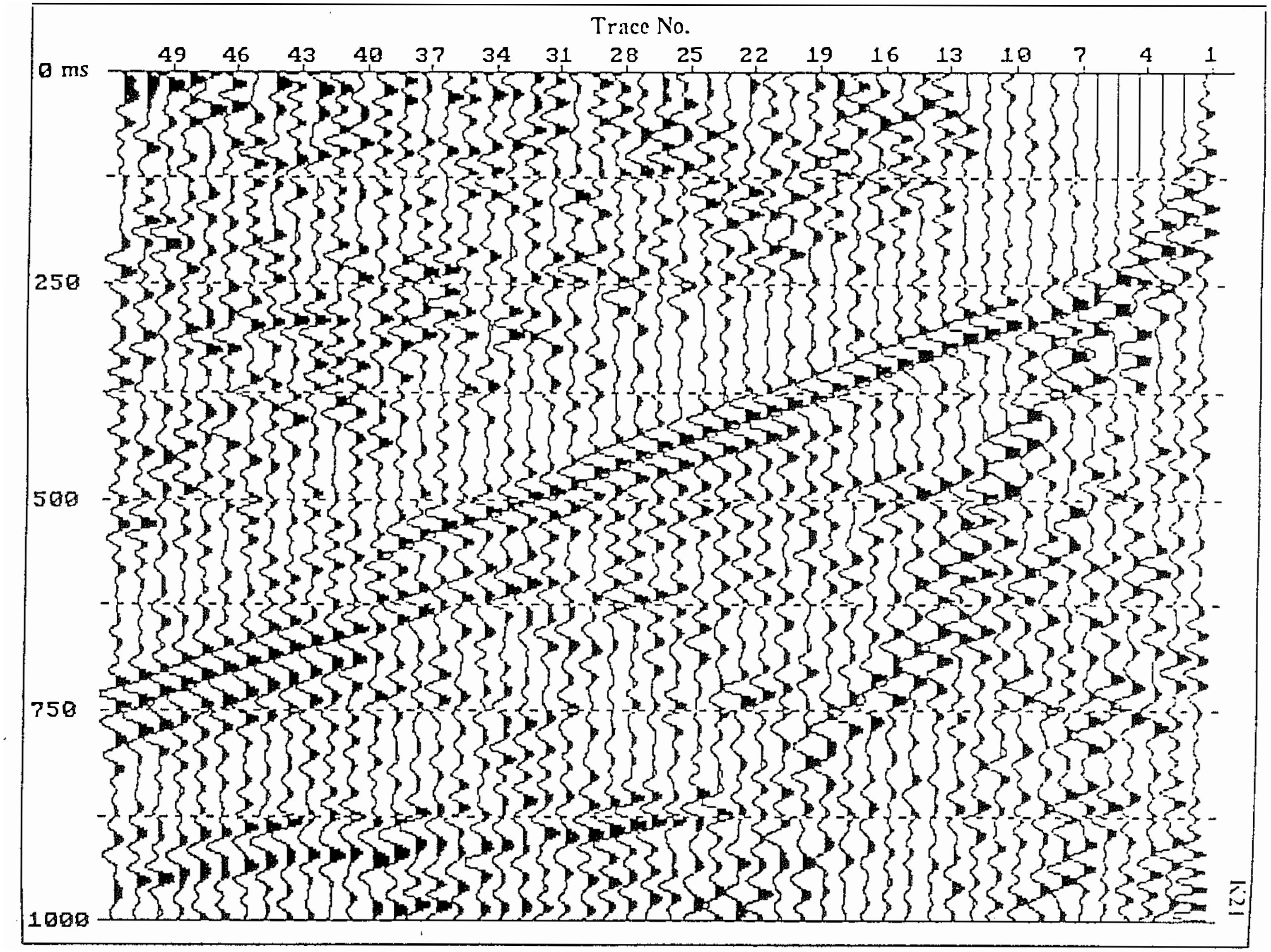

Figure A.19. Site K21 in Graves County (Symsonia Quadrangle).

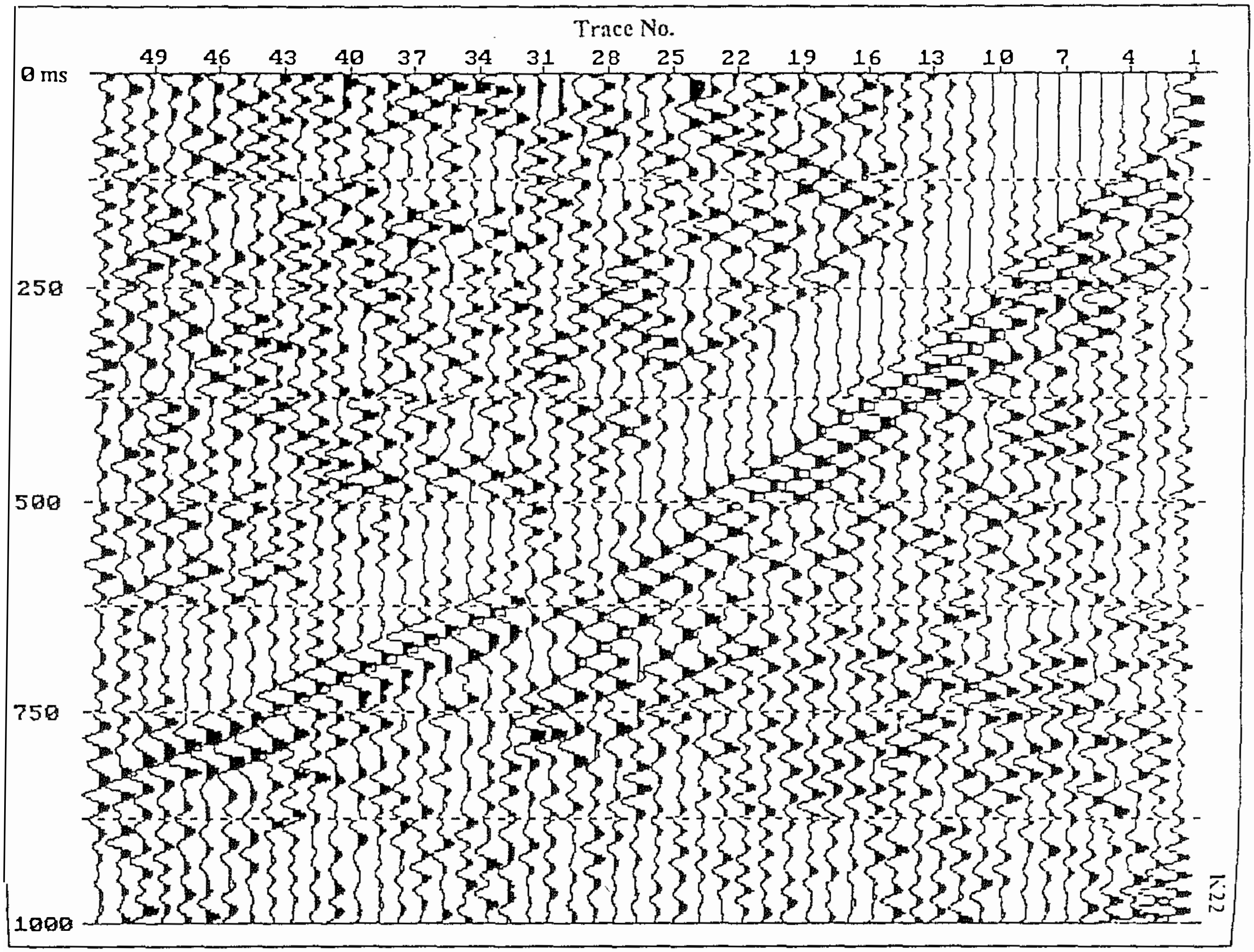

Figure A.20. Site K22 in McCracken County (Symsonia Quadrangle).

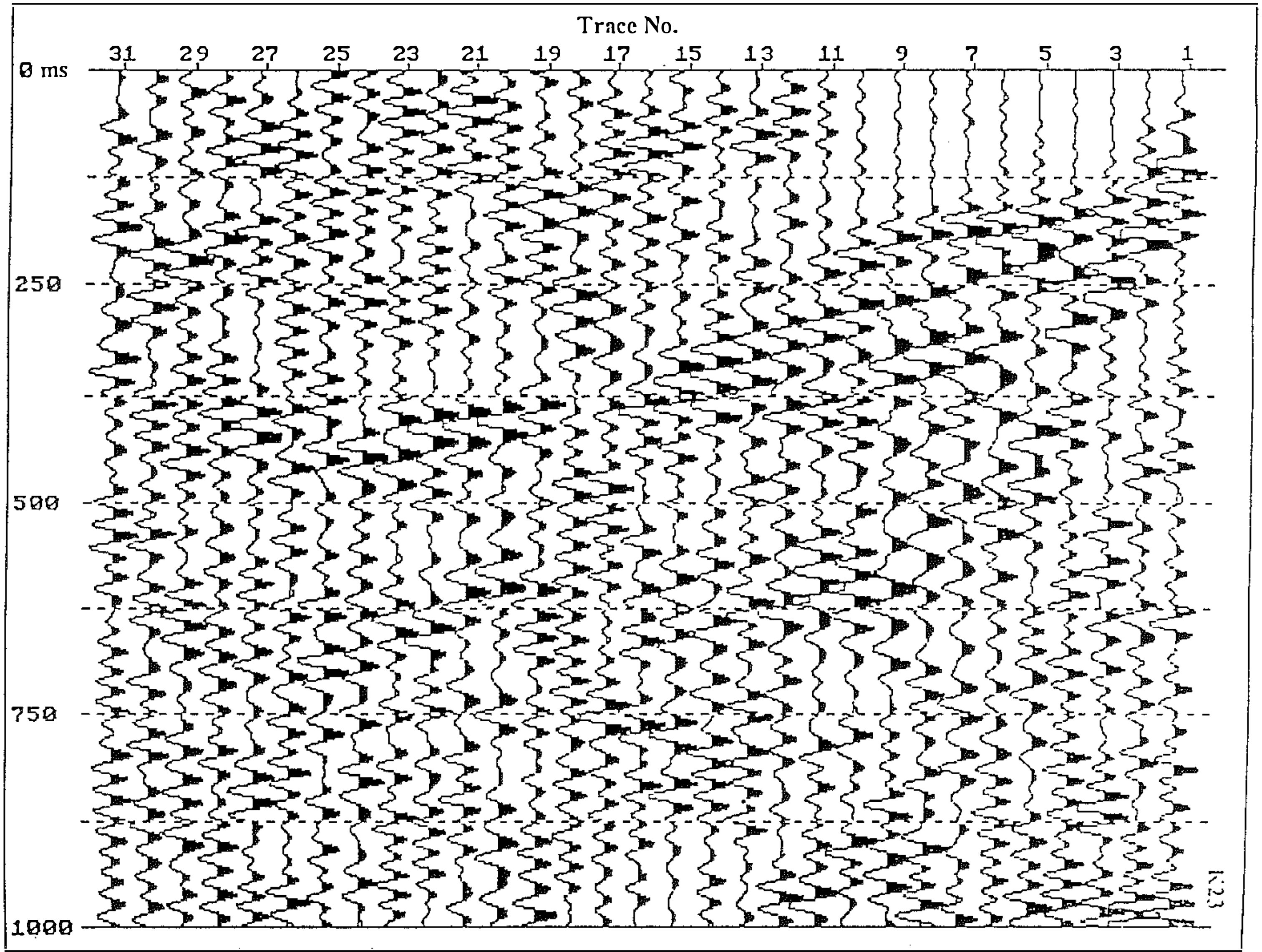

Figure A.21. Site K23 in McCracken County (Symsonia Quadrangle).

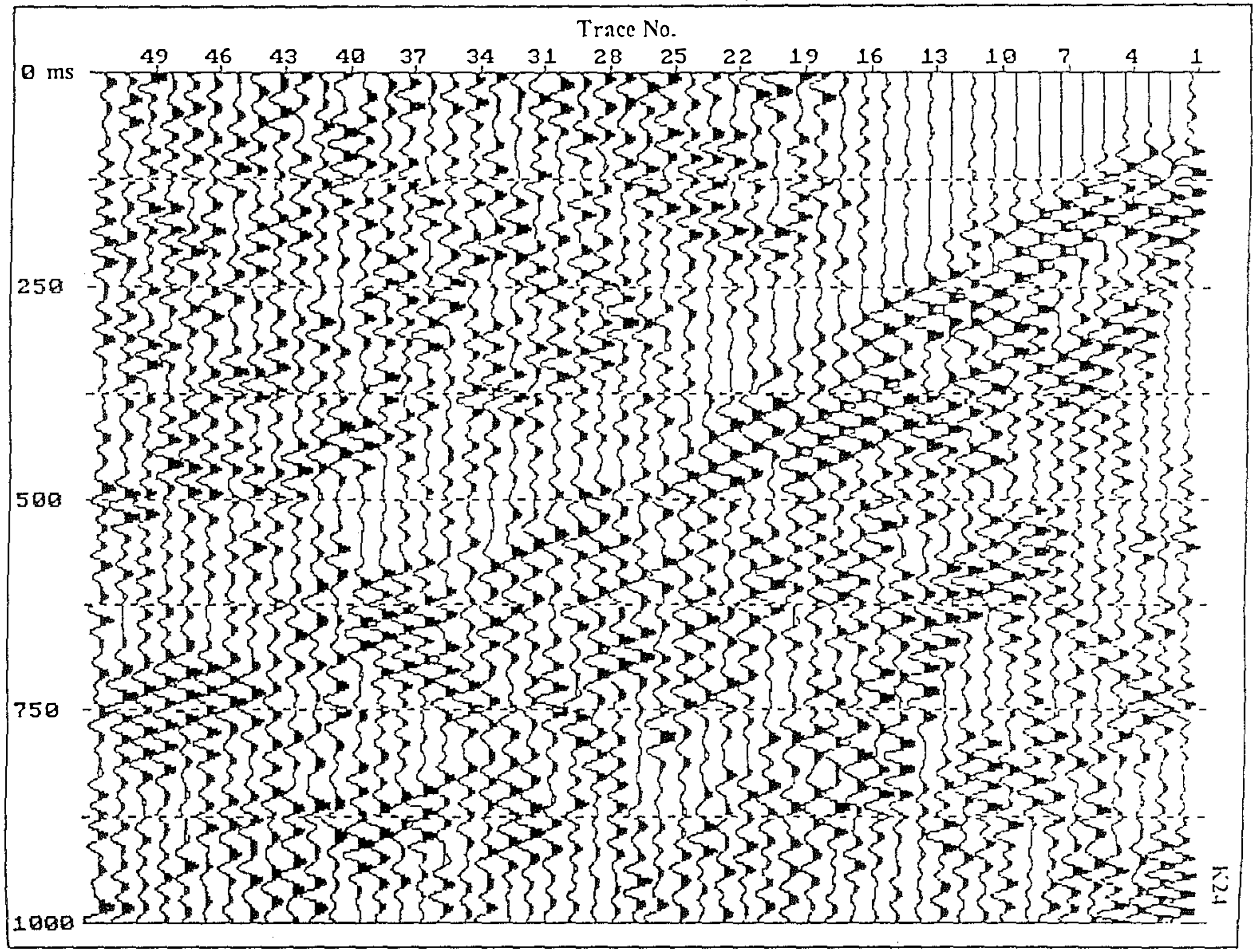

Figure A.22. Site K24 in McCracken County (Melber Quadrangle).

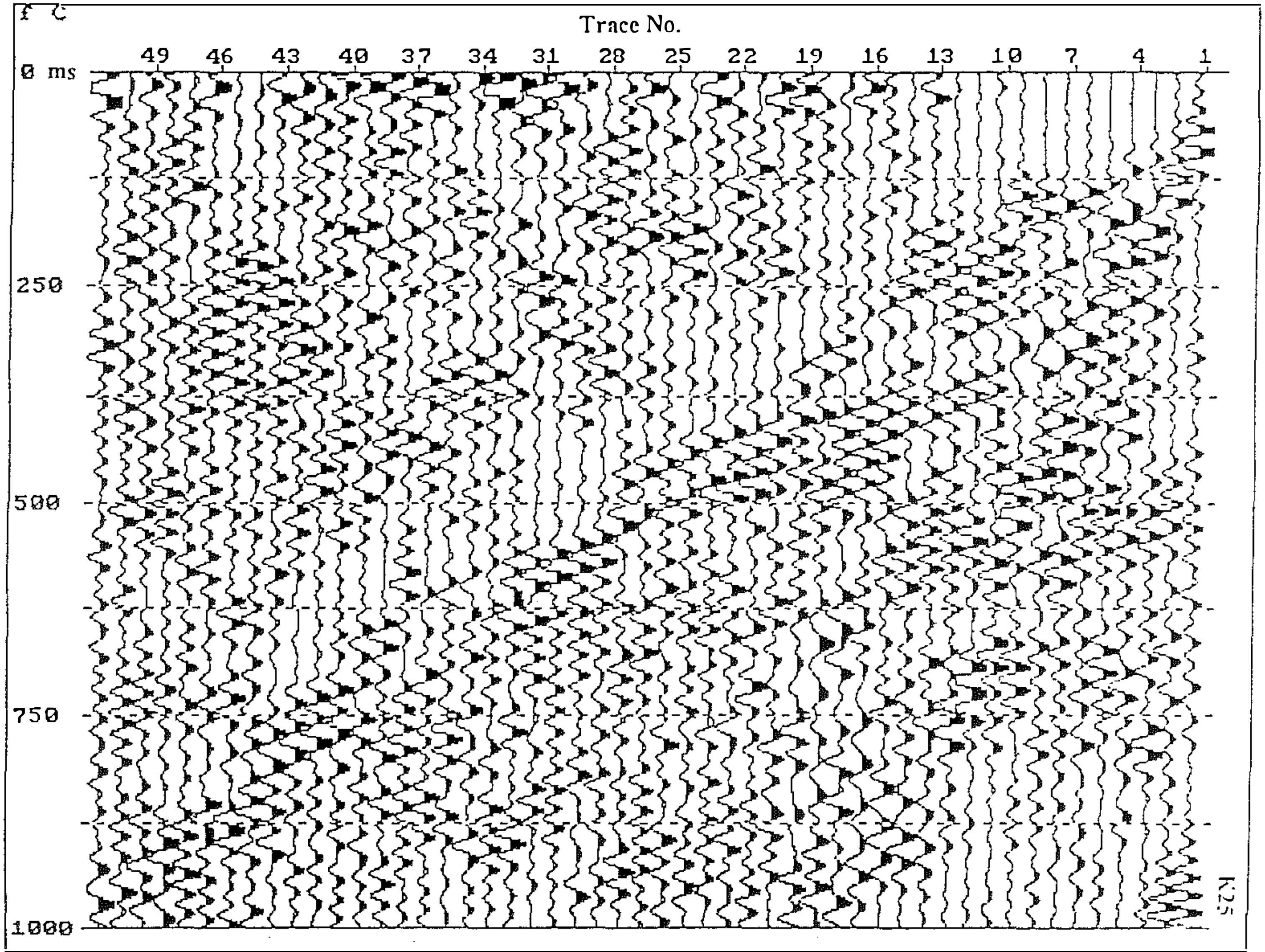

Figure A.23. Site K25 in Graves County (Melber Quadrangle).

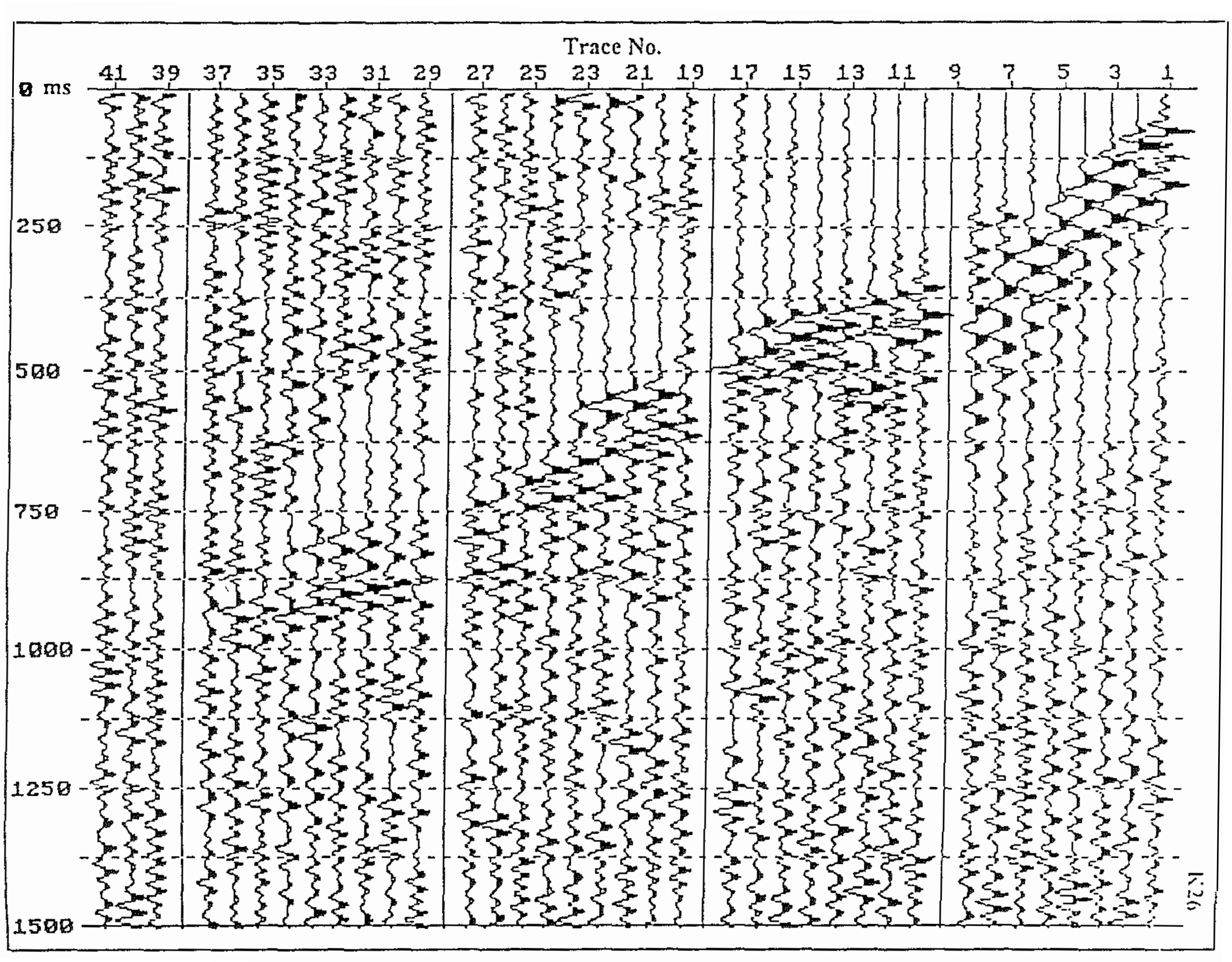

Figure A.24. Site K26 in McCracken County (Lovelaceville Quadrangle).

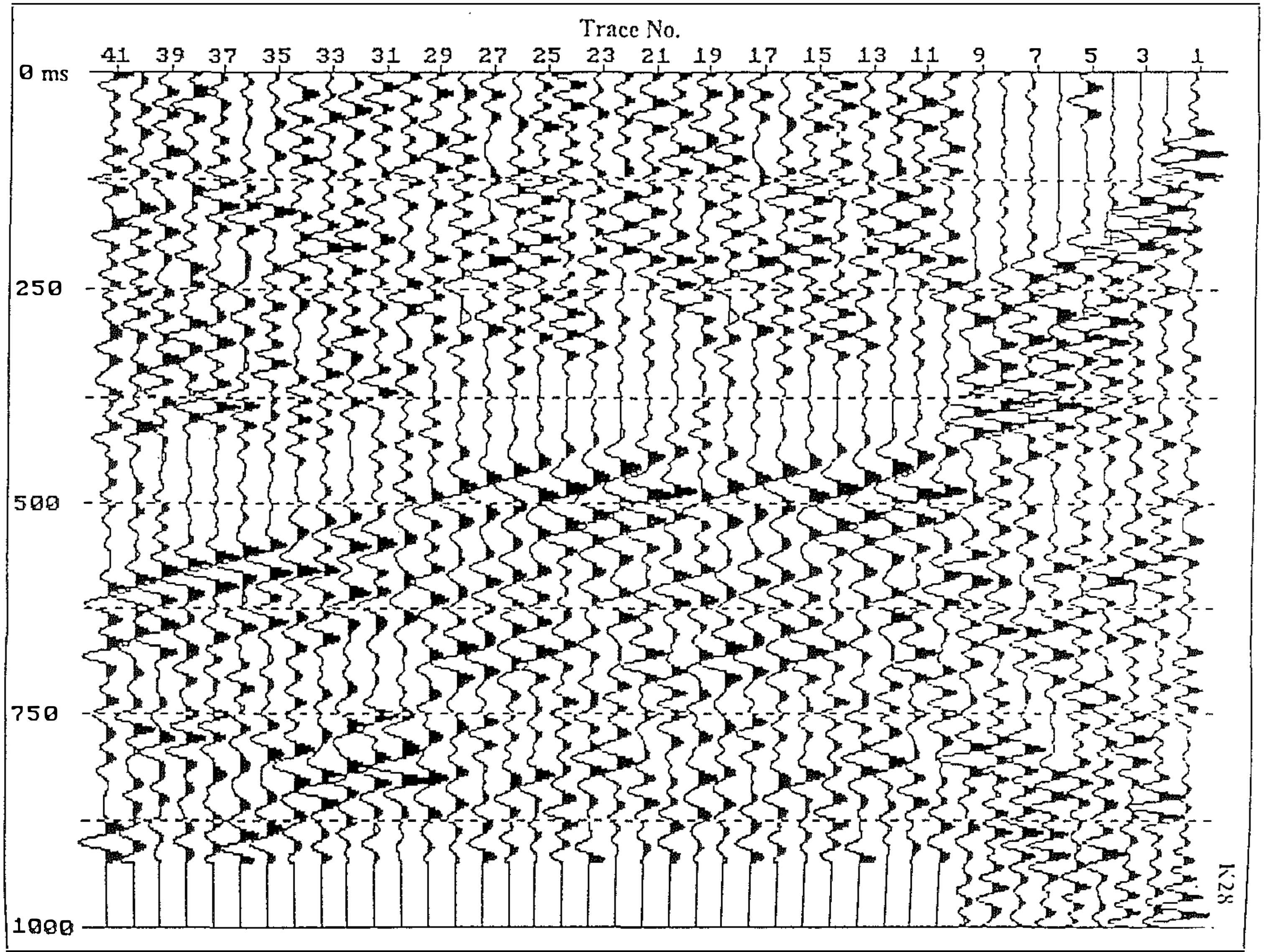

Figure A.25. Site K28 in Ballard County (Lovelaceville Quadrangle).

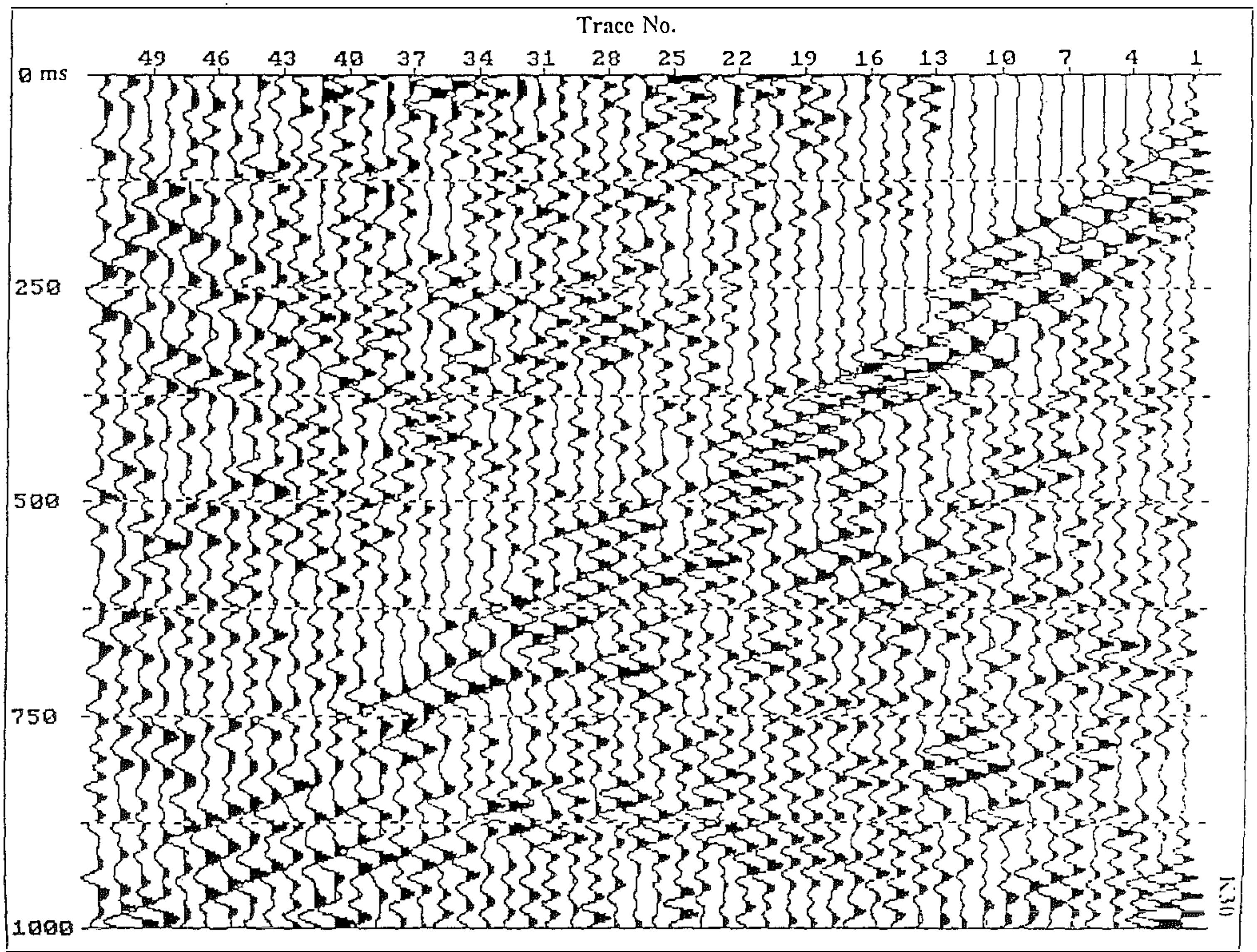

Figure A.26. Site K30 in Ballard County (Blandville Quadrangle).

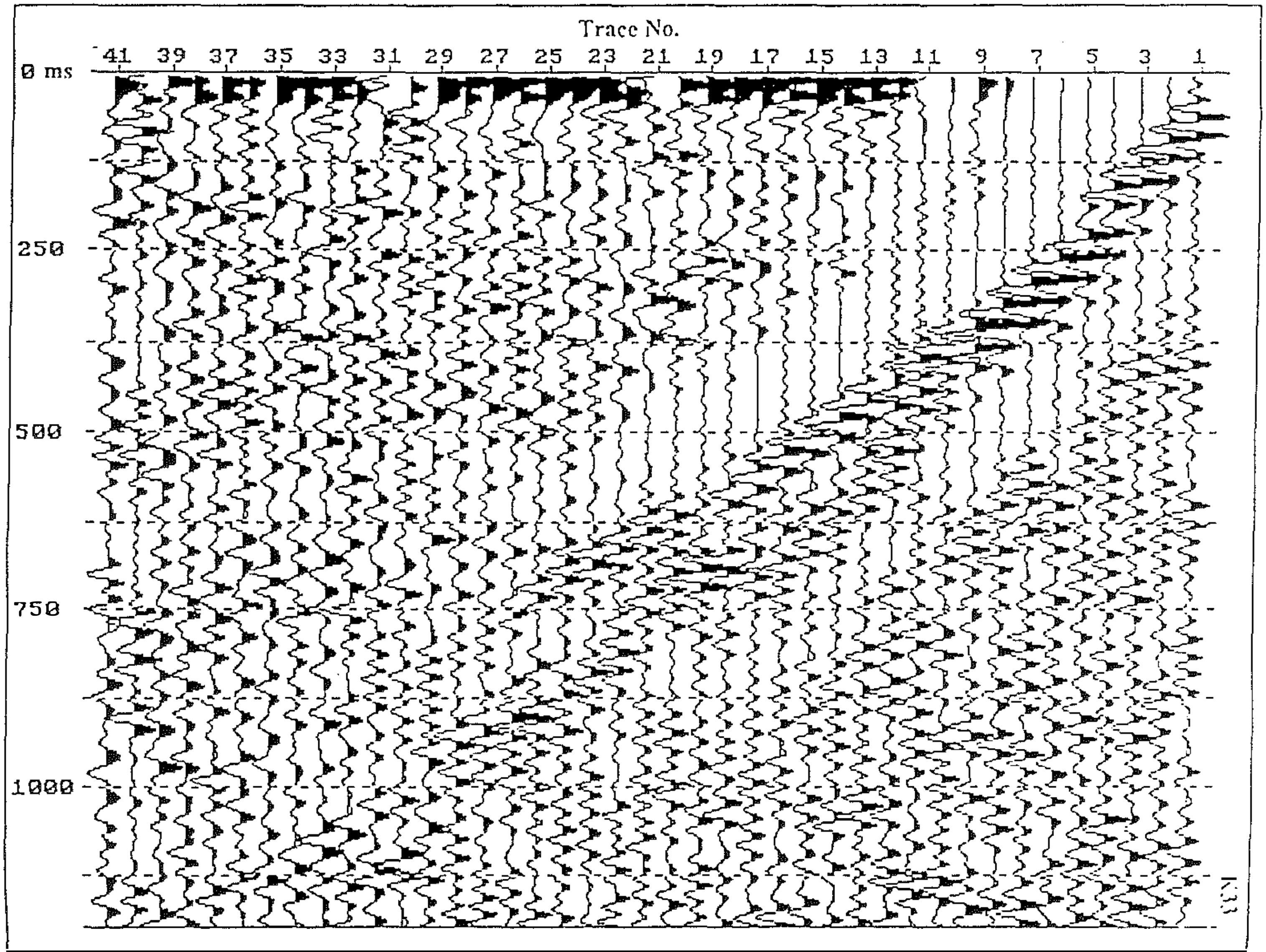

Figure A.27. Site K33 in Ballard County (Wickliffe Quadrangle).

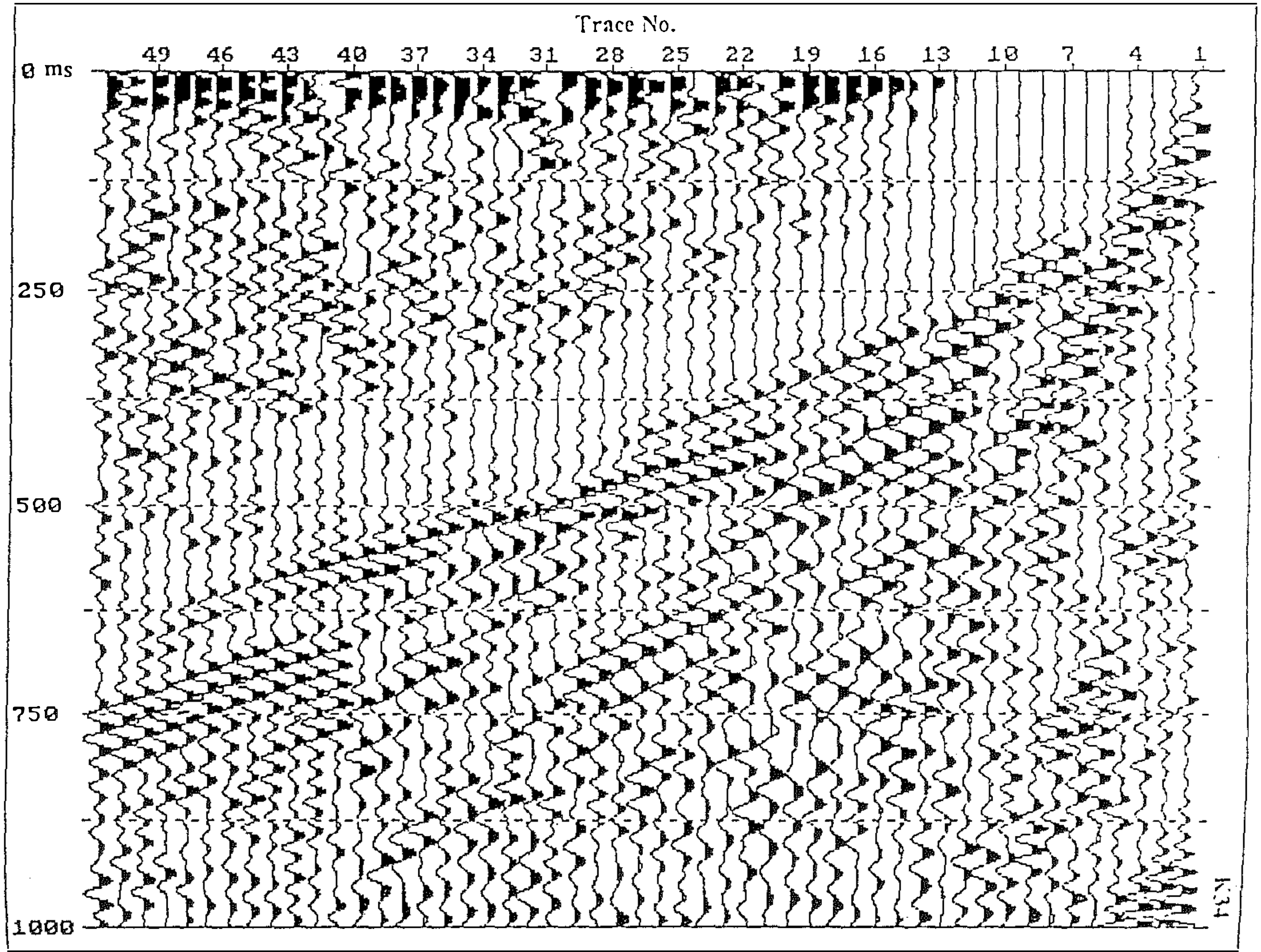

Figure A.28. Site K34 in Marshall County (Hardin Quadrangle).

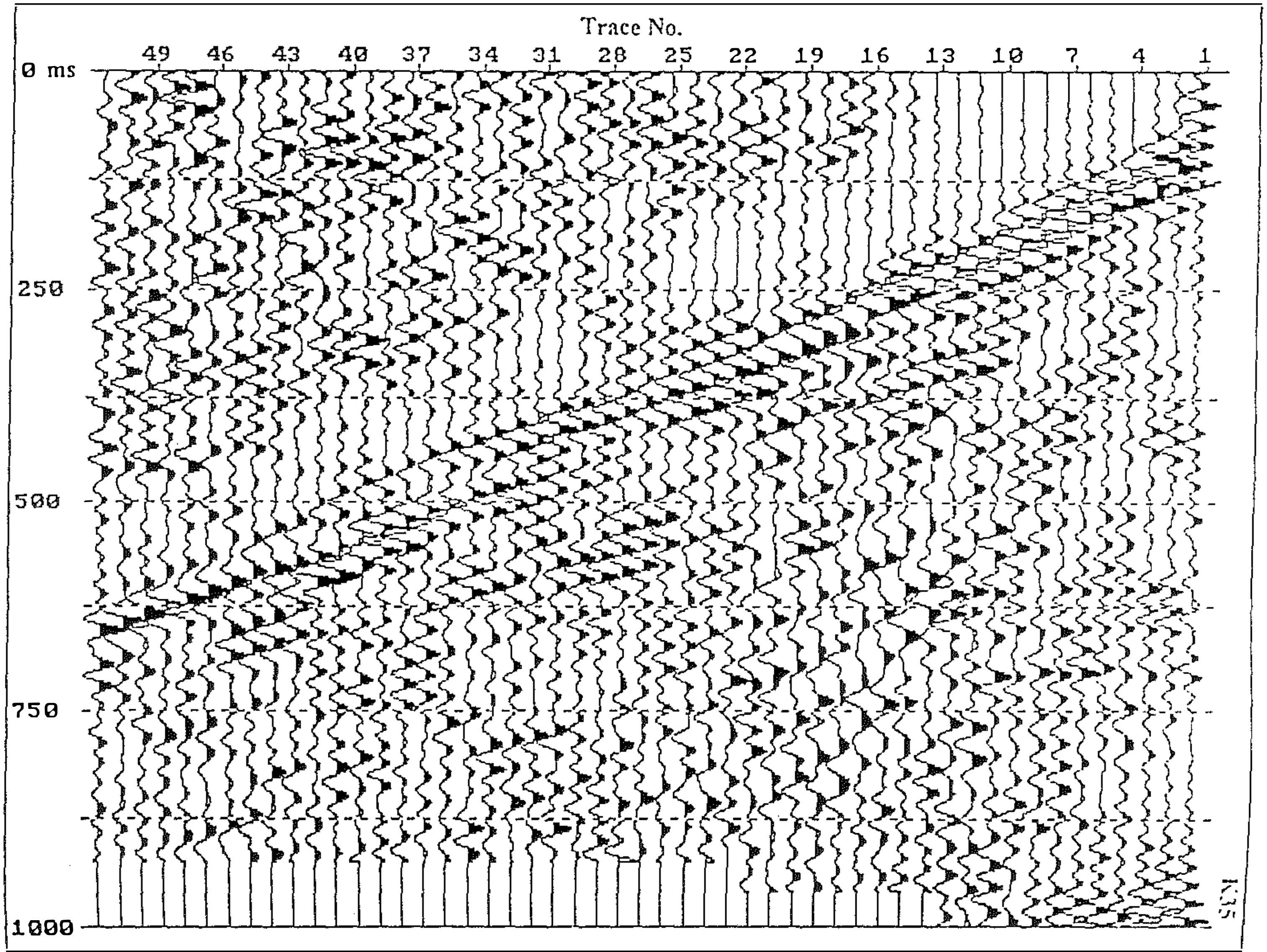

Figure A.29. Site K35 in Marshall County (Hardin Quadrangle).

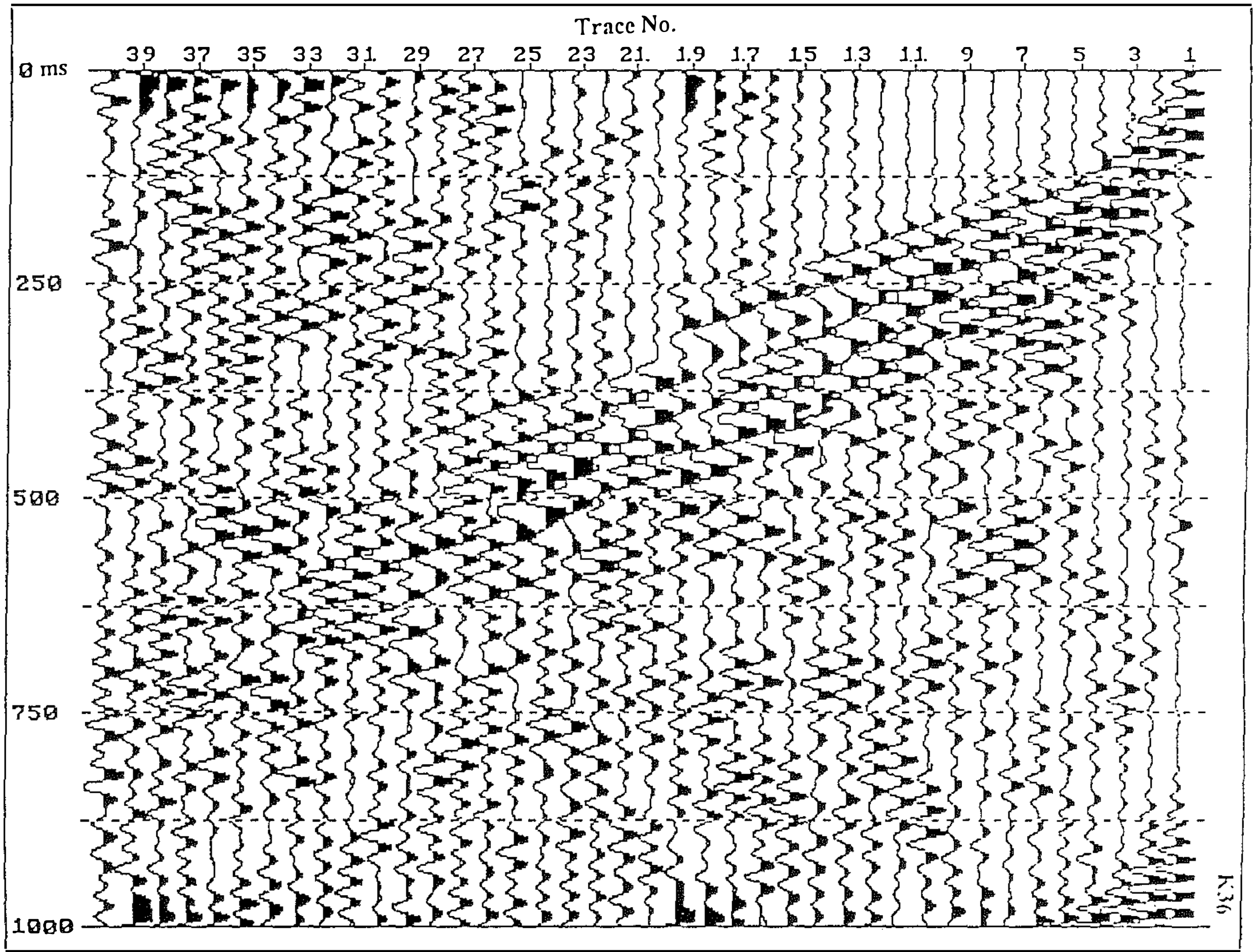

Figure A.30. Site K36 in Marshall County (Oak Level Quadrangle).

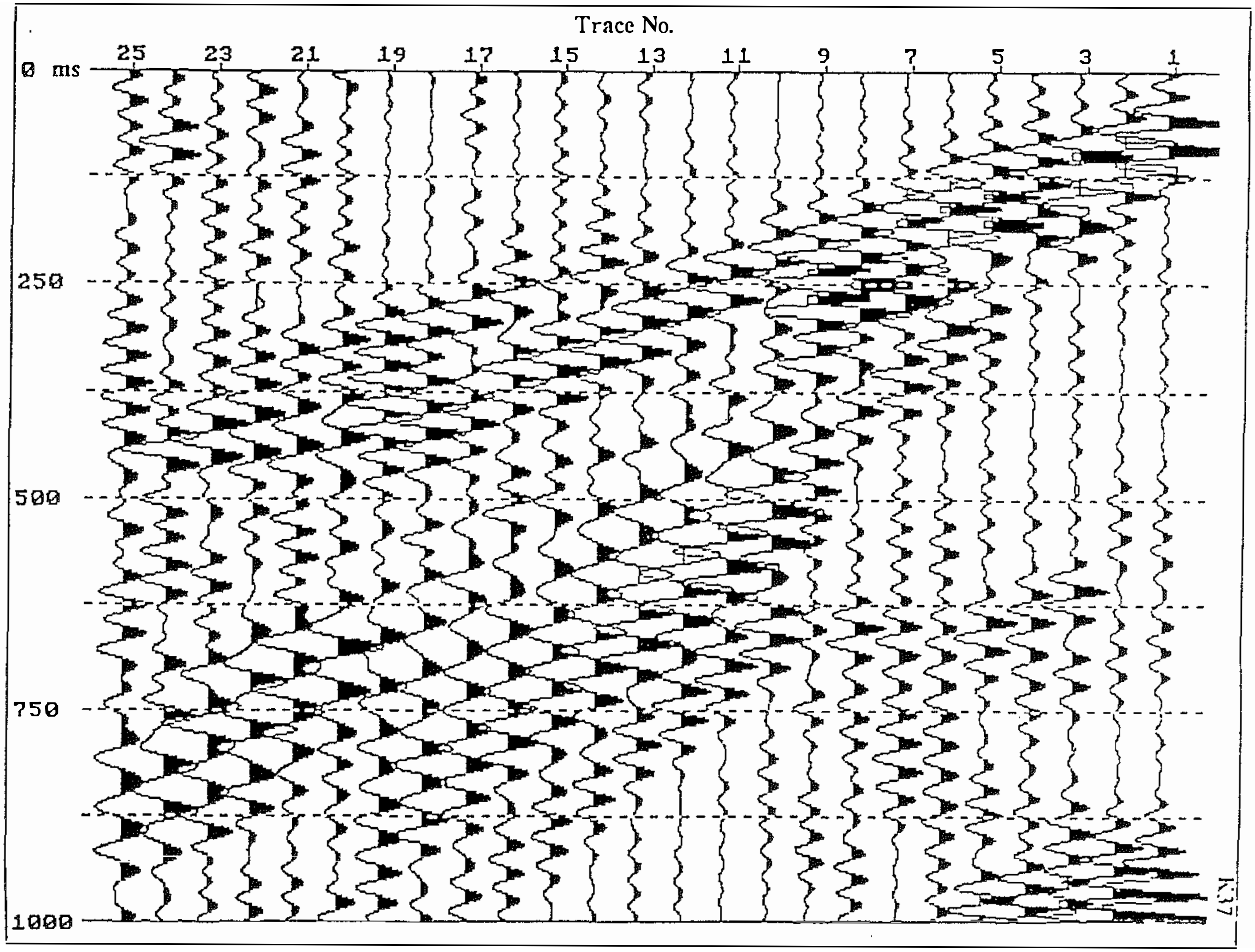

Figure A.31. Site K37 in Marshall County (Oak Level Quadrangle).

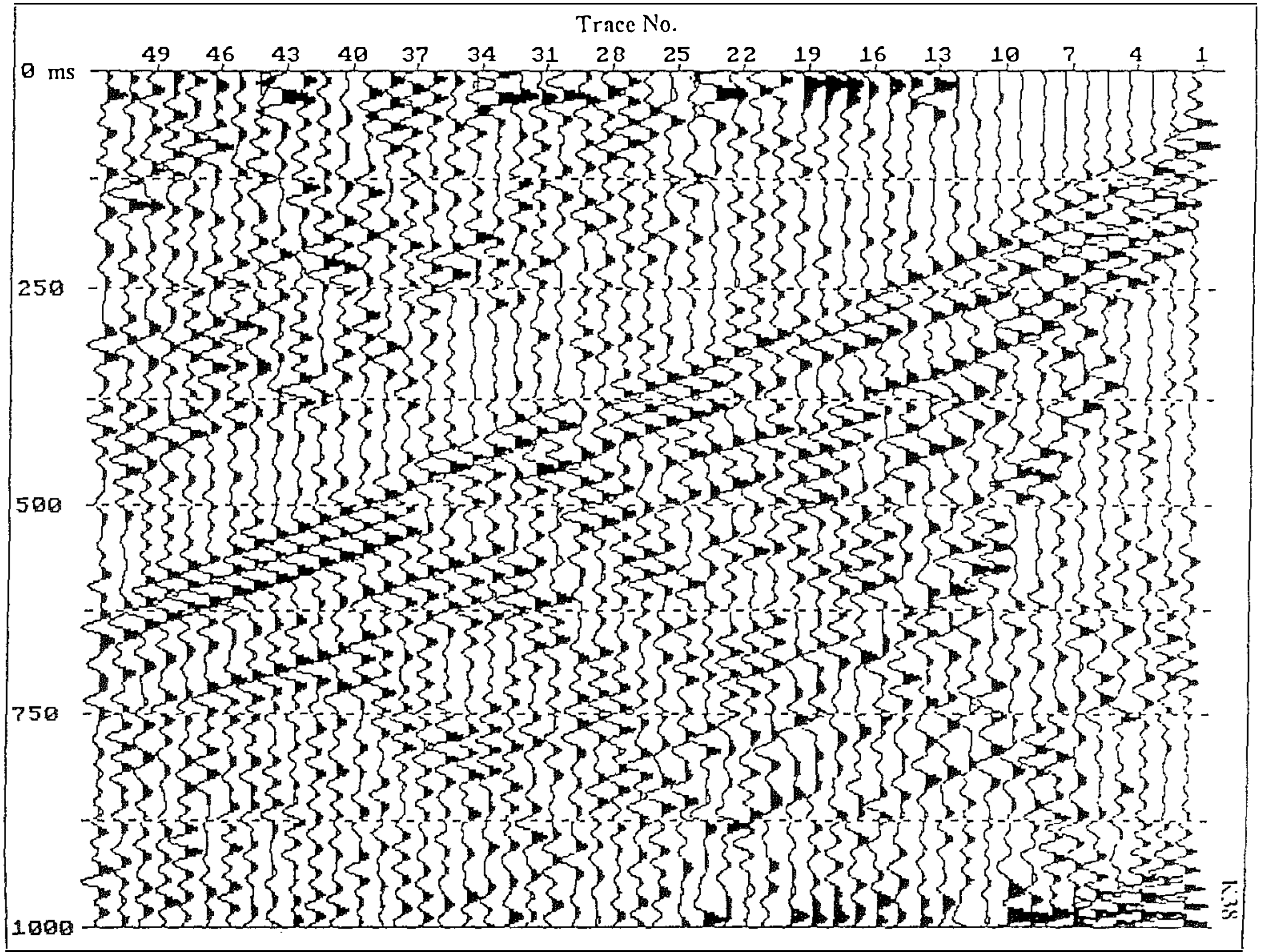

Figure A.32. Site K38 in Marshall County (Oak Level Quadrangle).

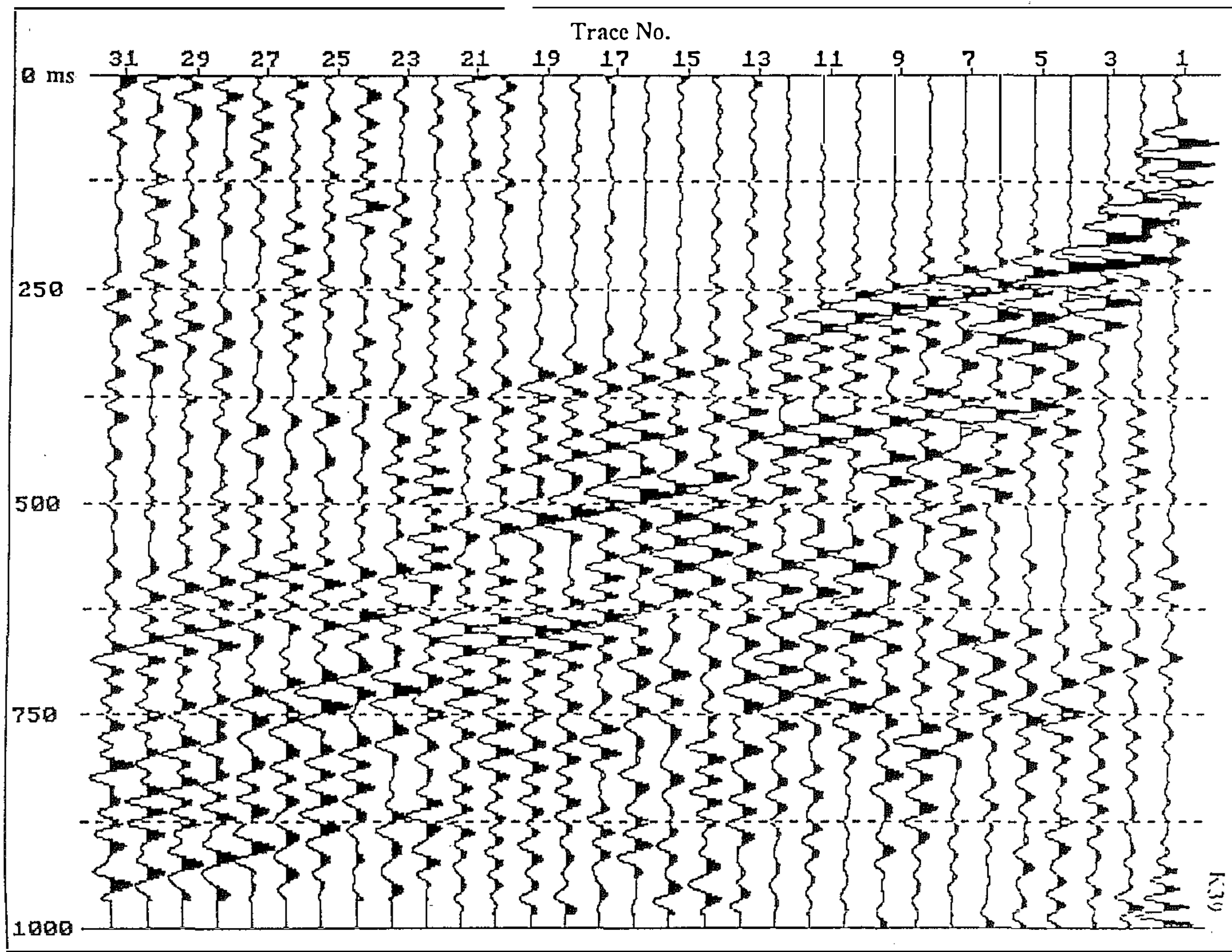

Figure A.33. Site K39 in Graves County (West Plains Quadrangle).

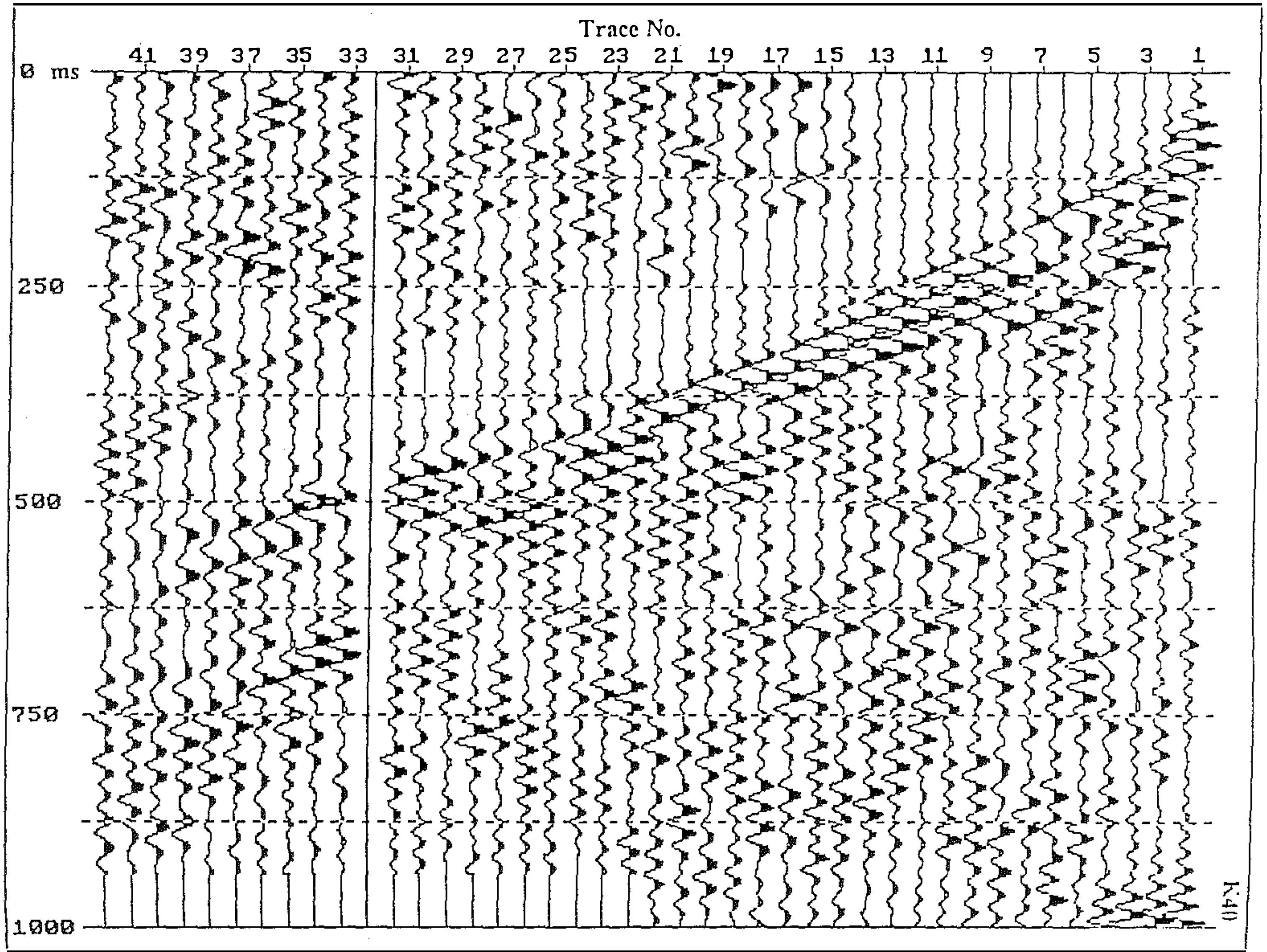

Figure A.34. Site K40 in Graves County (West Plains Quadrangle).

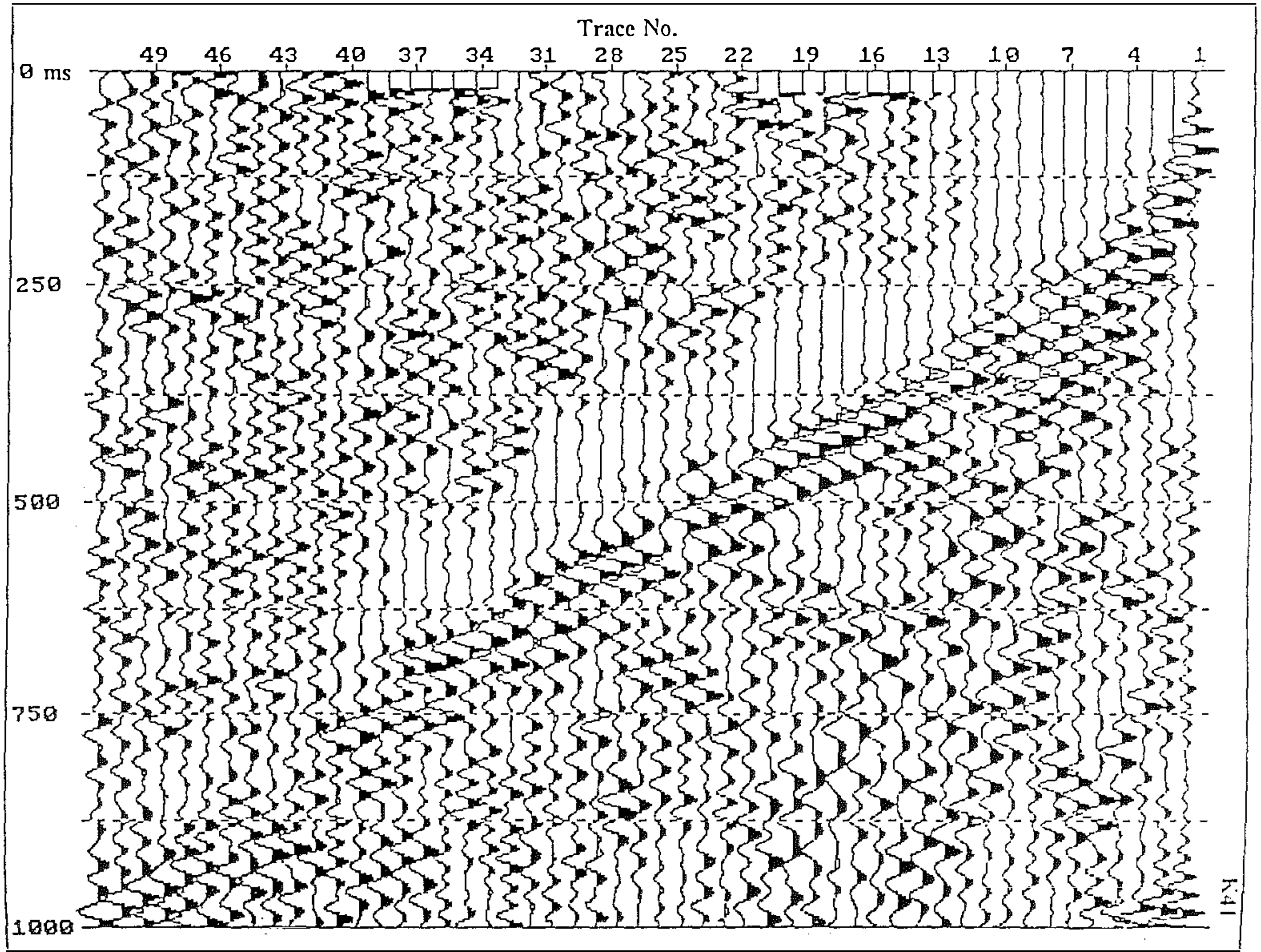

Figure A.35. Site K41 in Graves County (Hickory Quadrangle).

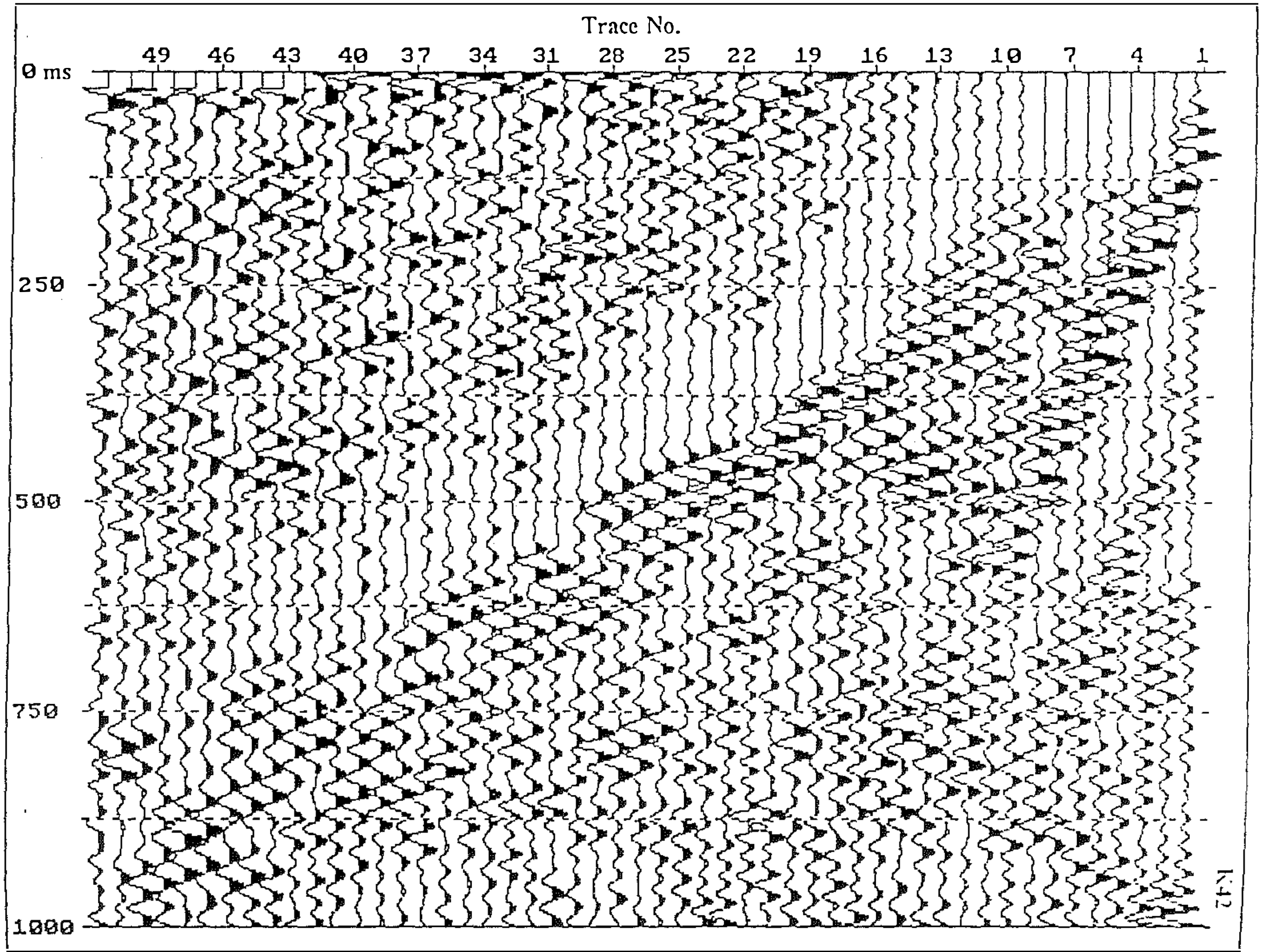

Figure A.36. Site K42 in Graves County (Hickory Quadrangle).

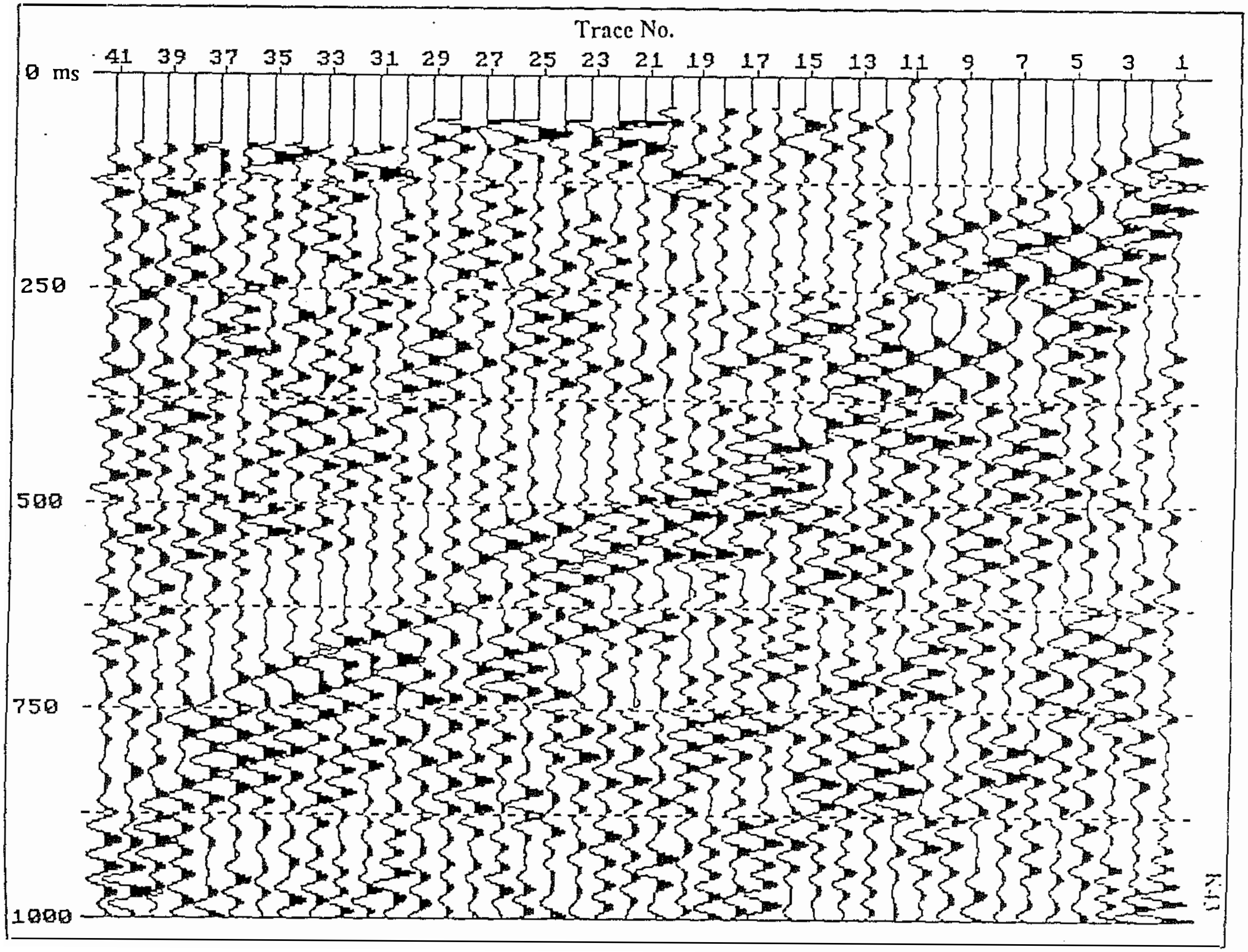

Figure A.37. Site K43 in Graves County (Fancy Farm Quadrangle).

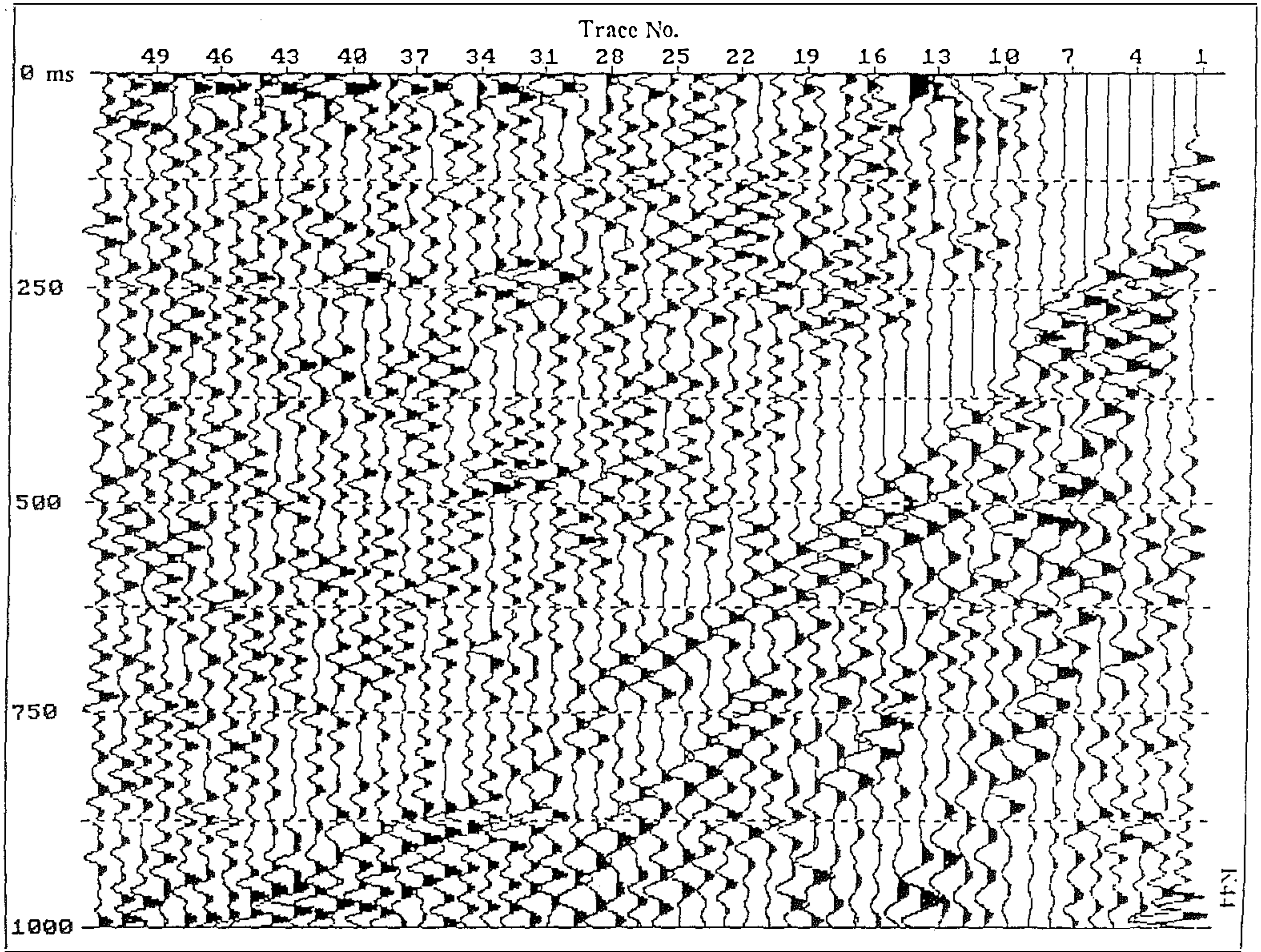

Figure A.38. Site K44 in Carlisle County (Milburn Quadrangle).

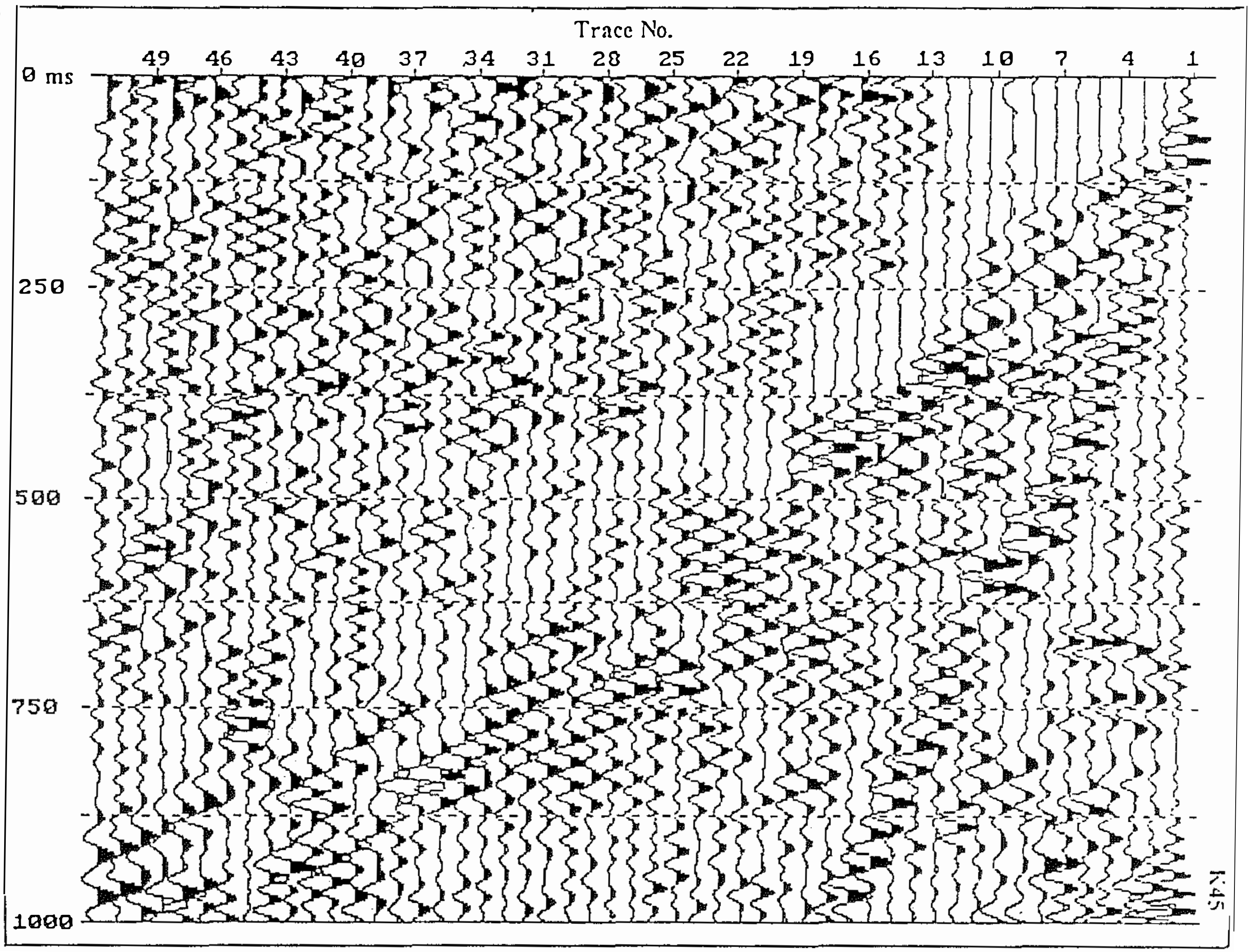

Figure A.39. Site K45 in Carlisle County (Milburn Quadrangle).

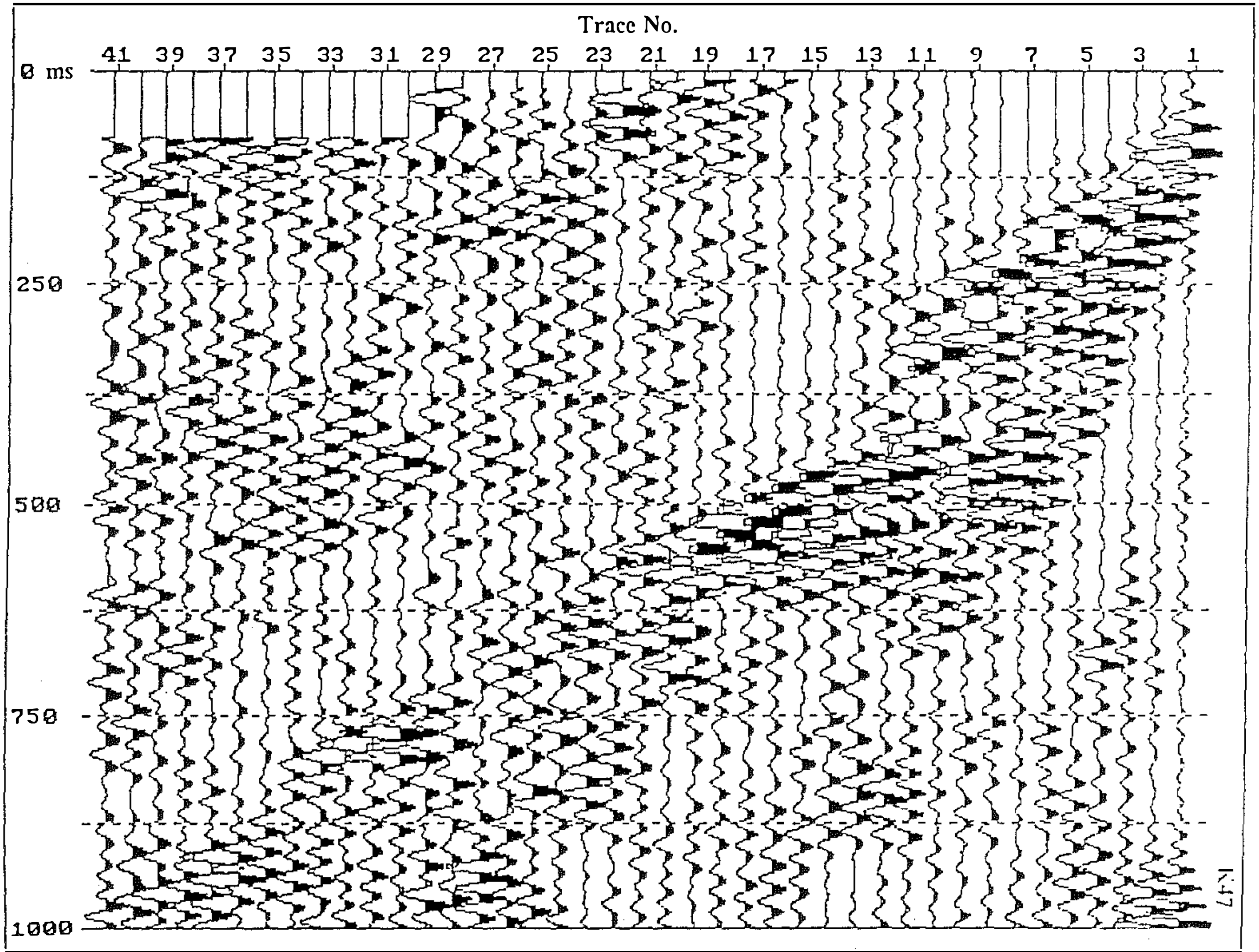

Figure A.40. Site K47 in Carlisle County (Milburn Quadrangle).

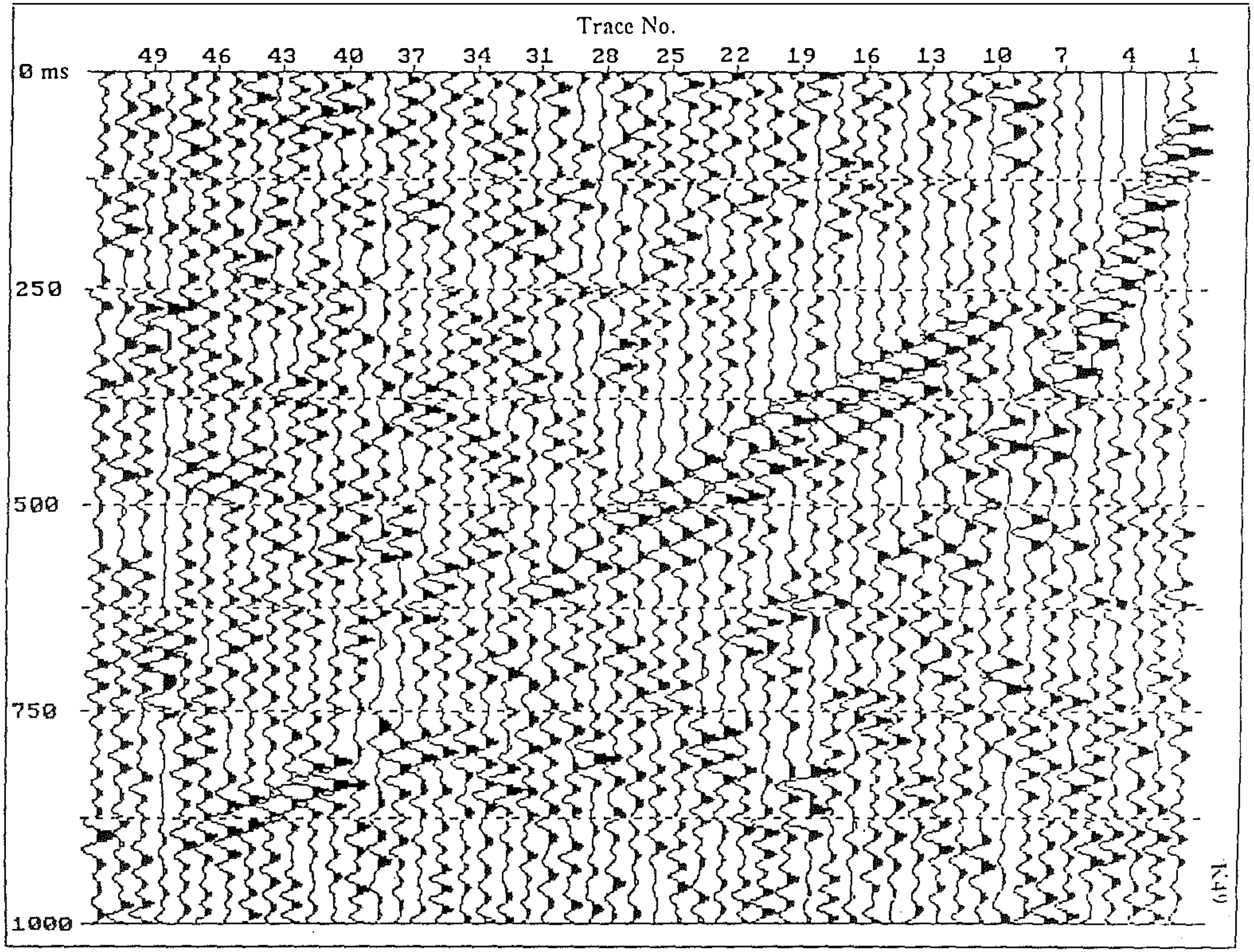

Figure A.41. Site K49 in Carlisle County (Arlington Quadrangle).

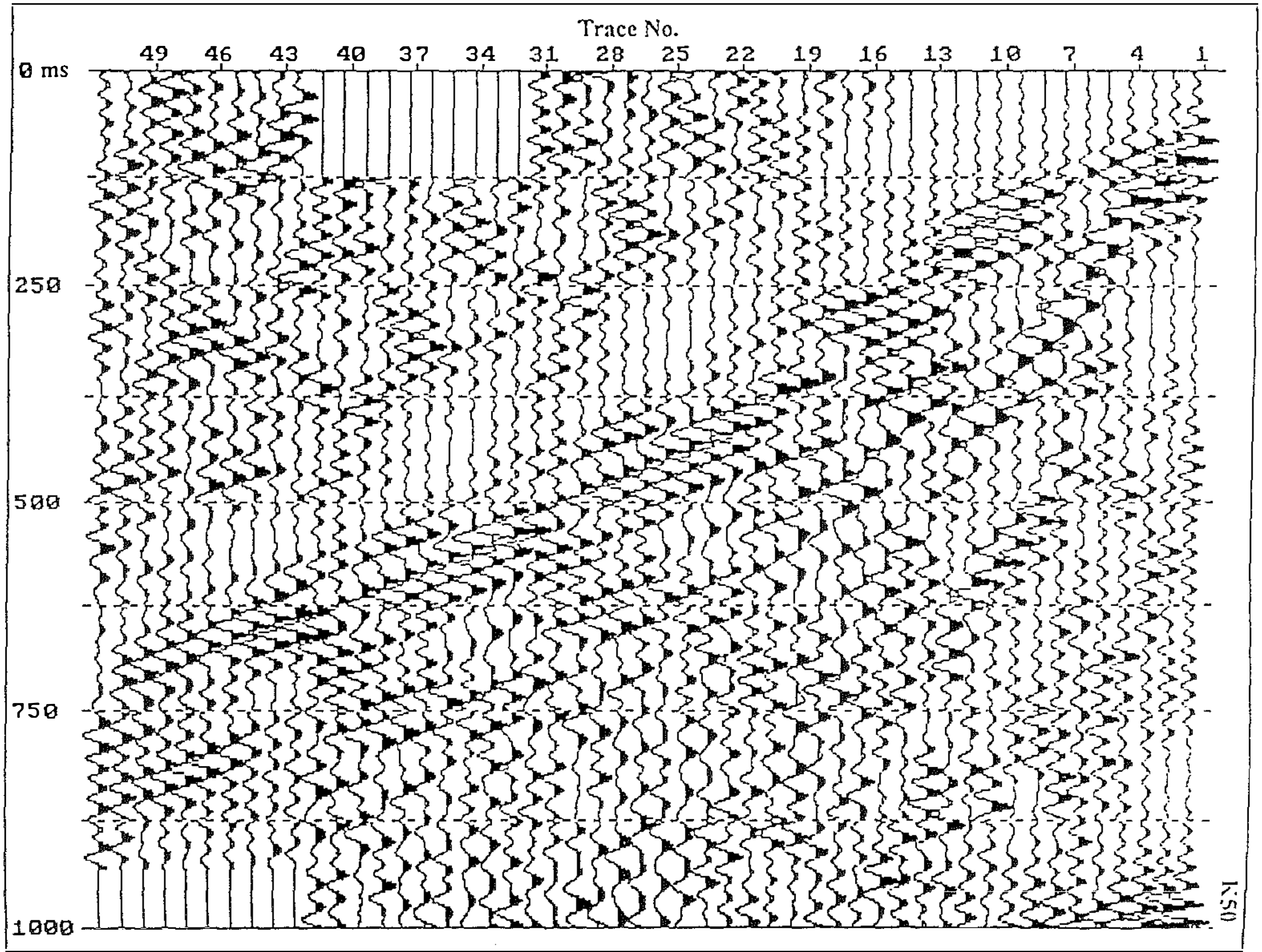

Figure A.42. Site K50 in Calloway County (Hico Quadrangle).

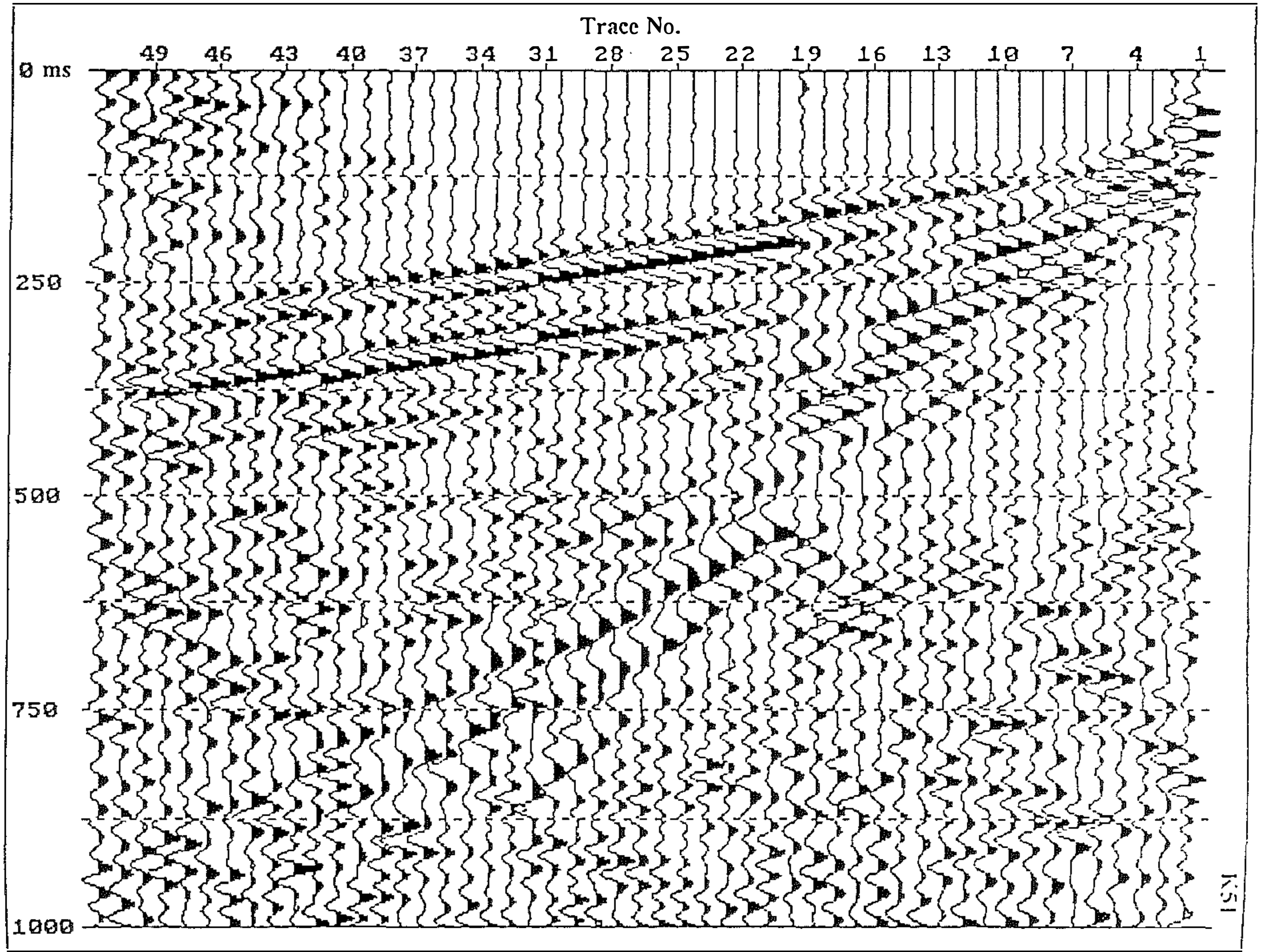

Figure A.43. Site K51 in Calloway County (Hico Quadrangle).

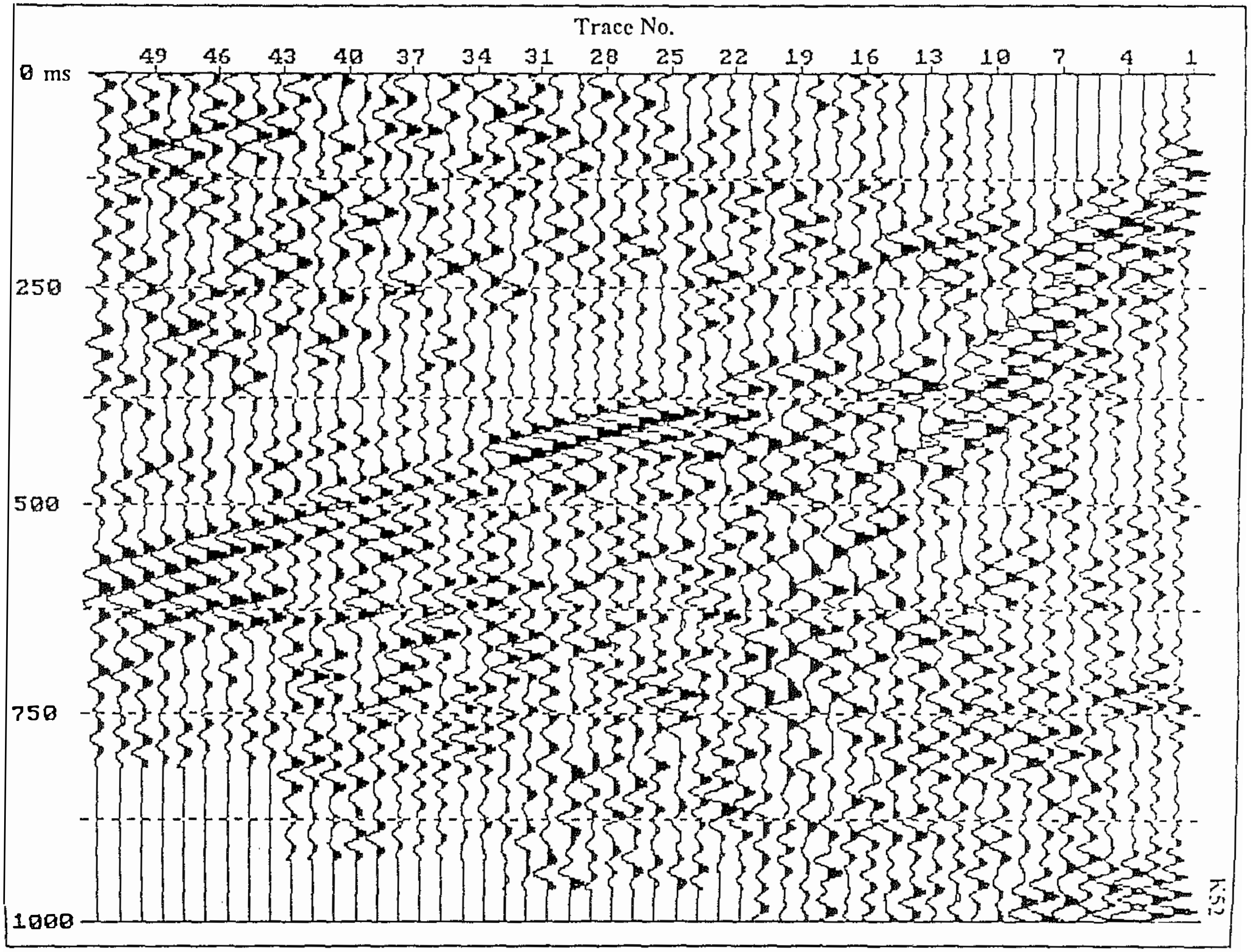

Figure A.44. Site K52 in Calloway County (Hico Quadrangle).

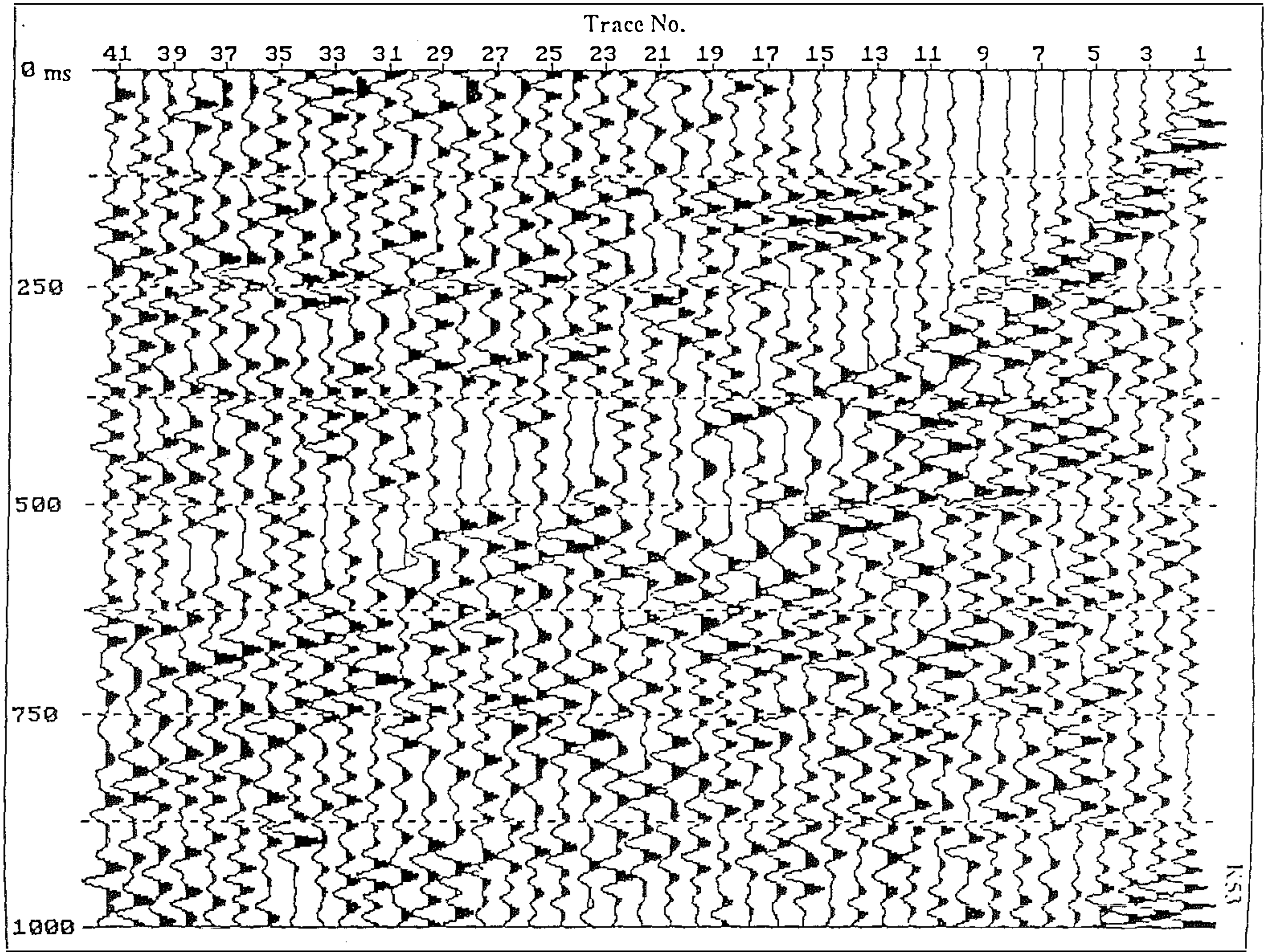

Figure A.45. Site K53 in Calloway County (Dexter Quadrangle).

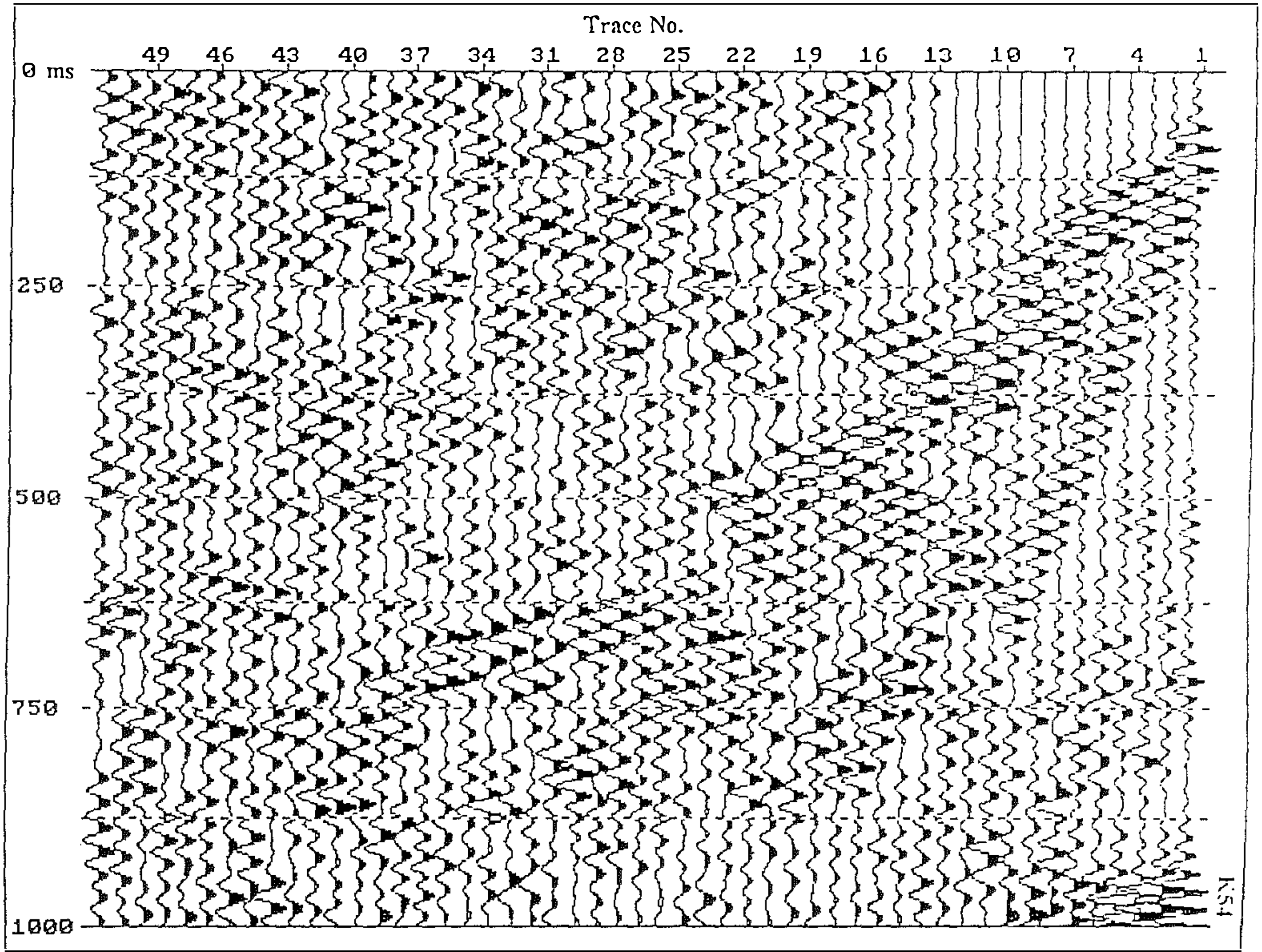

Figure A.46. Site K54 in Calloway County (Dexter Quadrangle).

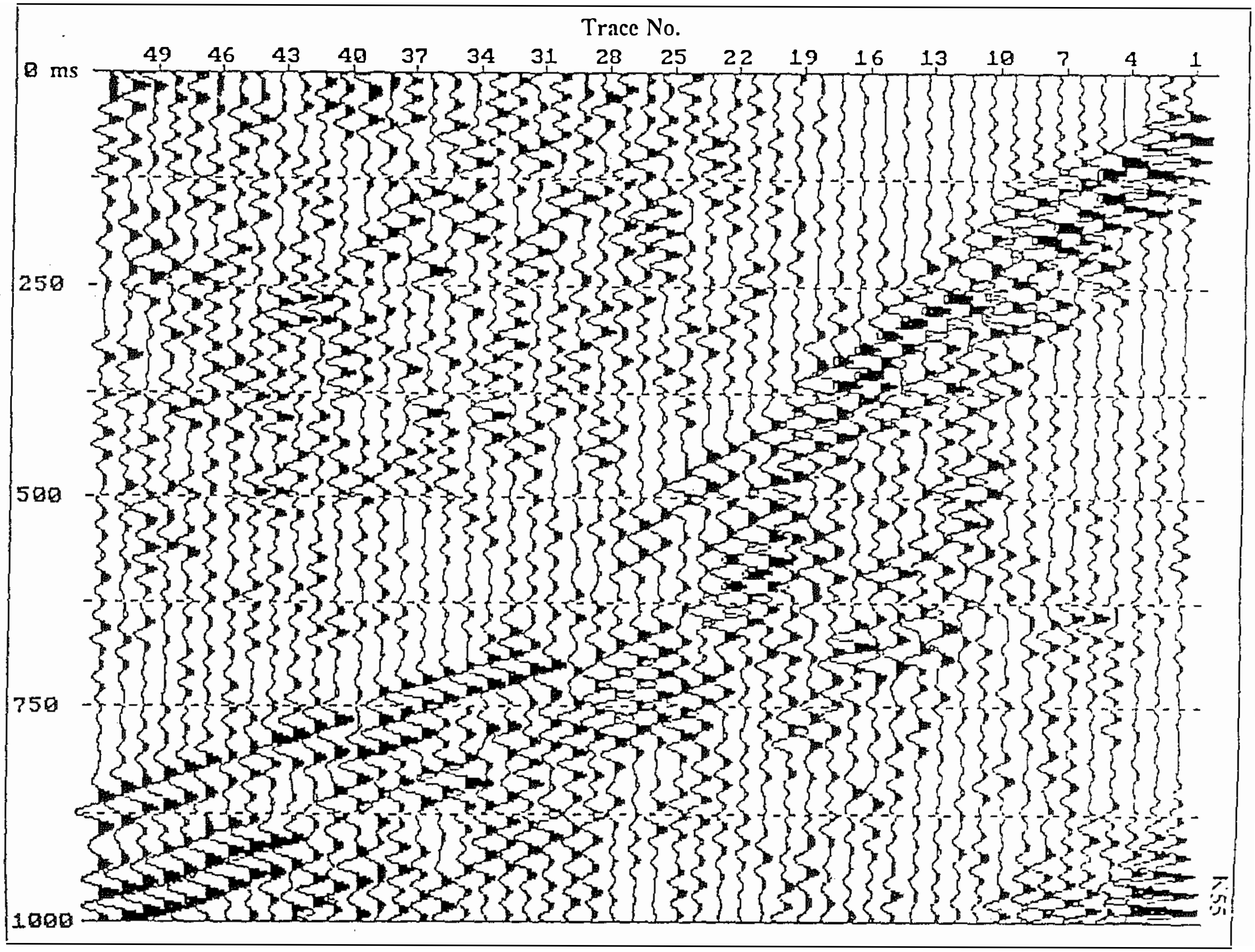

Figure A.47. Site K55 in Calloway County (Kirksey Quadrangle).

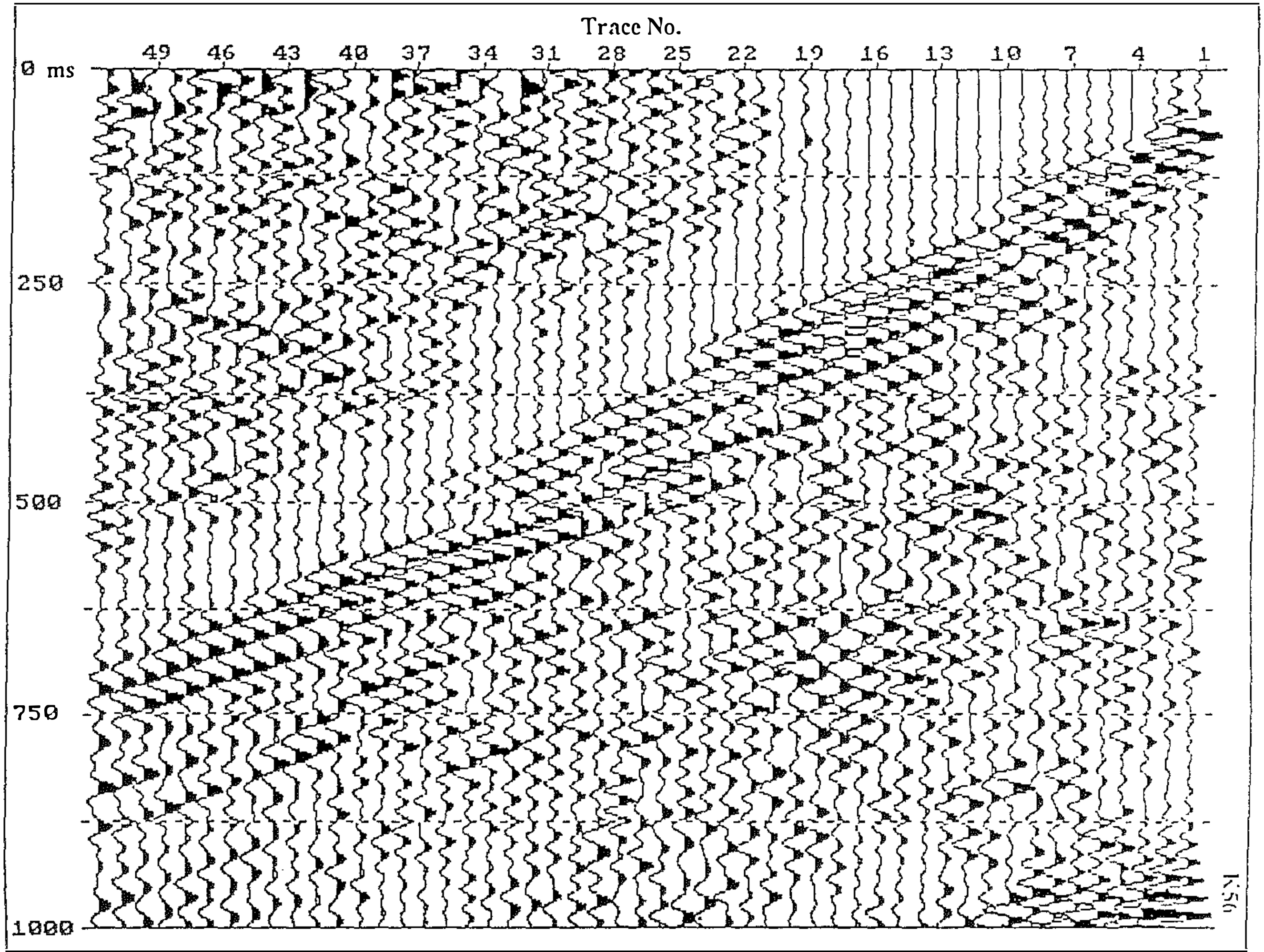

Figure A.48. Site K56 in Calloway County (Kirksey Quadrangle).

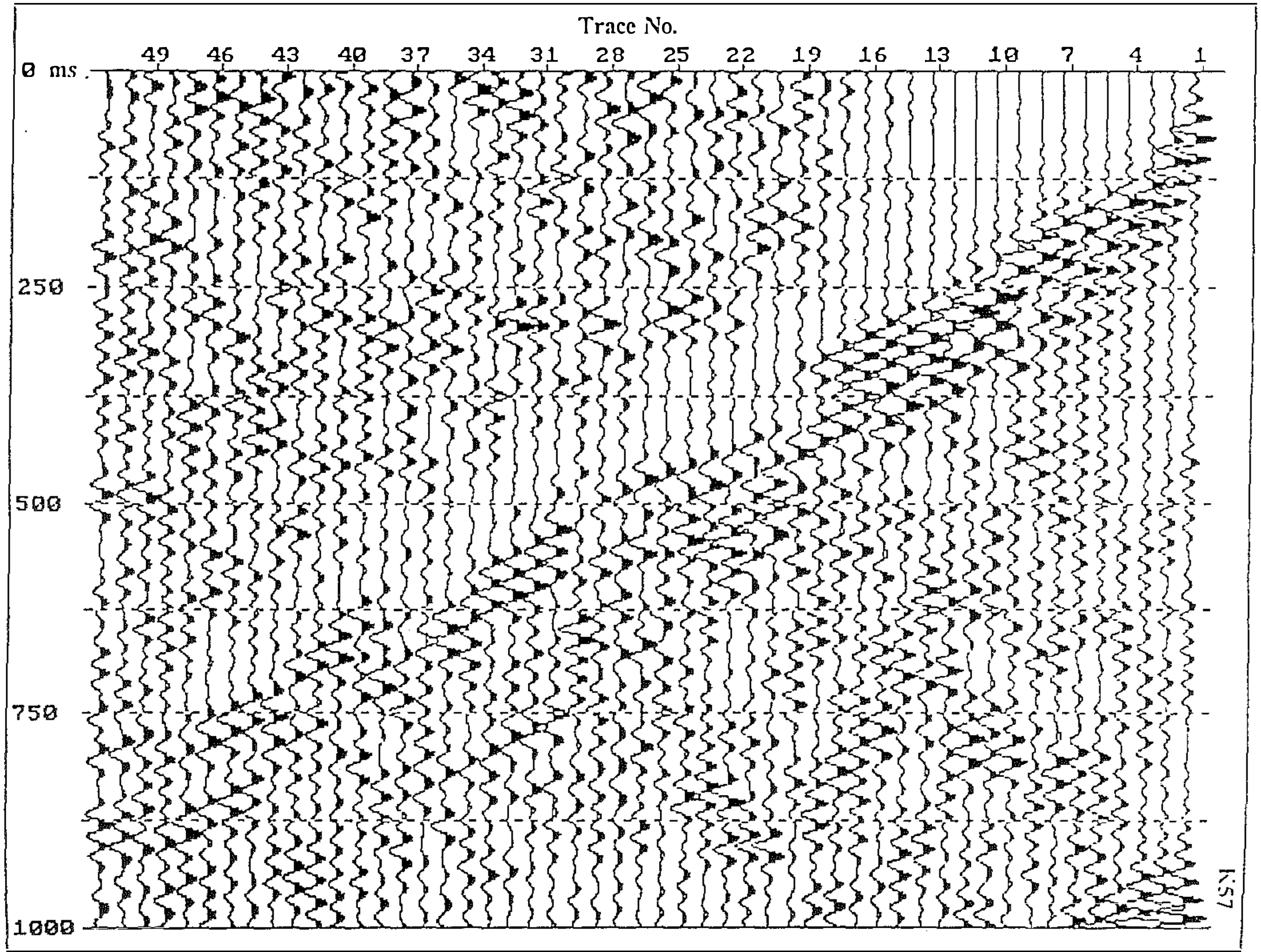

Figure A.49. Site K57 in Graves County (Farmington Quadrangle).

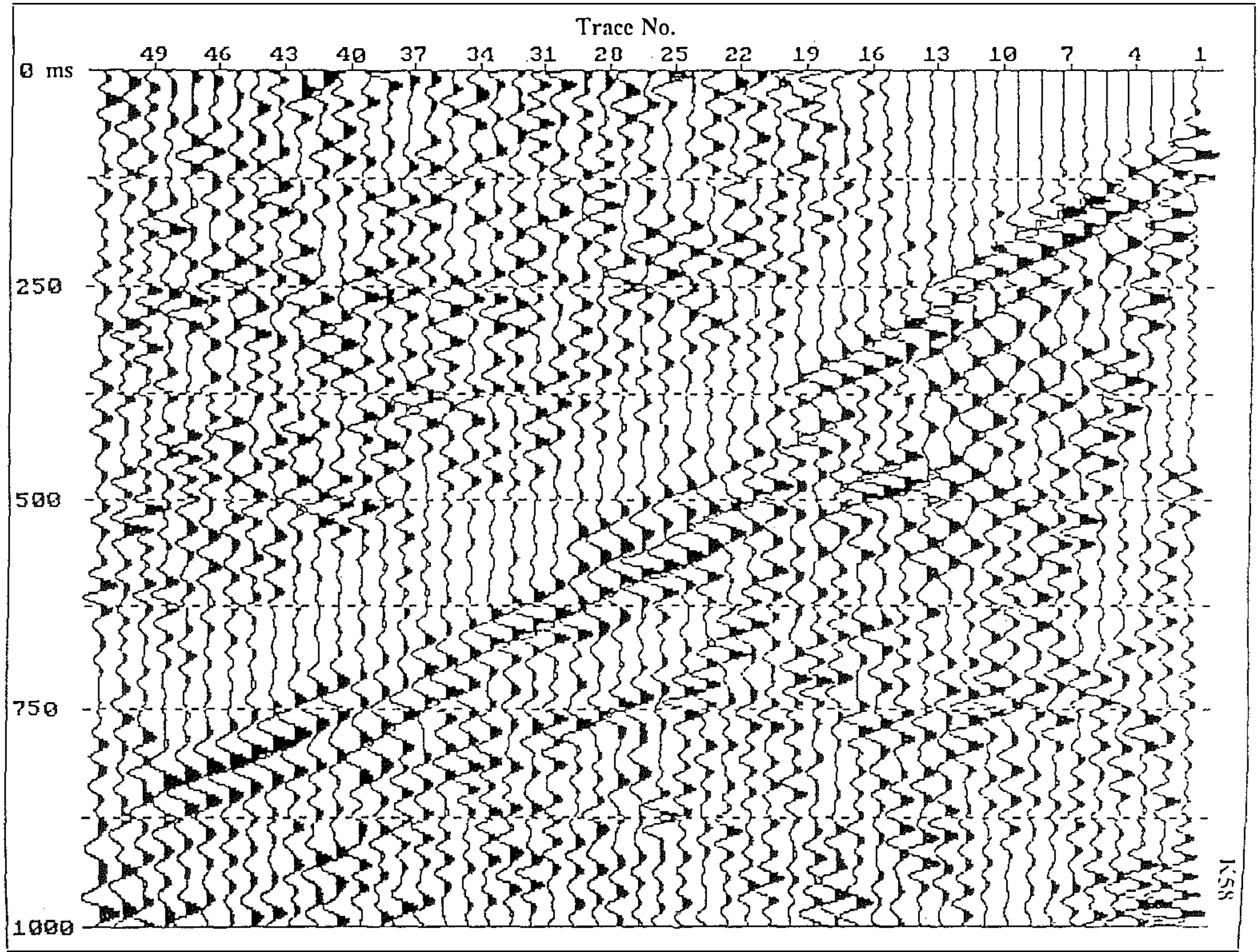

Figure A.50. Site K58 in Graves County (Farmington Quadrangle).

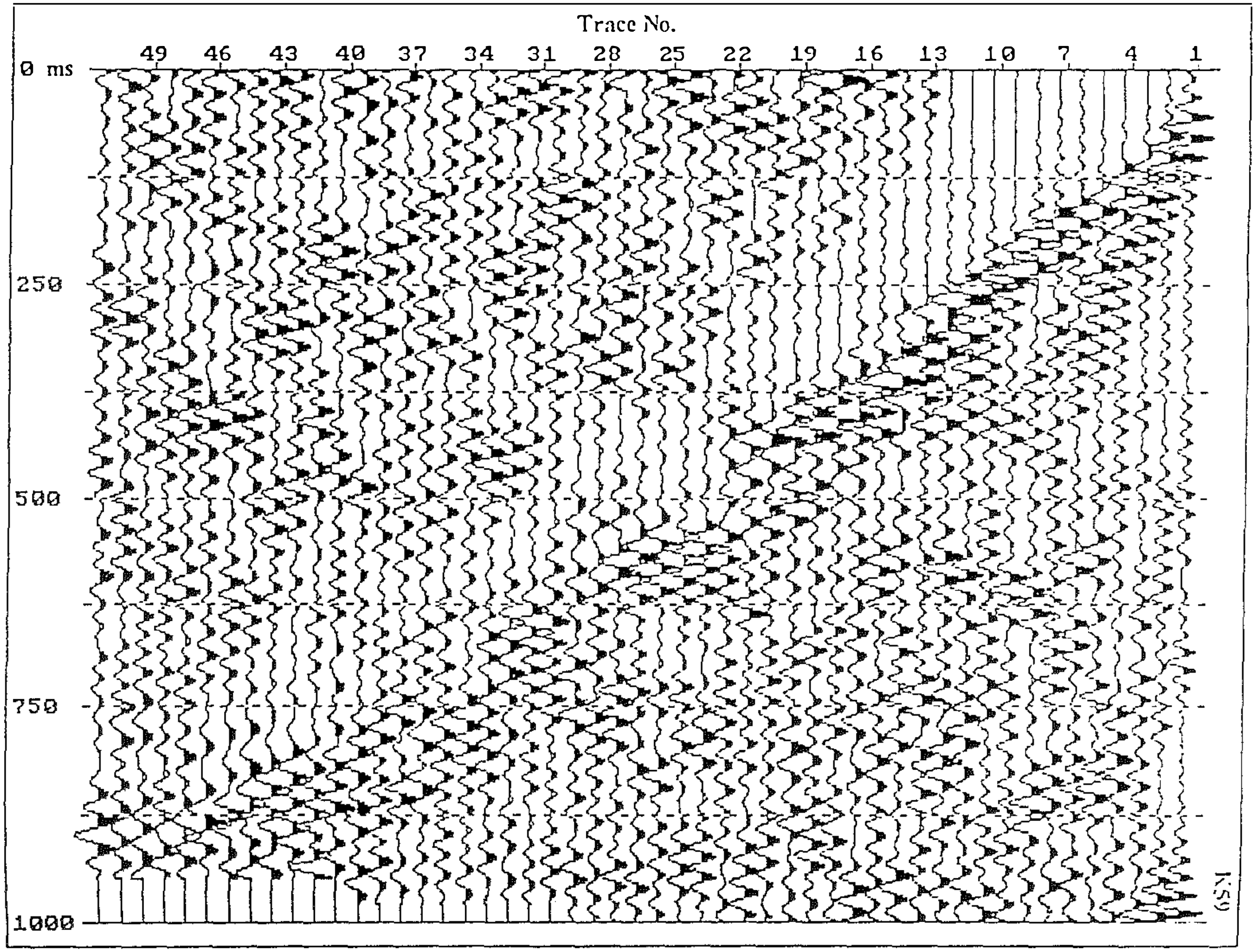

Figure A.51. Site K59 in Graves County (Mayfield Quadrangle).

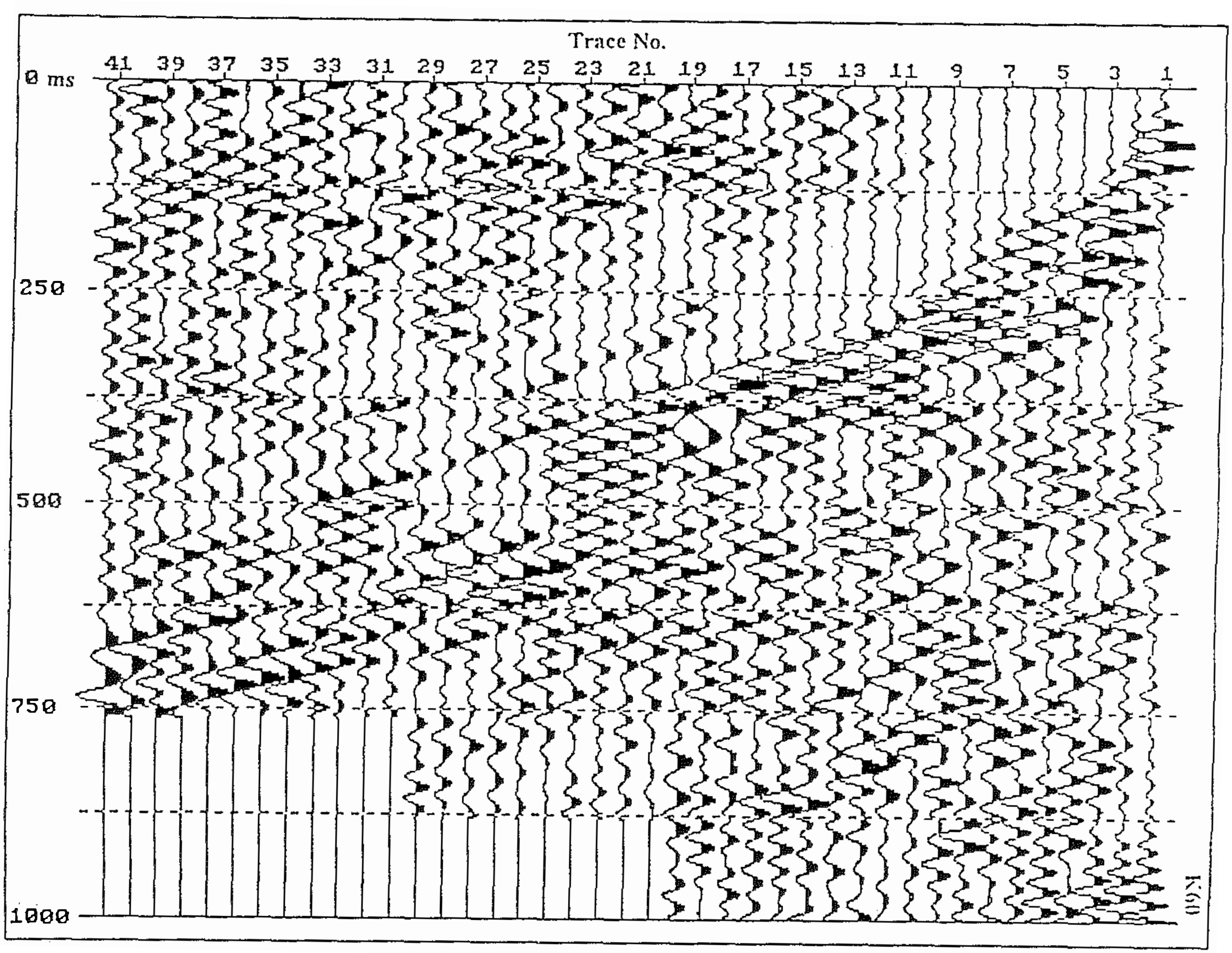

Figure A.52. Site K60 in Graves County (Dublin Quadrangle).

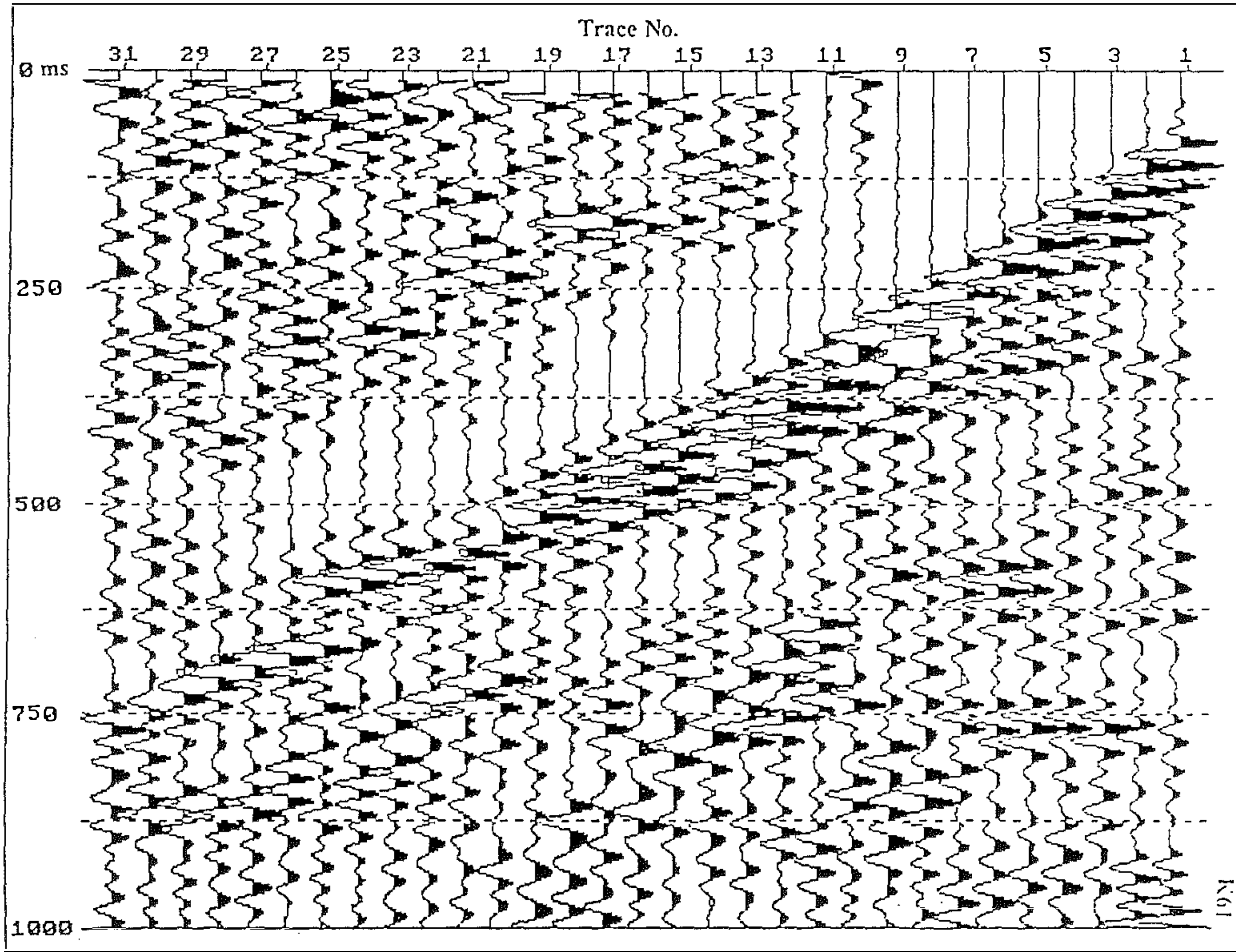

Figure A.53. Site K61 in Hickman County (Dublin Quadrangle).

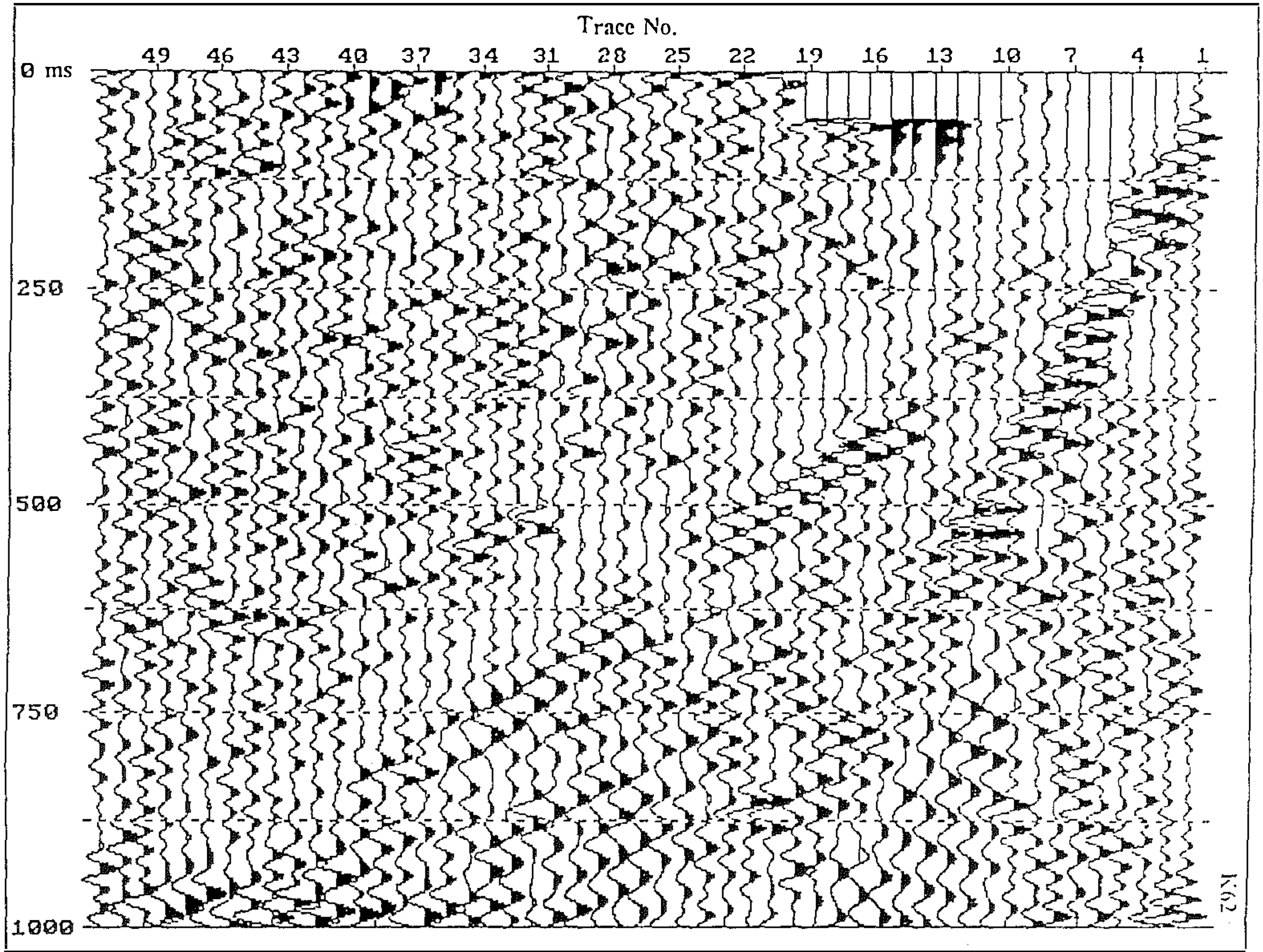

Figure A.54. Site K62 in Hickman County (Clinton Quadrangle).

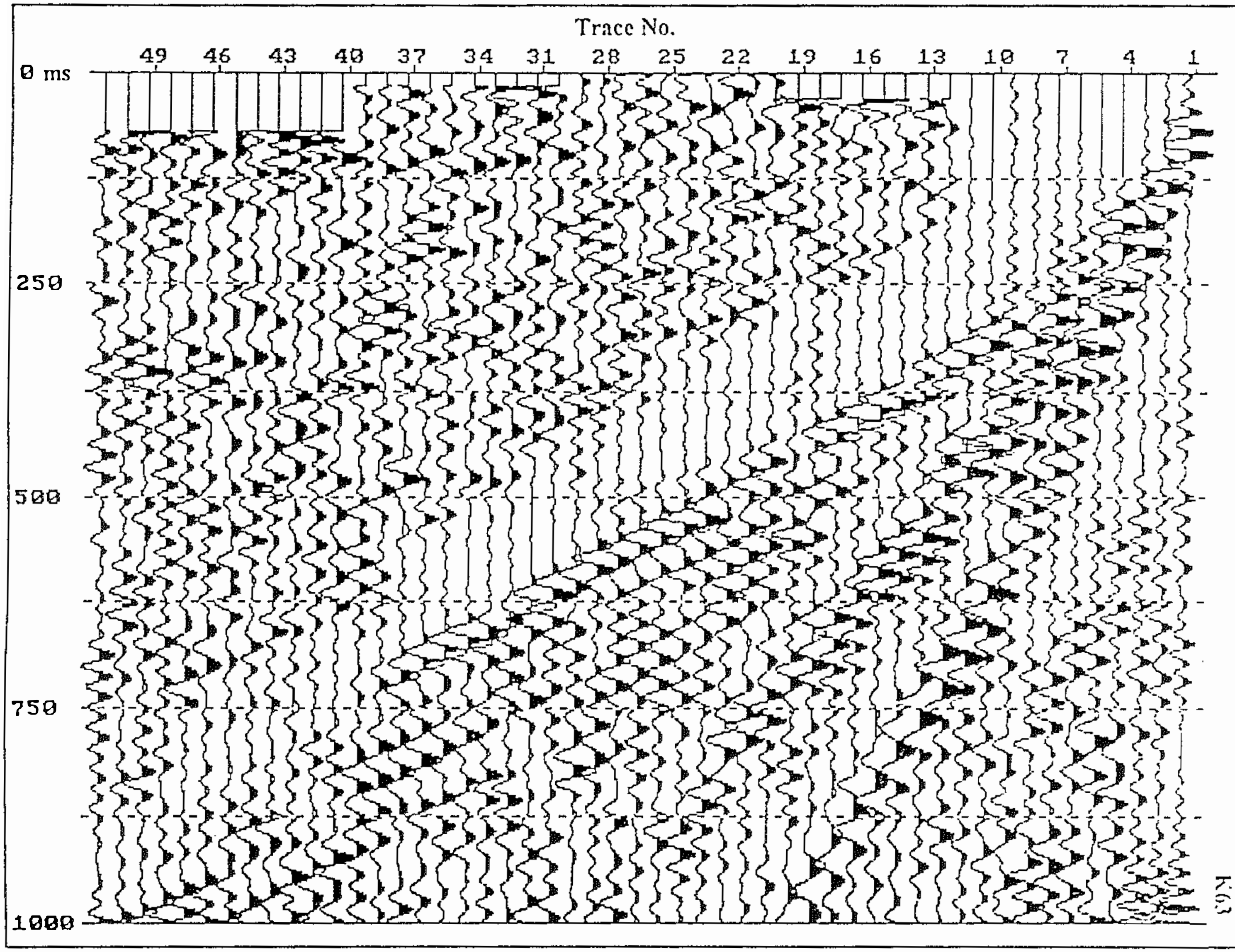

Figure A.55. Site K63 in Hickman County (Clinton Quadrangle).

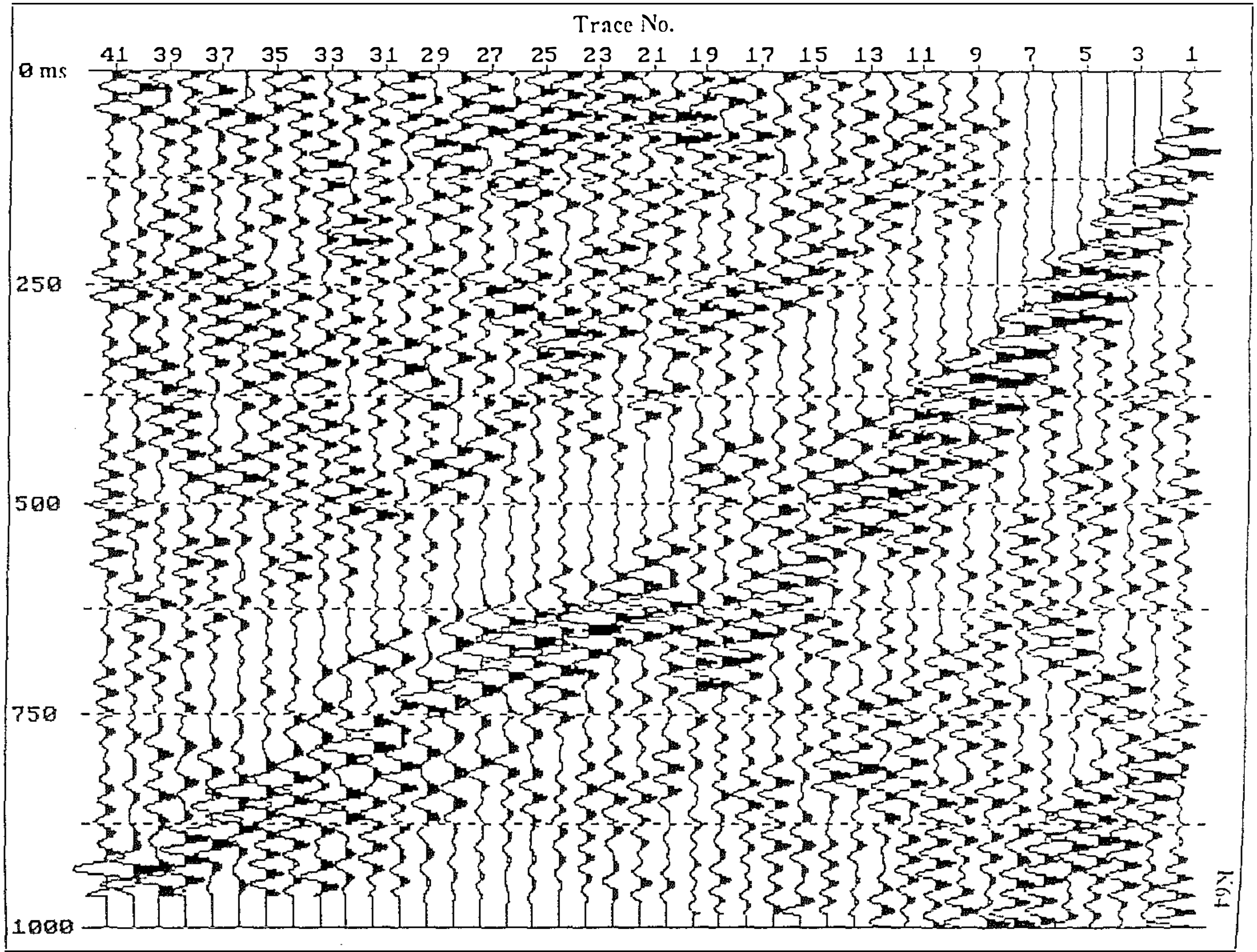

Figure A.56. Site K64 in Hickman County (Oakton Quadrangle).

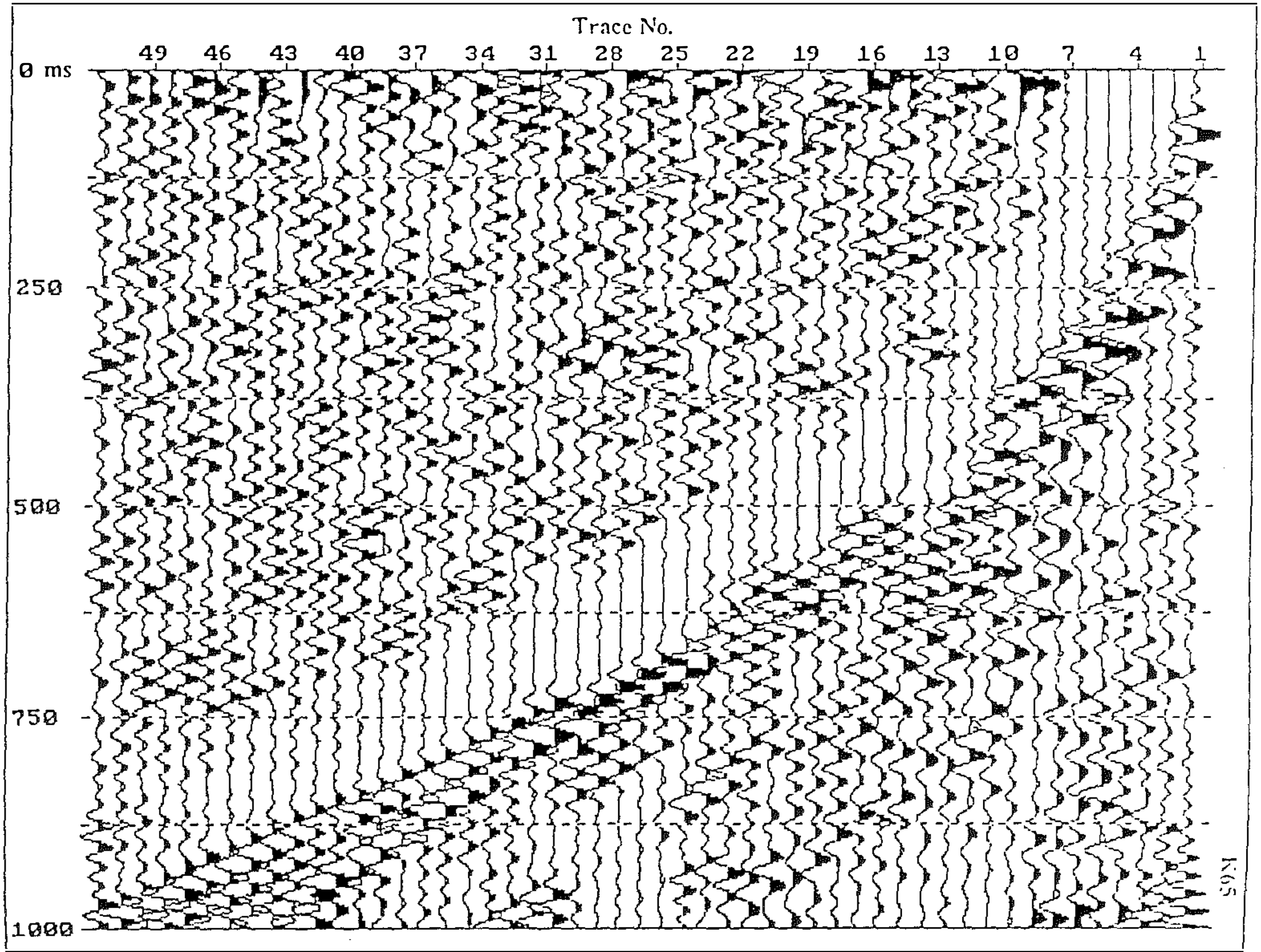

Figure A.56B. Site K65 in Hickman County (Oakton Quadrangle).

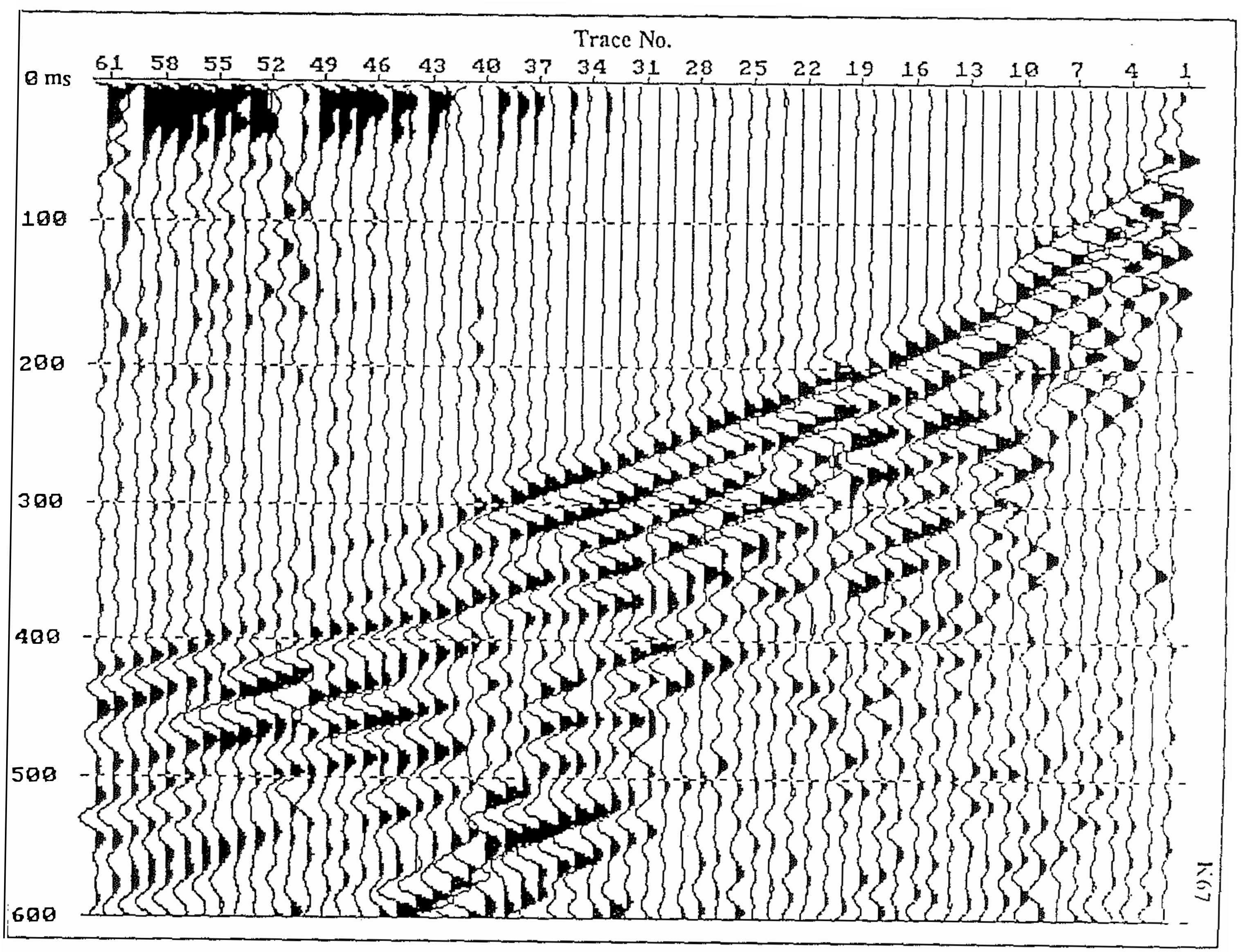

Figure A.57. Site K67 in Calloway County (New Concord Quadrangle).

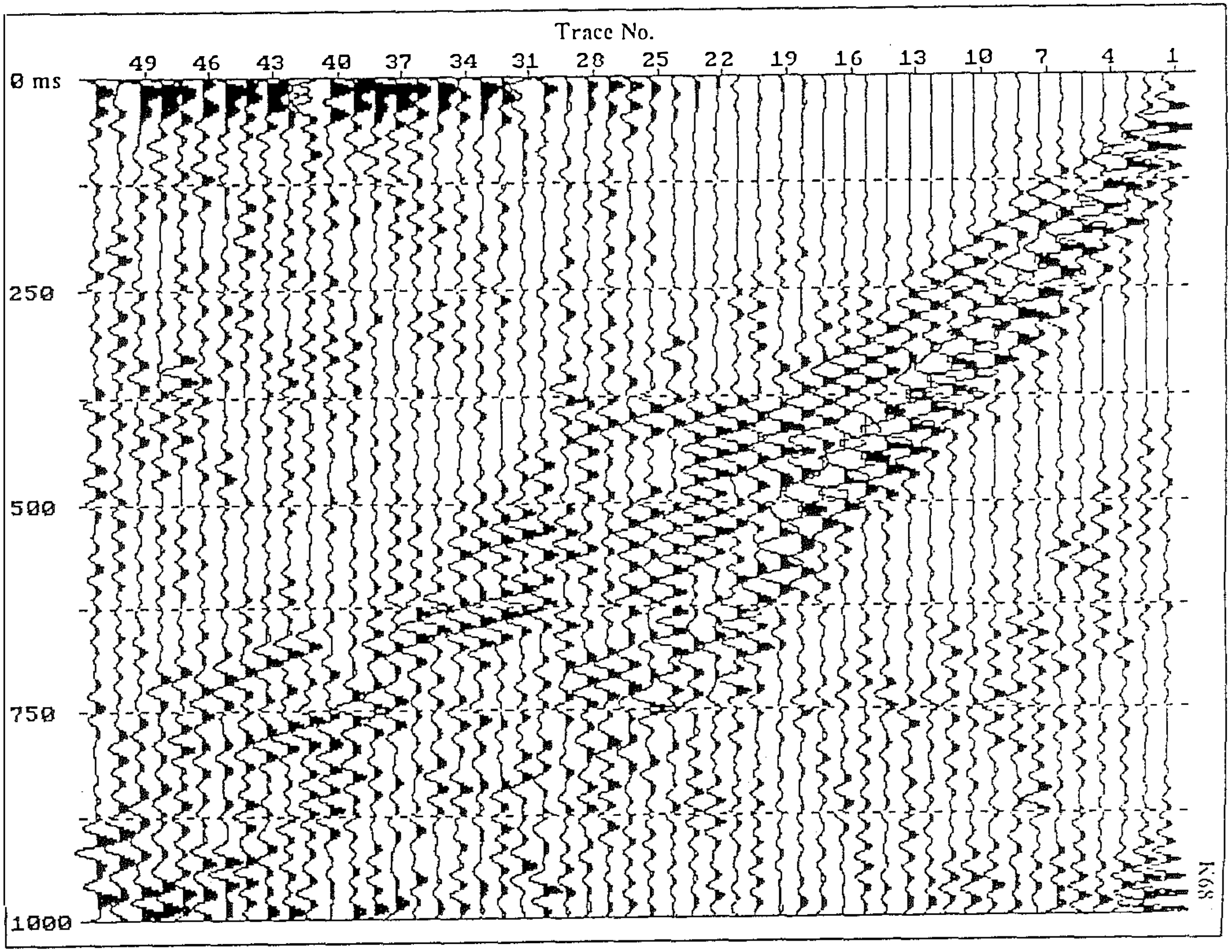

Figure A.58. Site K68 in Calloway County (New Concord Quadrangle).

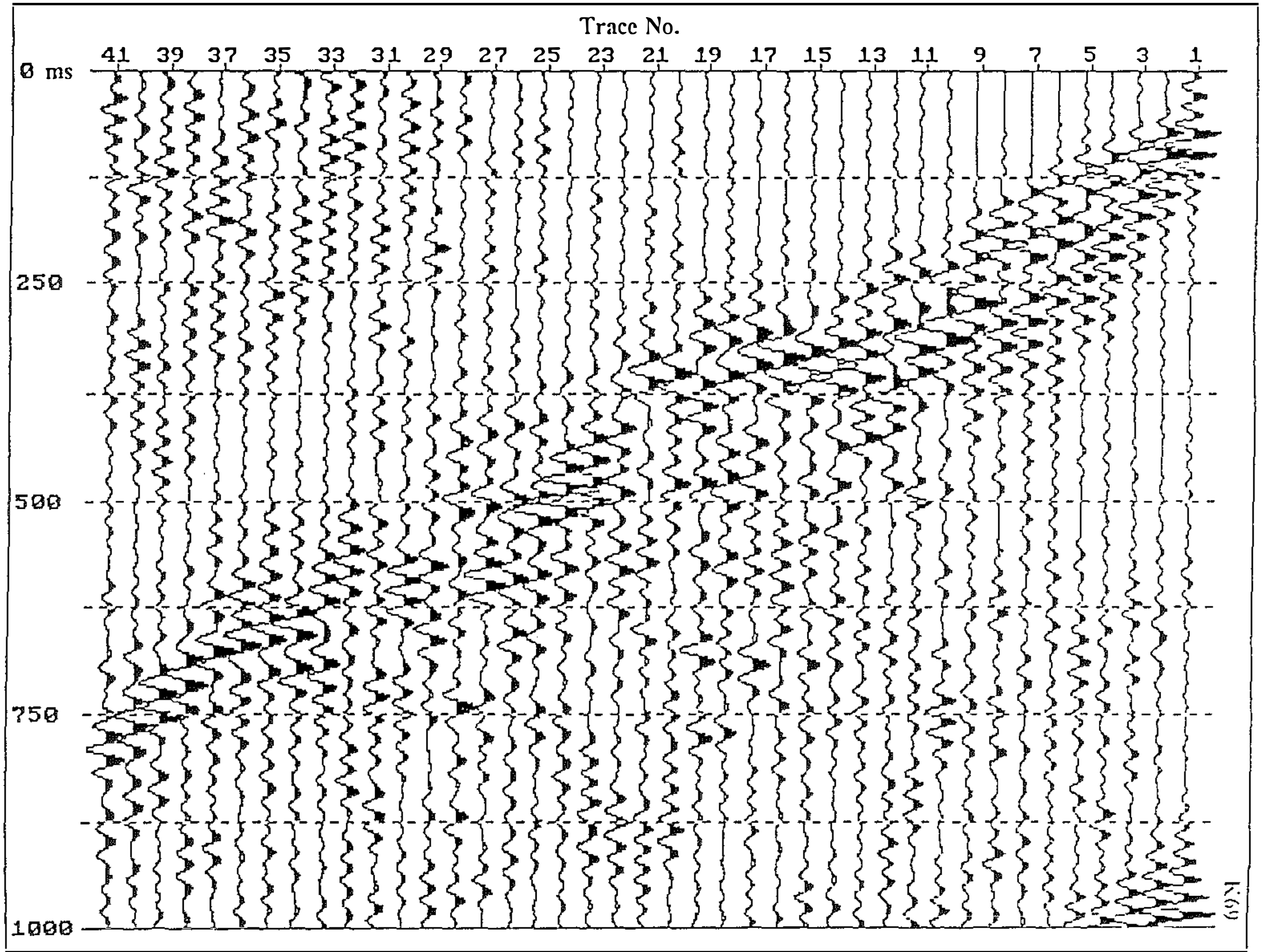

Figure A.59. Site K69 iu Calloway County (Murray Quadrangle).

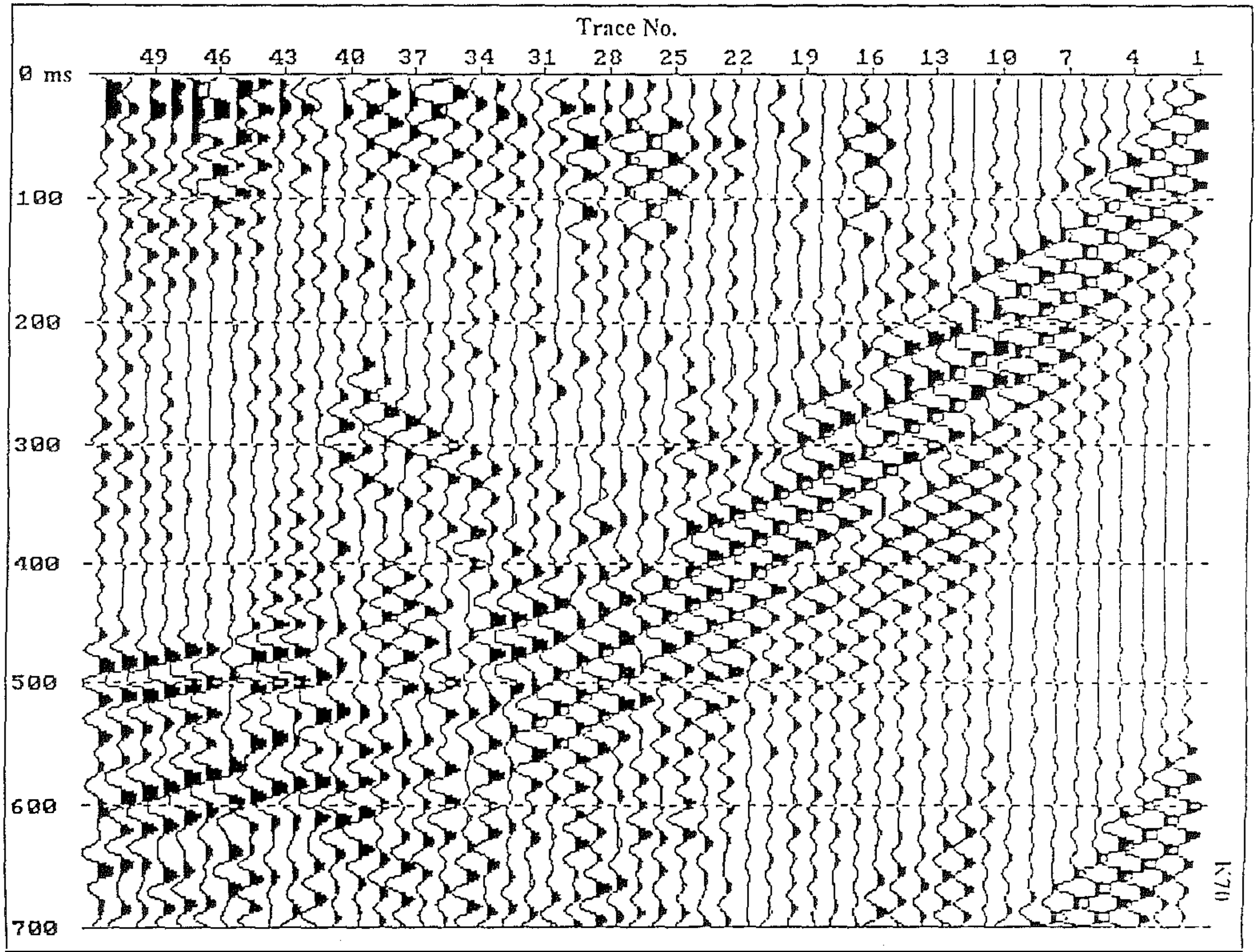

Figure A.60. Site K70 in Calloway County (Murray Quadrangle).

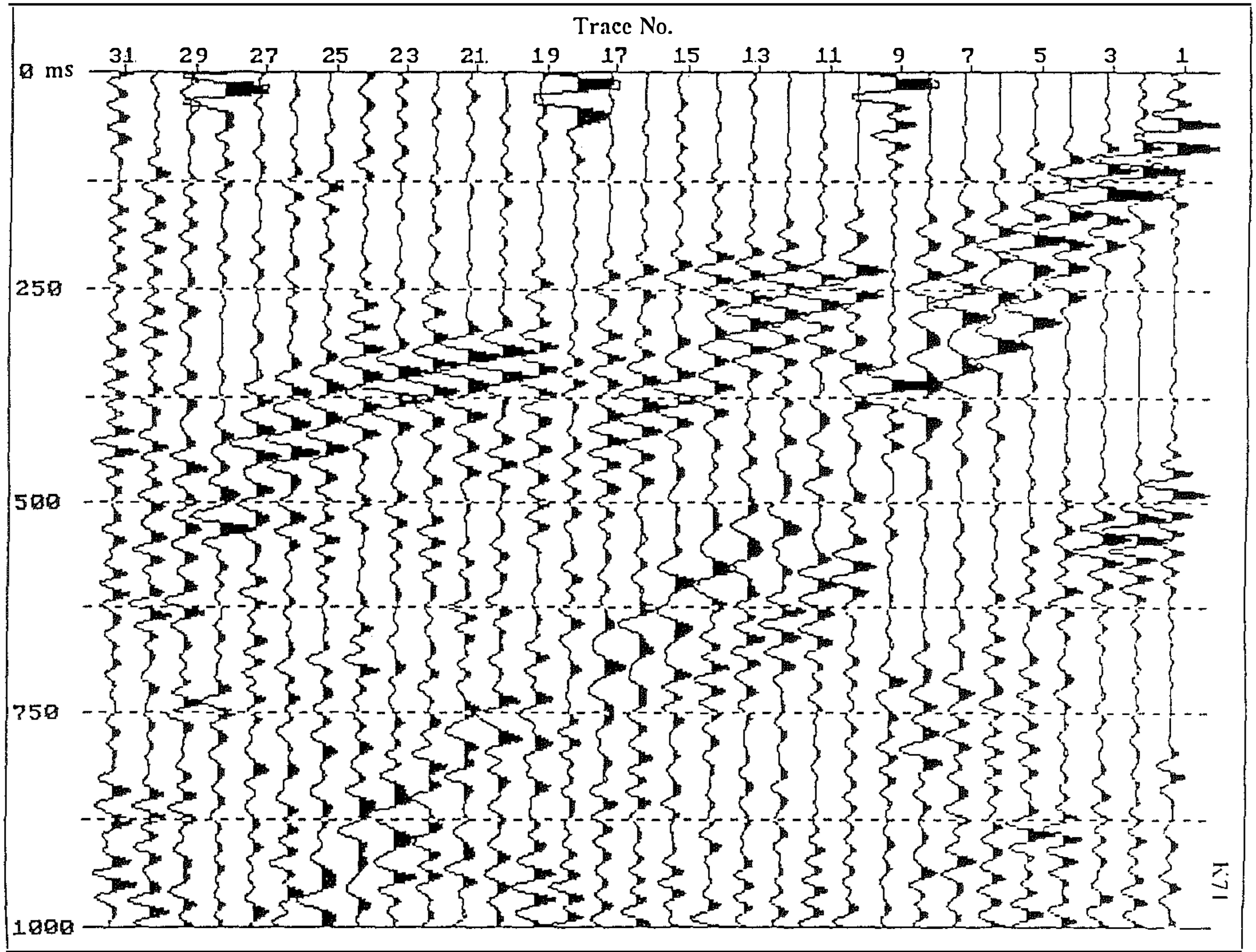

Figure A.61. Site K71 in Calloway County (Murray Quadrangle).

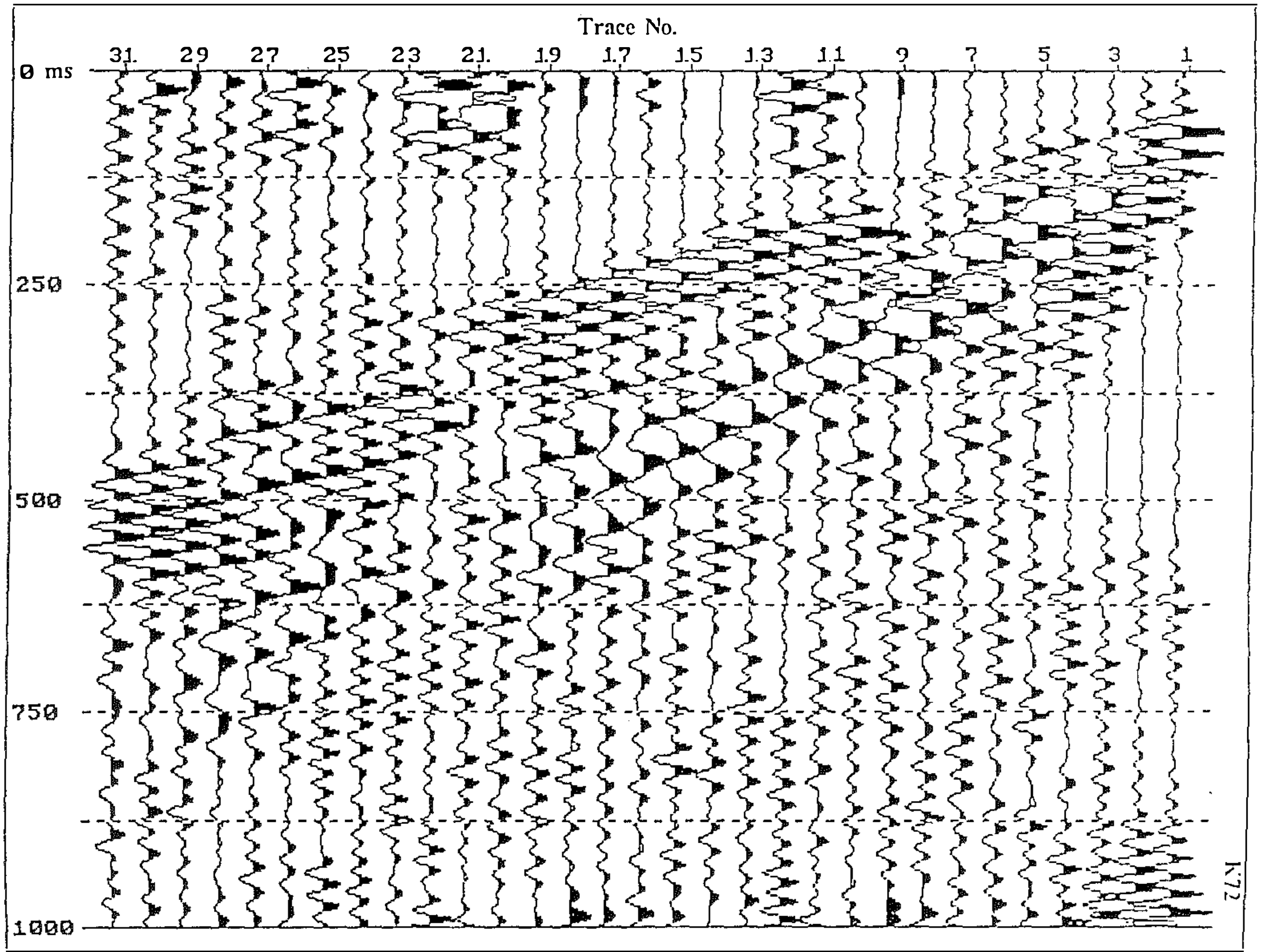

Figure A.62. Site K72 in Calloway County (Lynn Grove Quadrangle).

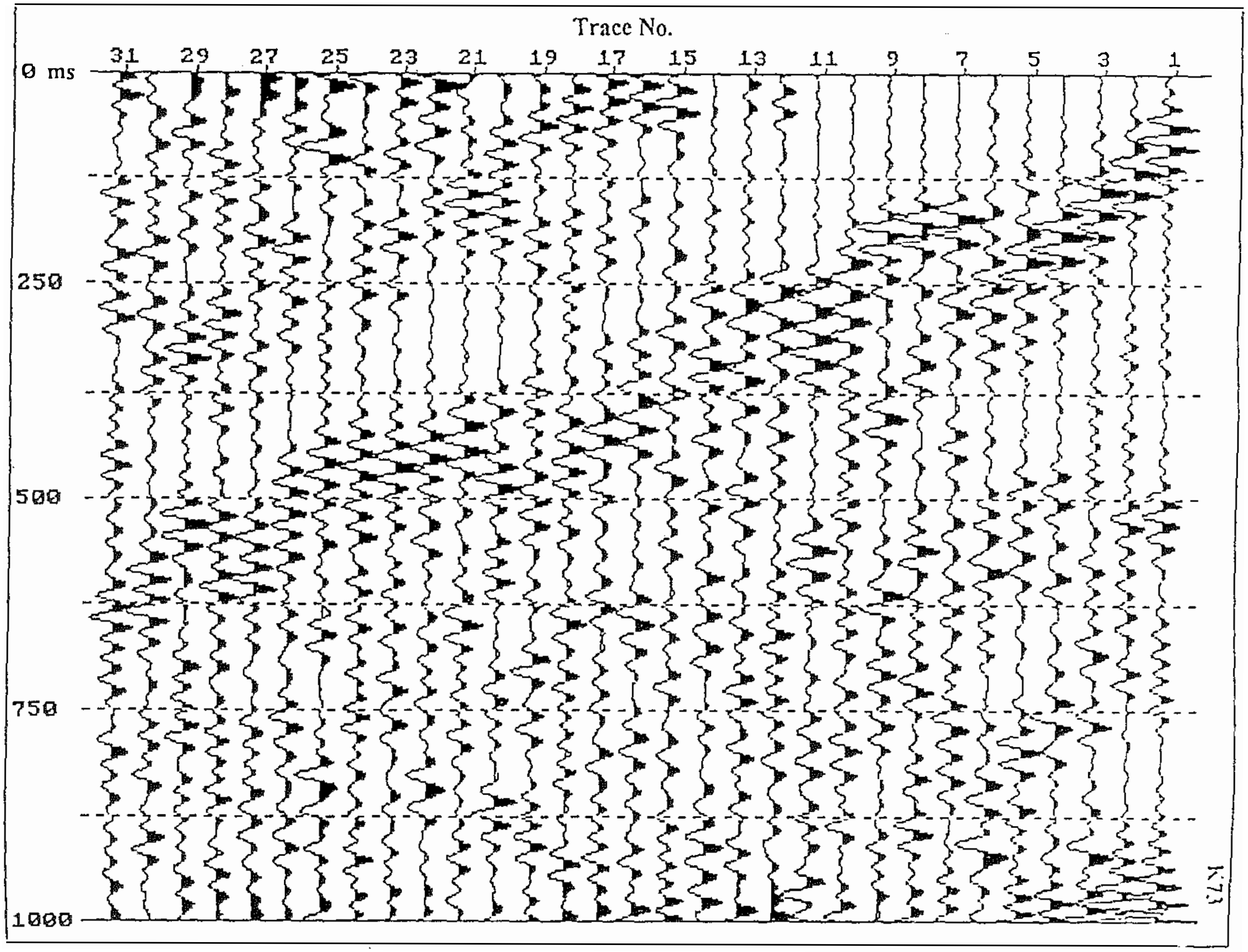

Figure A.63. Site K73 in Graves County (Lynnville Quadrangle).

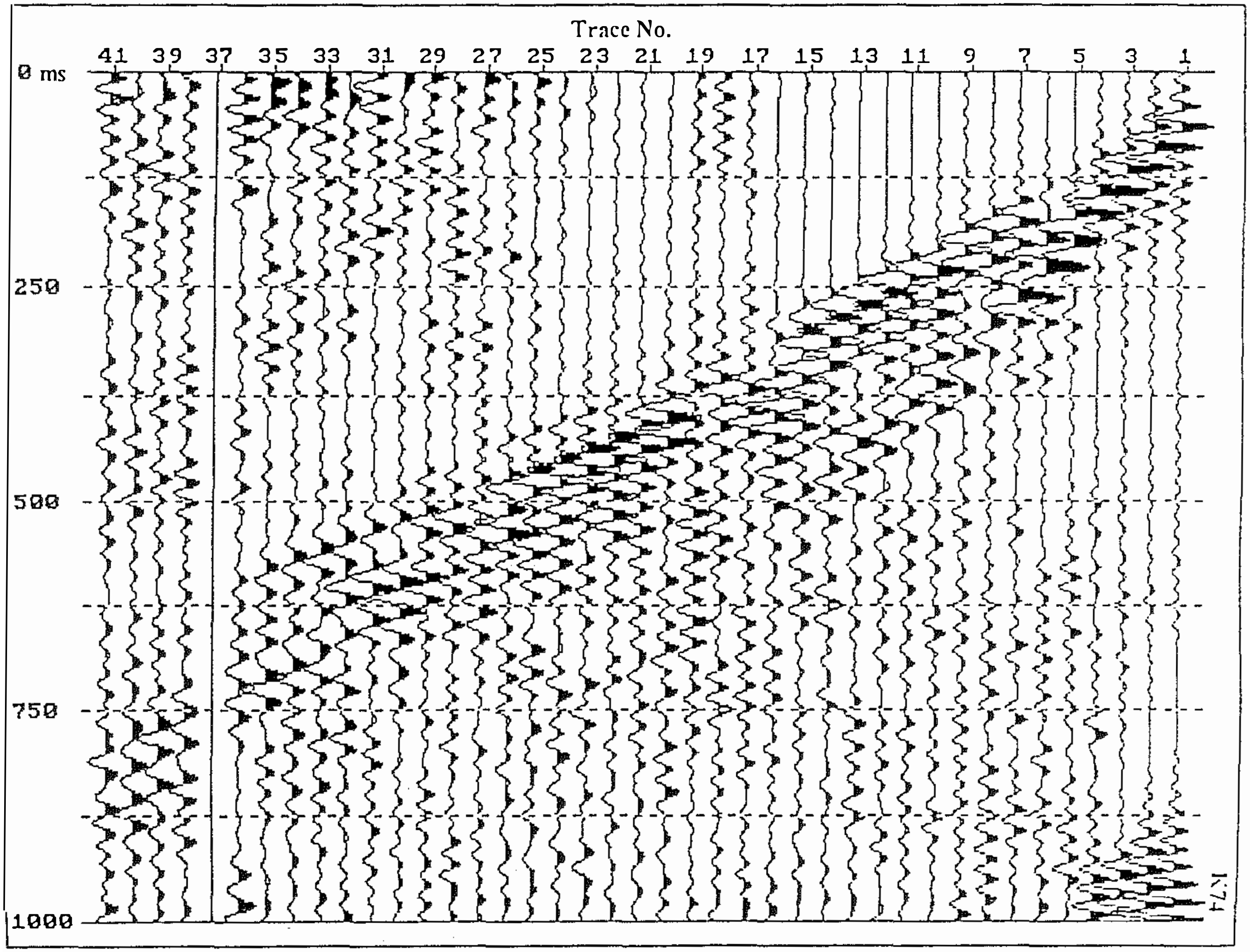

Figure A.64. Site K74 in Graves County (Lynnville Quadrangle).

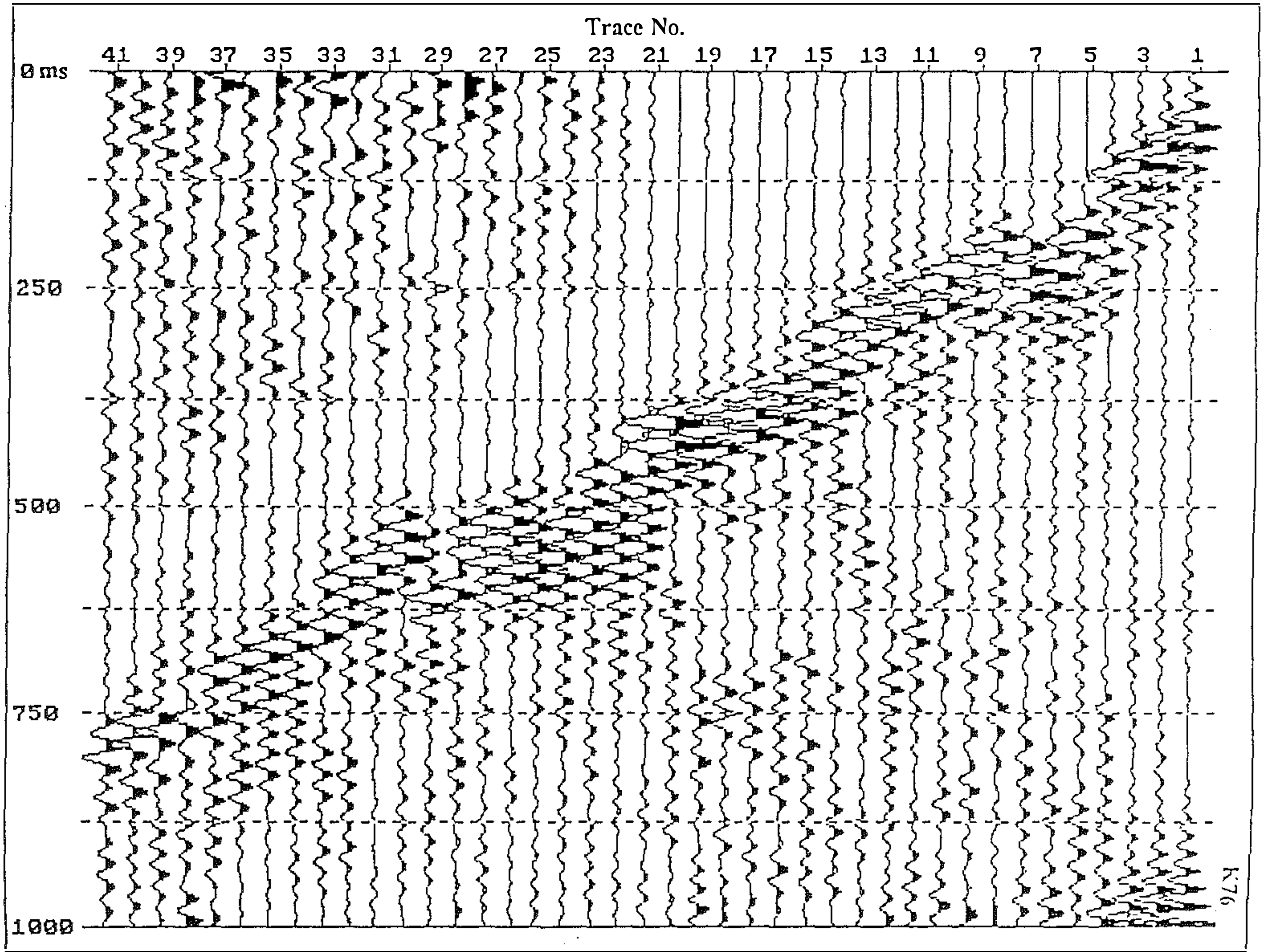

Figure A.65. Site K76 in Graves County (Cuba Quadrangle).

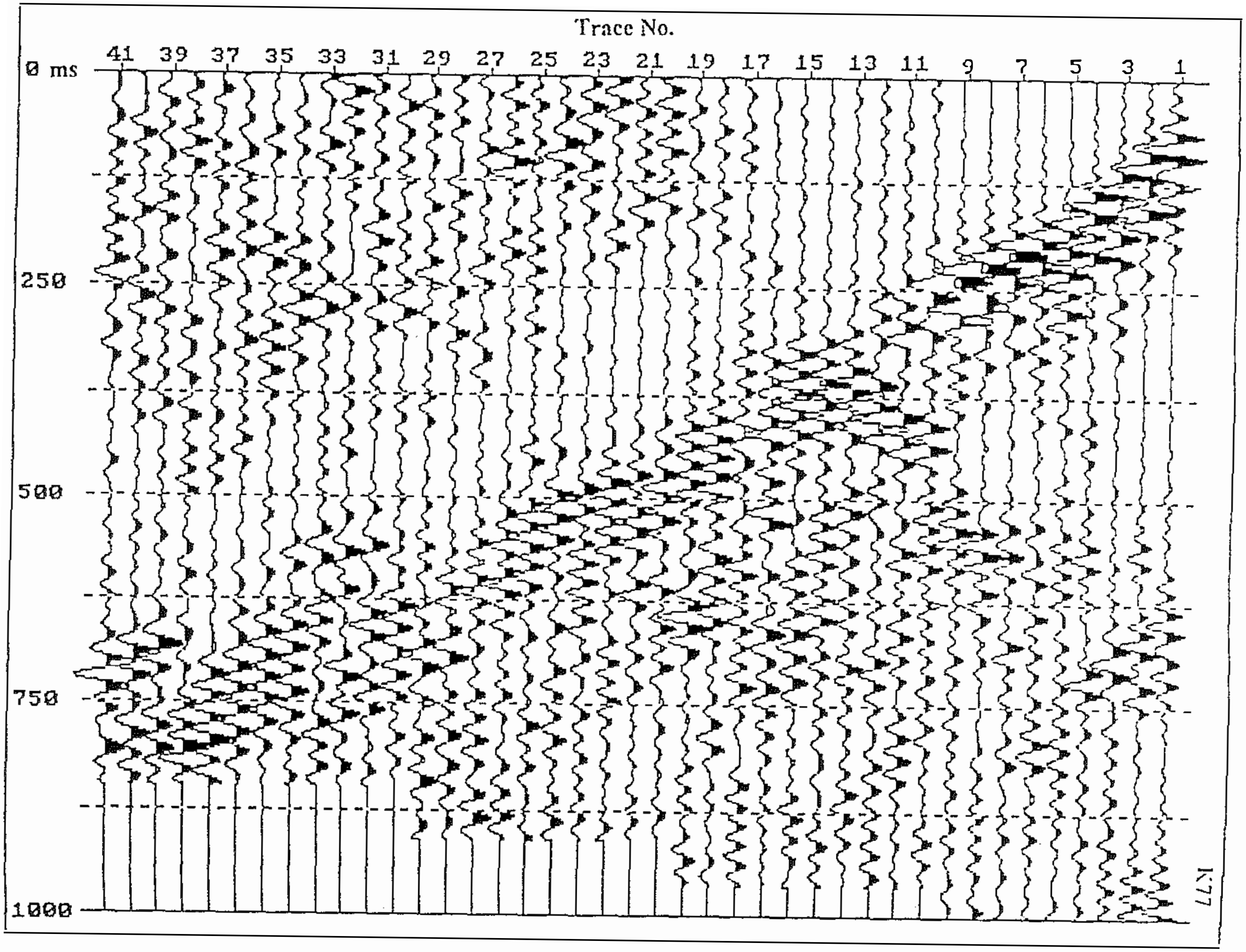

Figure A.66. Site K77 in Graves County (Water Valley Quadrangle).

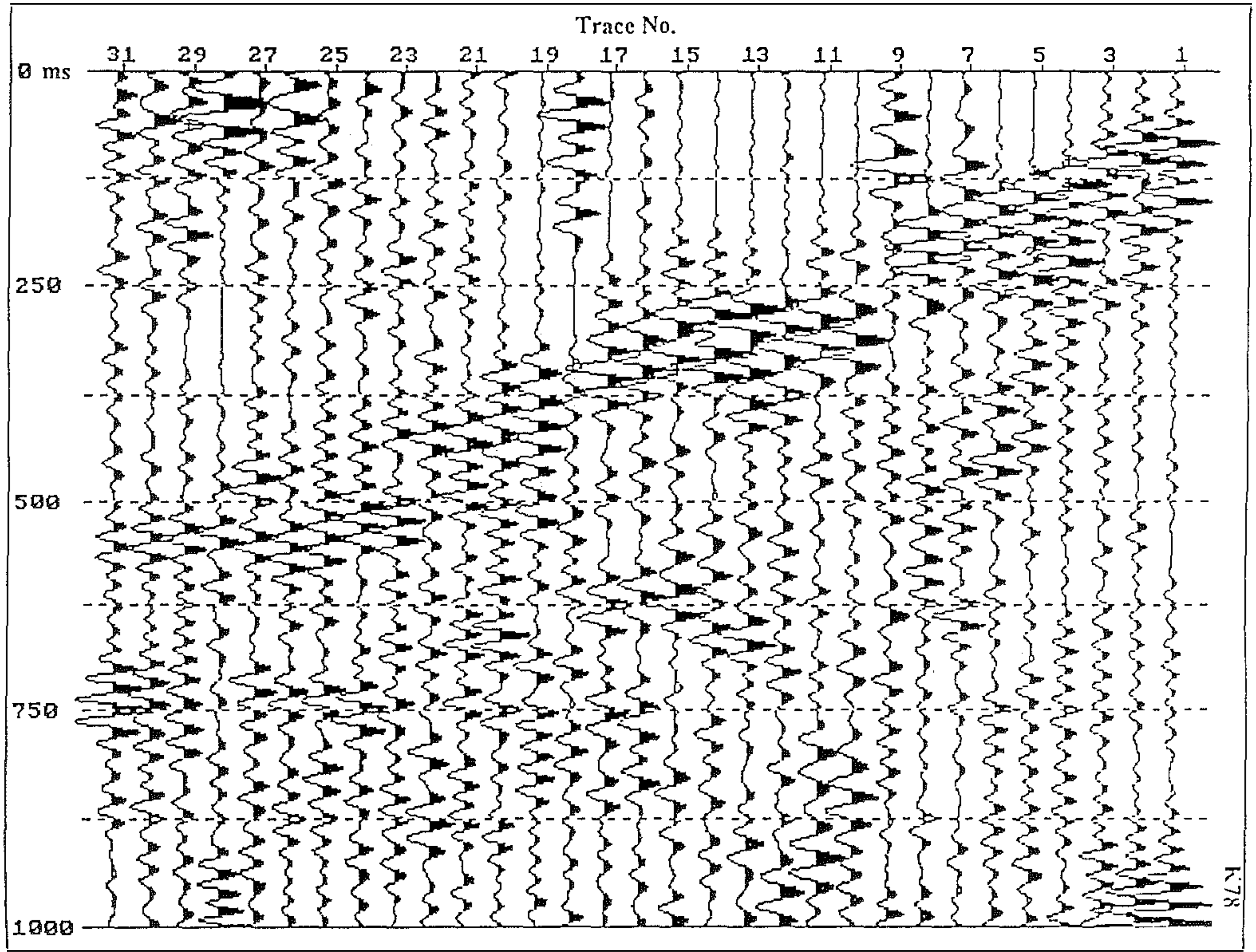

Figure A.67. Site K78 in Hickman County (Water Valley Quadrangle).

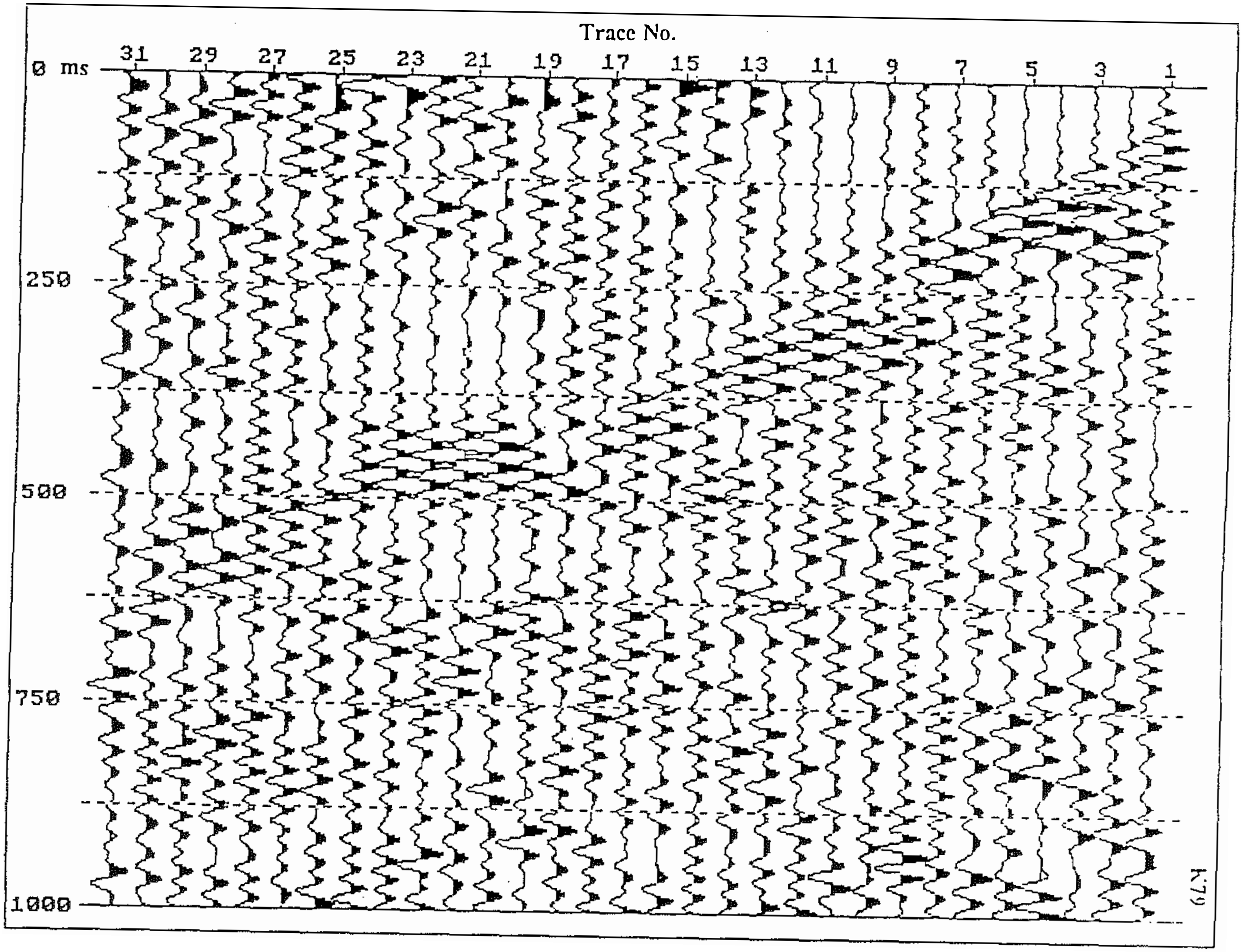

Figure A.68. Site K79 in Fulton County (Crutchfield Quadrangle).

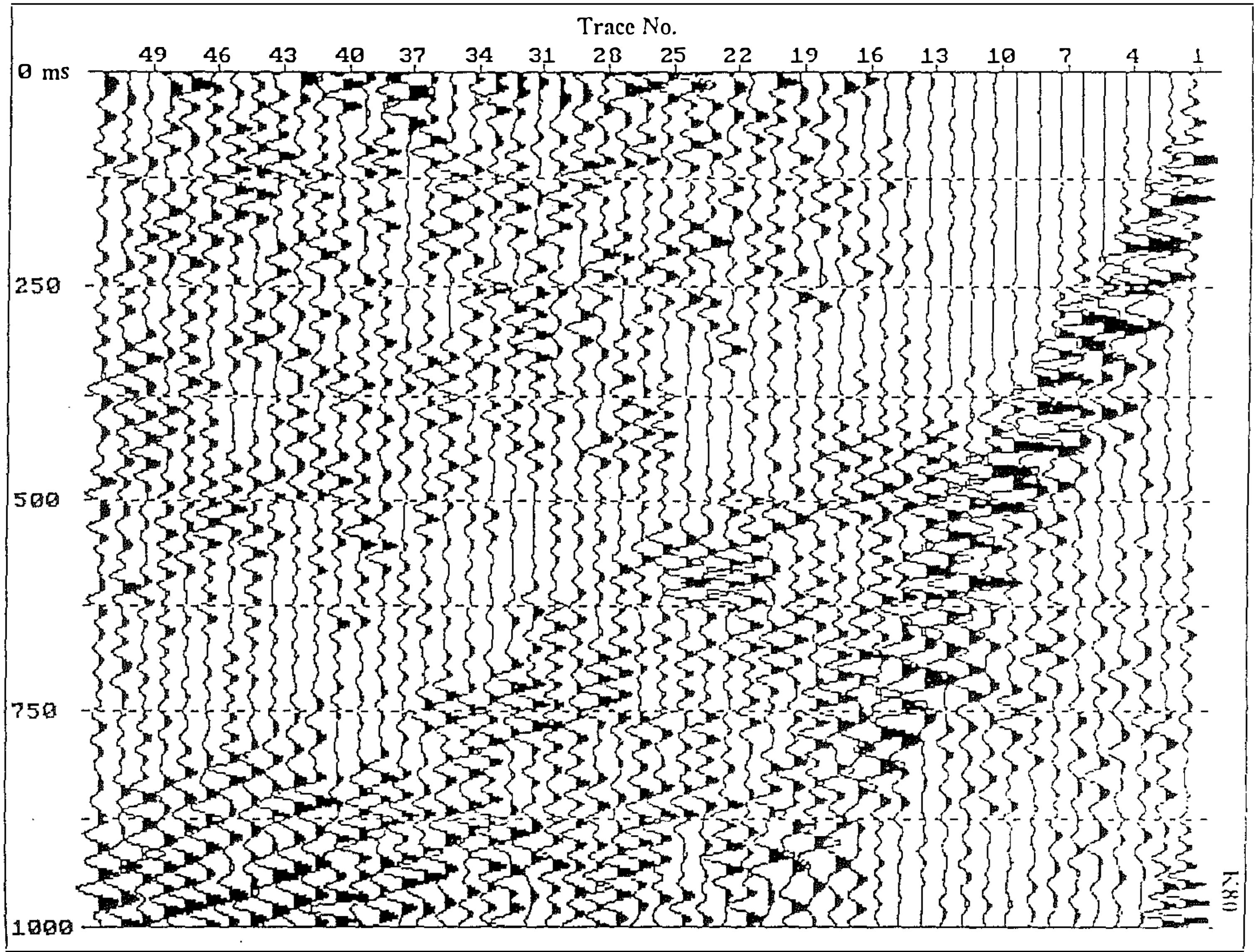

Figure A.69. Site K80 in Fulton County (Crutchfield Quadrangle).

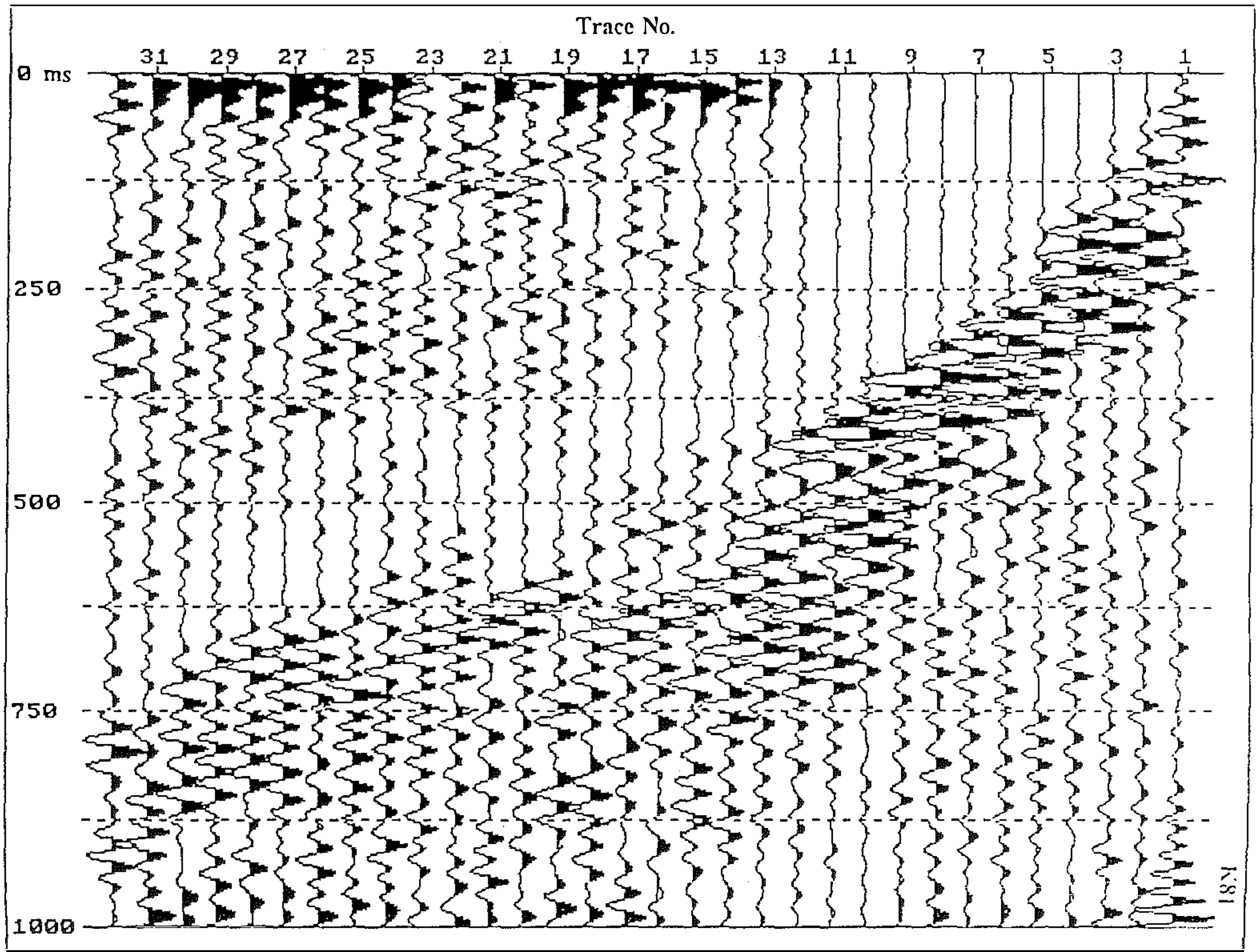

Figure A.70. Site K81 in Fulton County (Crutchfield Quadrangle).

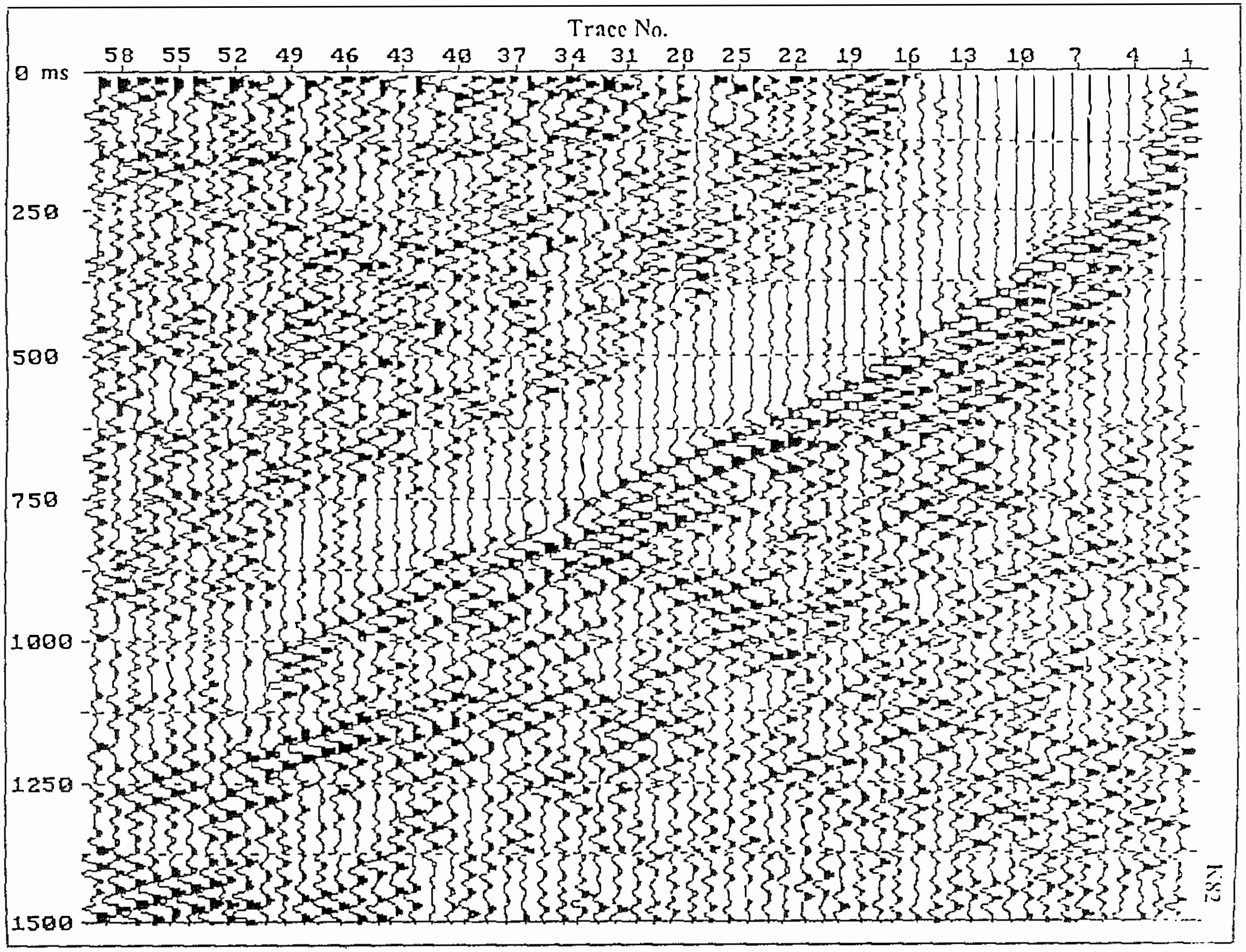

Figure A.71. Site K82 in Fulton County (Cayce Quadrangle).

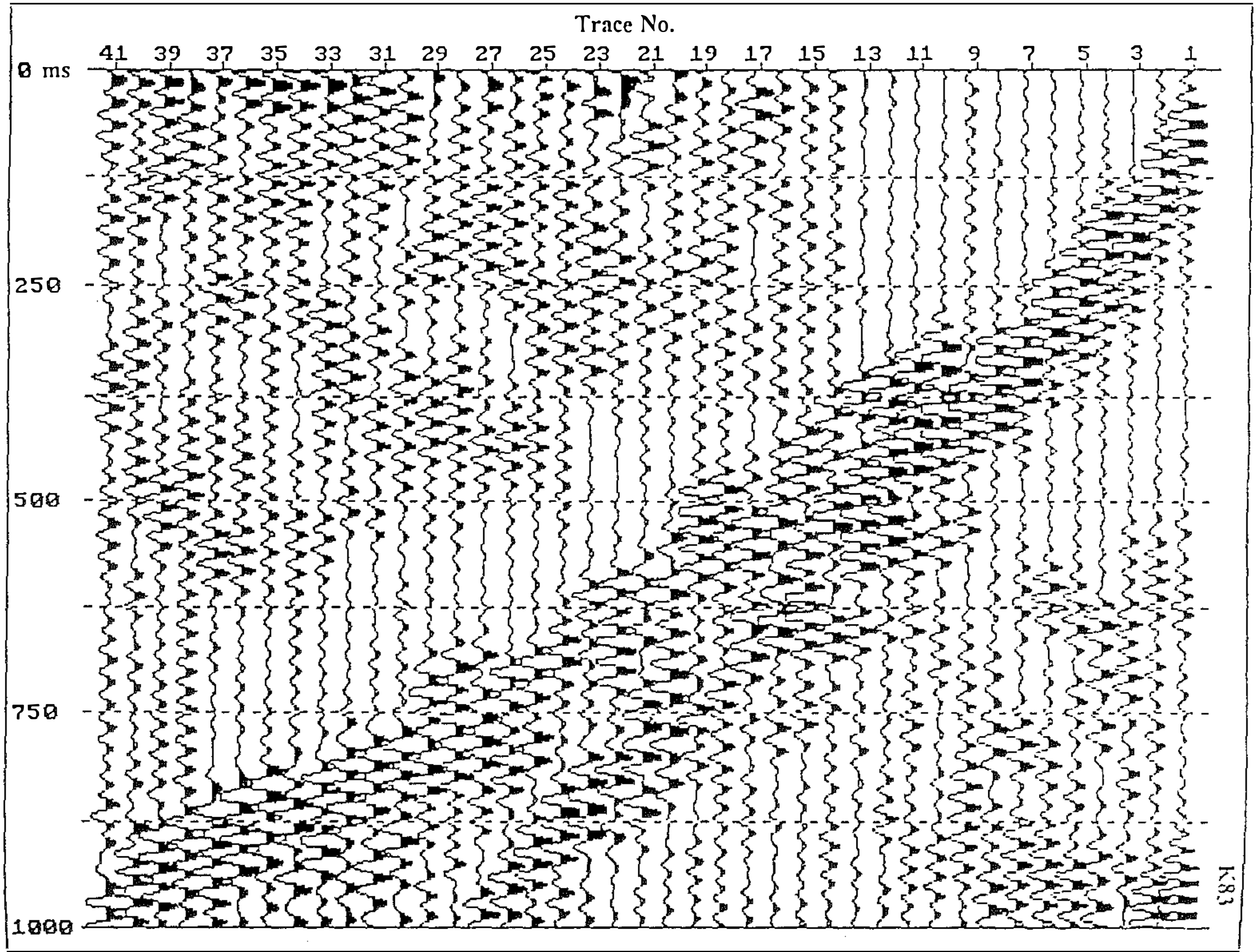

Figure A.72. Site K83 in Fulton County (Cayce Quadrangle).